www.cern.ch/n_TOF

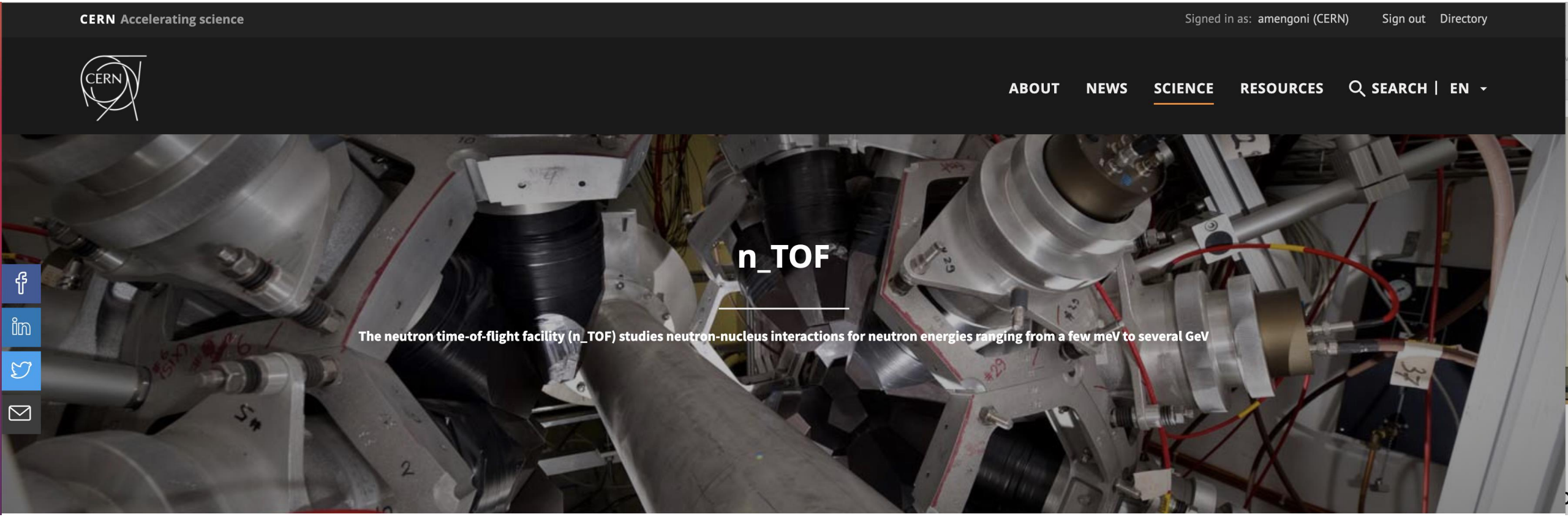



Alberto Mengoni

on behalf of the n_TOF Collaboration

# n_TOF @ CERN

- Based on an idea by Carlo Rubbia, n_TOF is a pulsed spallation neutron source, driven by the CERN PS, coupled to two flight paths (at 20 and at 200 meters) designed to study neutron-nucleus interactions for neutron kinetic energies ranging from a few milli-eV to several GeV. The neutron kinetic energy is determined by time-of-flight, hence the name n_TOF

- The study of neutron-induced reactions is of paramount importance in a variety of research fields, ranging from **big bang to stellar nucleosynthesis**, symmetry breaking effects in compound nuclei, investigation of nuclear level densities, to applications to **advanced nuclear technology**, including the transmutation of nuclear waste, accelerator driven systems and nuclear fuel cycle investigations

CERN

nTOF

# n_TOF @ CERN

C. Rubbia et al., A high resolution spallation driven facility at the CERN-PS to measure neutron cross sections in the interval from 1 eV to 250 MeV CERN/LHC/98-02(EET) 1998

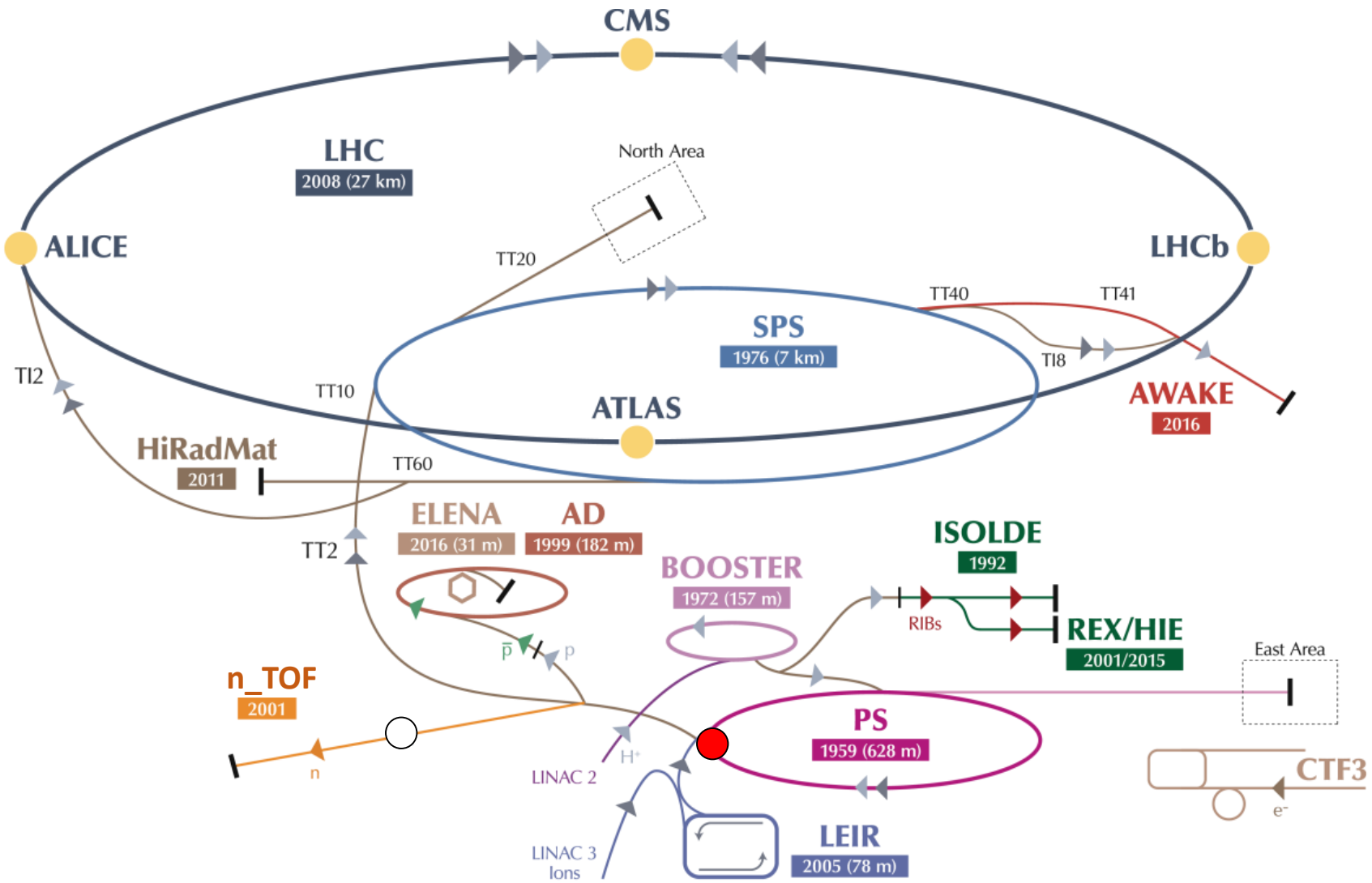

# n_TOF @ CERN

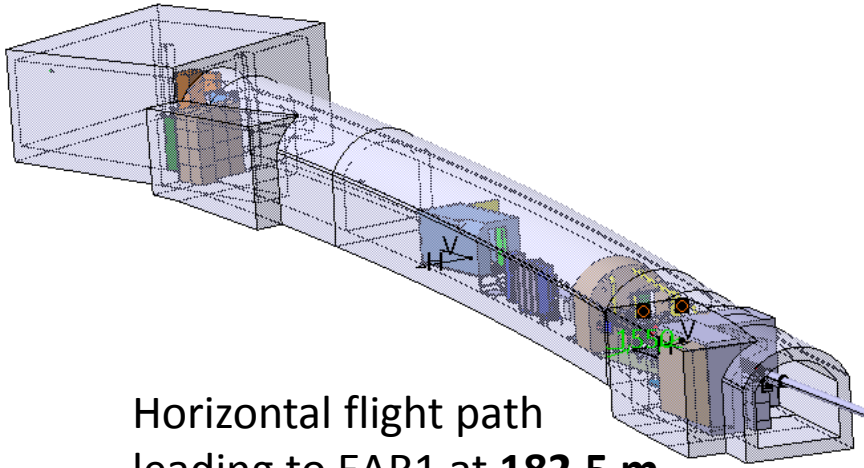


Bldg 380

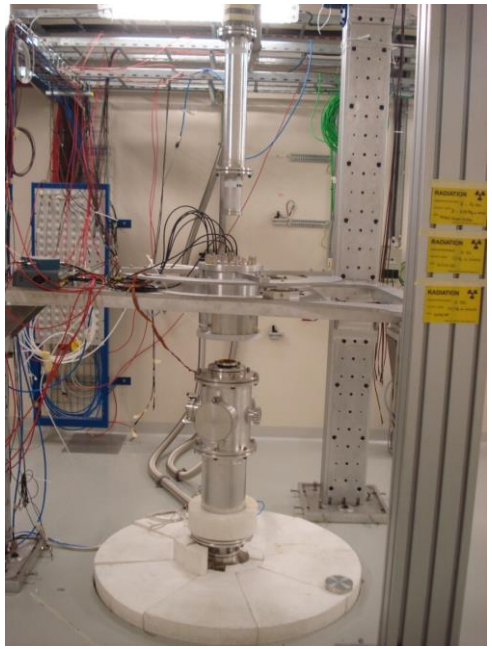

Horizontal flight path
leading to EAR1 at **182.5 m**

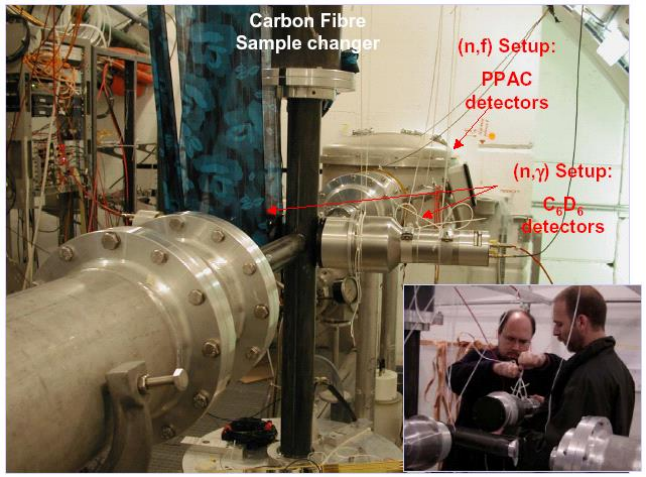


Vertical flight path
leading to EAR2 at **18.2 m**

proton beam from the PS

# n_TOF @ CERN

| | |
|---|---|
| proton beam momentum | 20 GeV/c |
| intensity (dedicated mode) | $7 \times 10^{12}$ protons/pulse |
| repetition frequency | 1 pulse/1.2s |
| pulse width | 6 ns (rms) |
| n/p | 300 |
| lead target dimensions | 80x80x60 $cm^3$ |
| cooling & moderation material | $H_2O$ (borated) |
| moderator thickness in the exit face | 5 cm |
| neutron beam dimension in EAR-1 (capture mode) | 2 cm (FWHM) |

# n_TOF @ CERN: 3rd-generation target

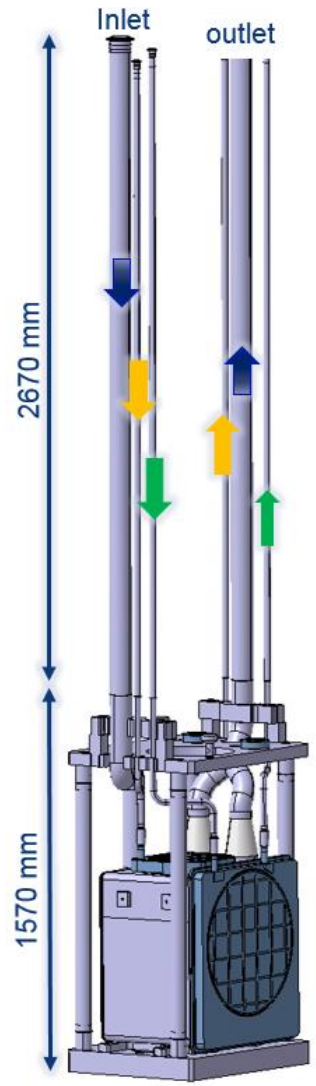


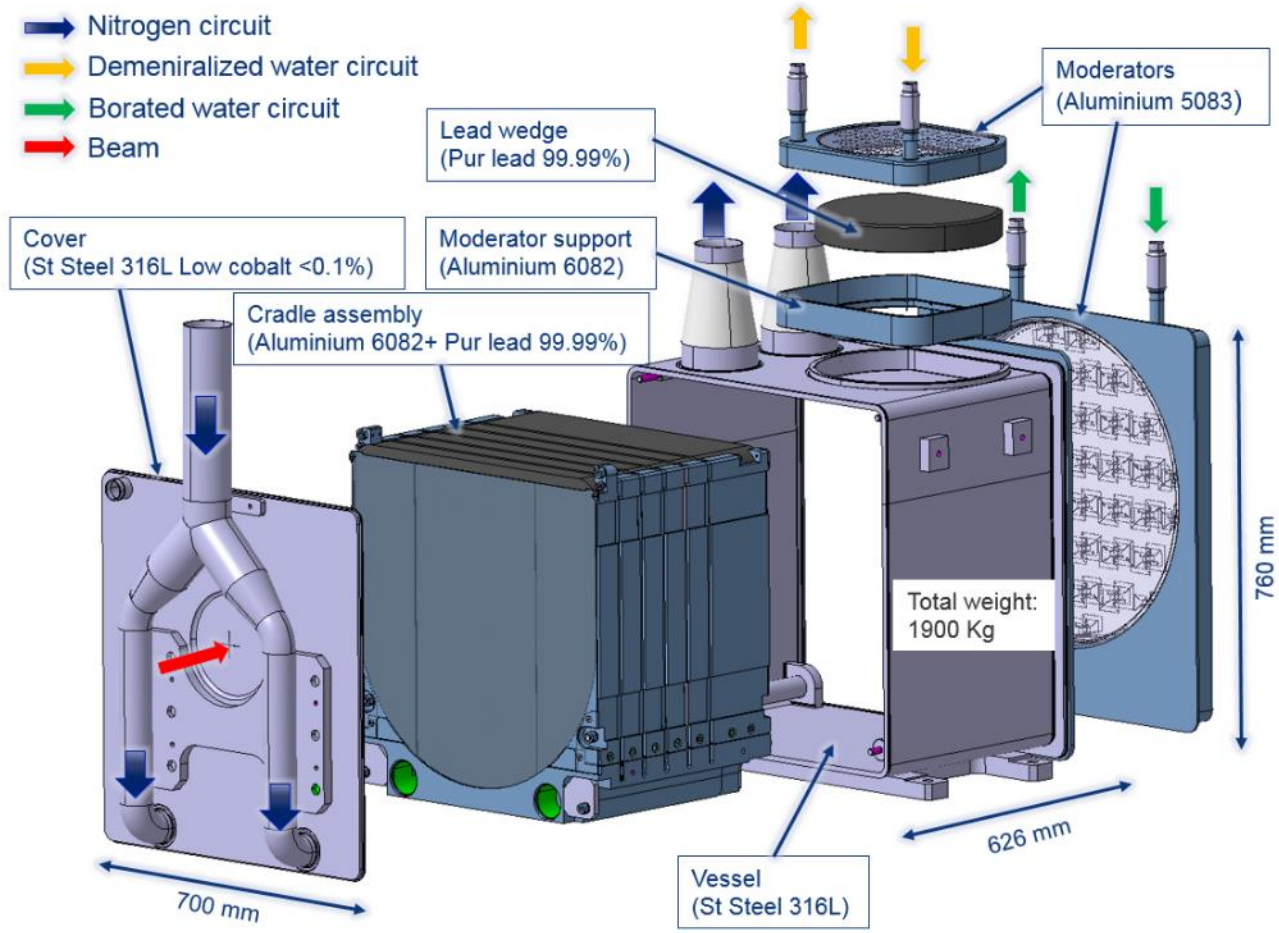


courtesy of Oliver Aberle, CERN

# n_TOF @ CERN: 3rd-generation target

| | |
|---|---|
| proton beam momentum | 20 GeV/c |
| intensity (dedicated mode) | 7 x $10^{12}$ protons/pulse |
| repetition frequency | 1 pulse/1.2s |
| pulse width | 6 ns (rms) |
| n/p | 300 |
| lead target dimensions | 70x76x63 $cm^3$ |
| cooling & moderation material | $N_2$ & $H_2O$ (borated) |
| moderator thickness in the exit face | 5 cm |
| neutron beam dimension in EAR-1 (capture mode) | 2 cm (FWHM) |

CERN

nTOF

# n_TOF @ CERN

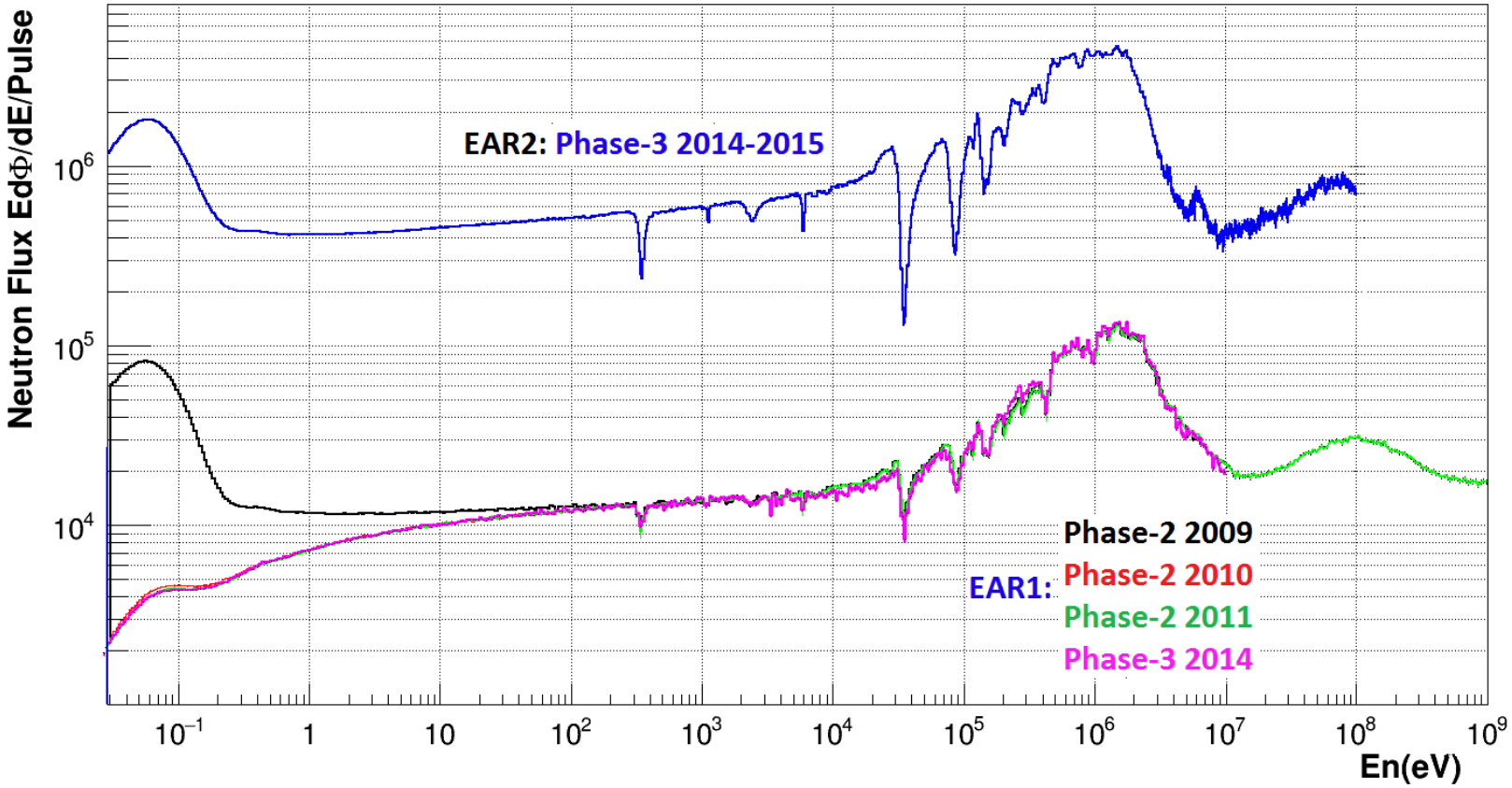


1 meV < $E_n$ < 1 GeV

$\Delta E/E \sim 10^{-4}$ @ EAR1

# Detectors & Physics at n_TOF

## WARNING

Physics & detection systems are mixed in this presentation.

Some of the detection systems are simple, other are complex. Therefore, some of the slides are simple, other are full of infos which I will not be able to explain in details.

Please refer to my slides for details, for references and (hyper)links.

# SiMON: Silicon monitors

based on the $^{6}Li(n,t)^{4}He$ reaction

~ 600 $\mu g/cm^2$ $^{6}LiF$

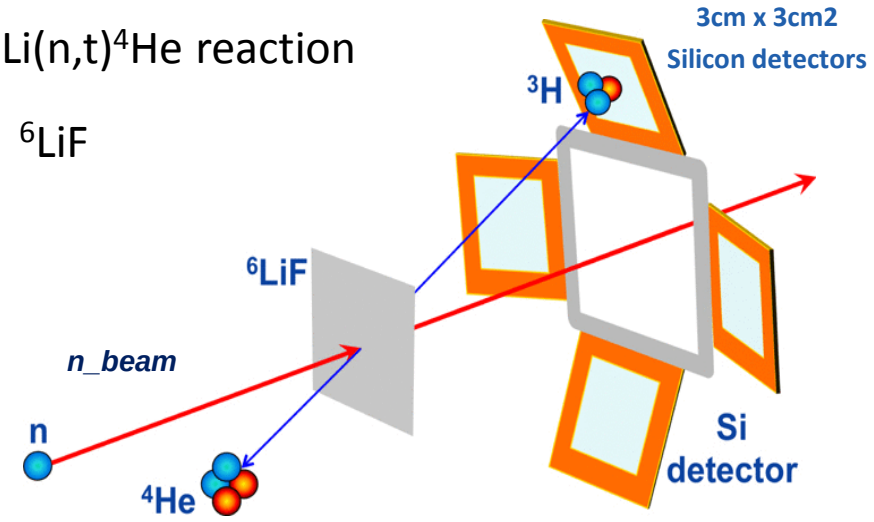



Eur. Phys. J. A (2017) **53**: 210

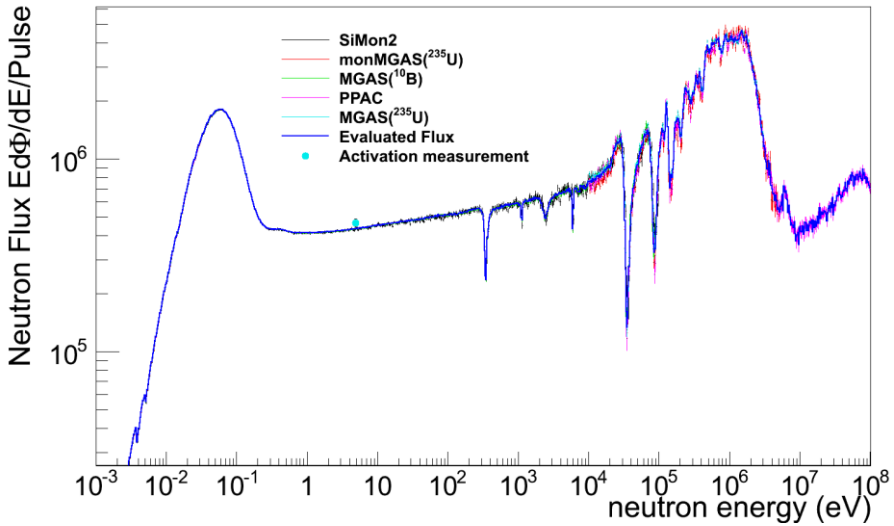


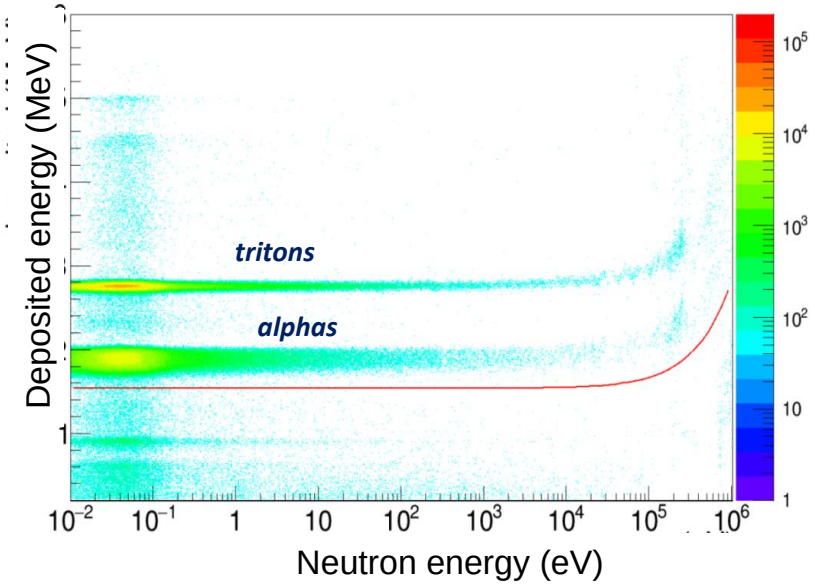

# $^{235}$U(n,f) relative $^{6}$Li(n,t) and $^{10}$B(n,α) standards

**six silicon detectors** (single 5x5 cm$^2$) **and six samples** (two for each material) all larger than the neutron beam width, in **forward/backward configuration**

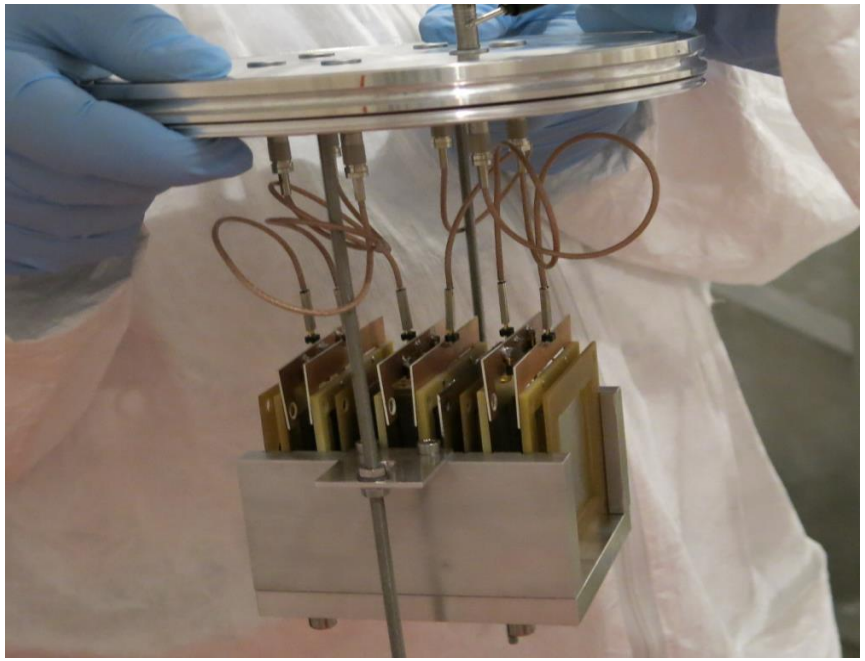

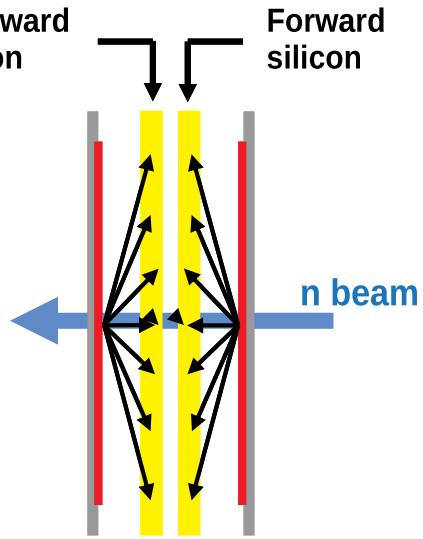


| Material | Enrichement | Size (mm) | Thickness | Atoms/cm$^2$ | Backing |
|---|---|---|---|---|---|
| LiF | 95% $^{6}$Li | □ 47 × 47 | 1.89 (3) $\mu$m | $1.14 \cdot 10^{19}$ | 50 $\mu$m |
| $B_4C$ | 100% $^{10}$B | □ 70 × 70 | 0.08 (5) $\mu$m | $8.28 \cdot 10^{17}$ | 18 $\mu$m |
| $H_2O_2U$ | 99.93% $^{235}$U | ⊘ 40 | 0.145 (16) $\mu$m | $6.18 \cdot 10^{17}$ | 250 $\mu$m |


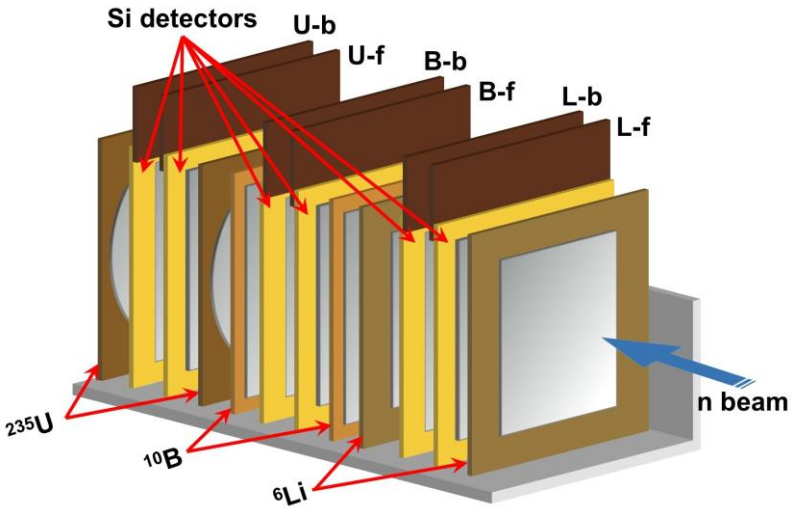


S Amaducci et al. (The n_TOF Collaboration), EPJA 56, 120 (2019)

# $^{235}$U(n,f) relative $^{6}$Li(n,t) and $^{10}$B(n,α) standards

Eur. Phys. J. A (2019) **55**: 120



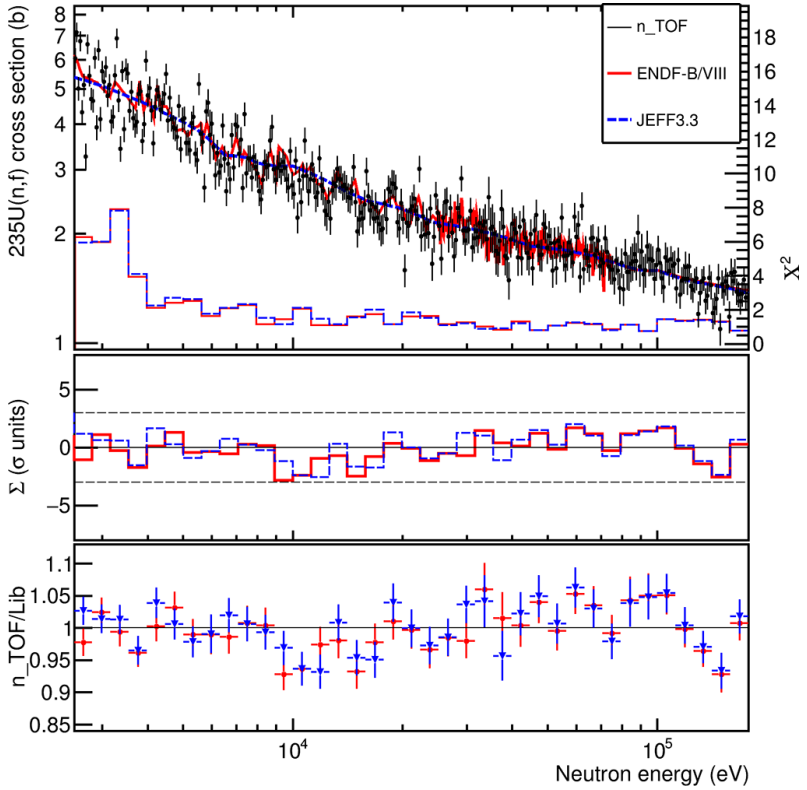


**Fig. 19.** $^{235}$U(n, f) measured cross section of this work, in the 2–100 keV neutron energy range (with $\chi^2$, $\Sigma$ and ratio), compared to the ENDF-B/VIII and JEFF3.3 evaluations.

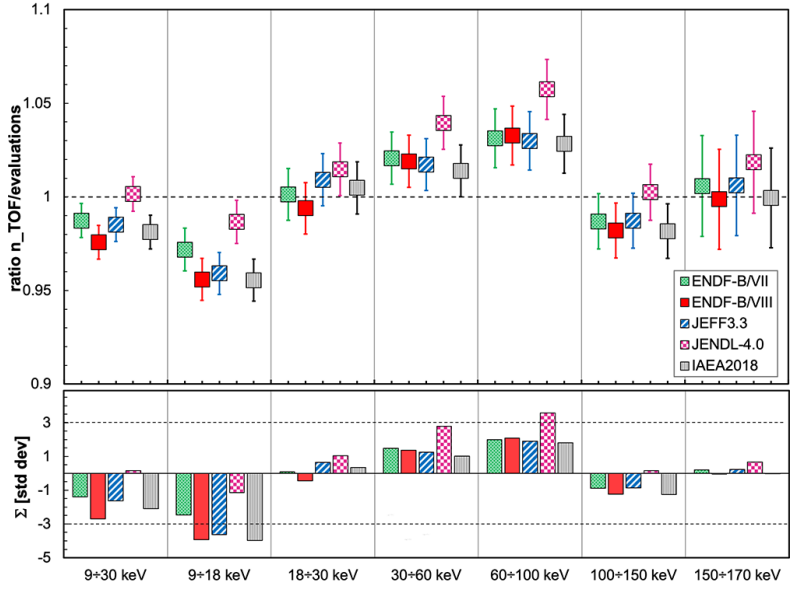


**Fig. 20.** Top panel: ratio between the measured cross section, integrated in a few relevant intervals, and the corresponding values for the five reference libraries ENDF-B/VII, ENDF-B/VIII, JEFF3.3, JENDL-4.0, IAEA. Bottom panel: the corresponding normalized deviation $\Sigma$ (standard deviation units).

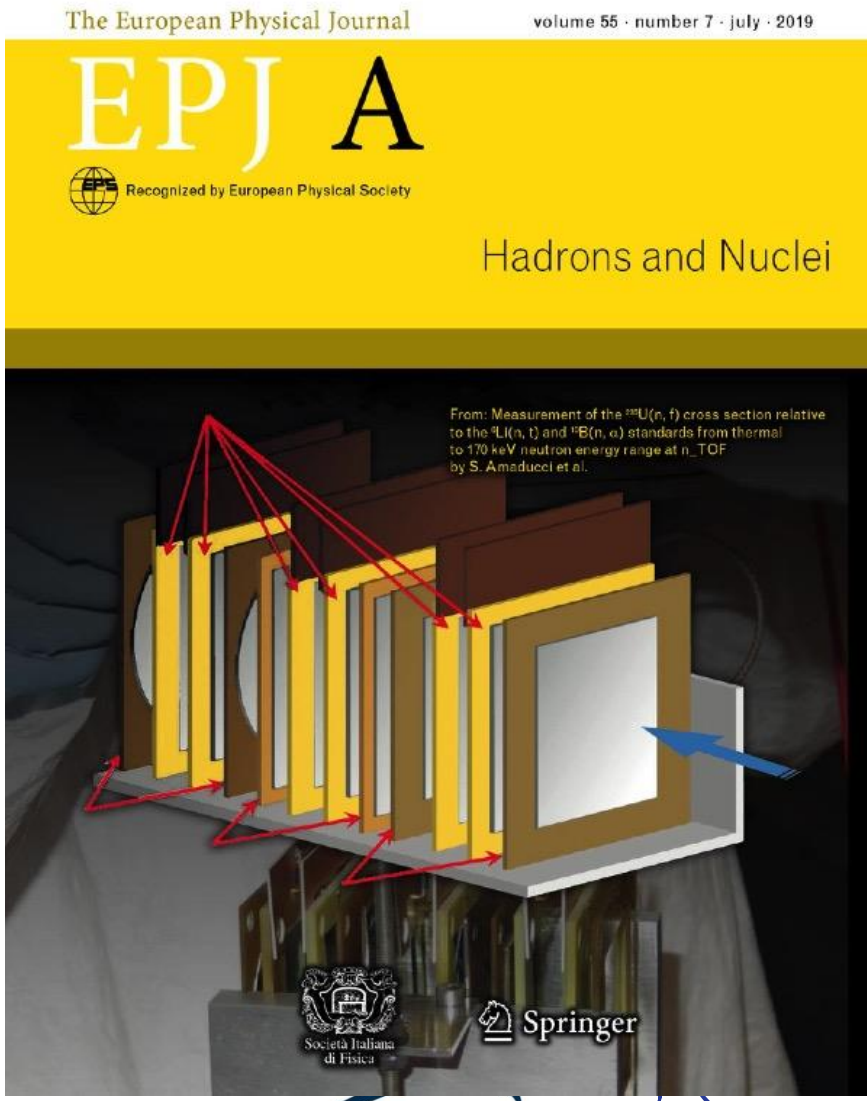


Main result: $^{235}$U(n,f) cross section itself adopted in the IAEA Standards database

# The n_TOF neutron beam profile with Micromegas detectors

@186 m from the spallation target
~ 2 cm neutron beam diameter

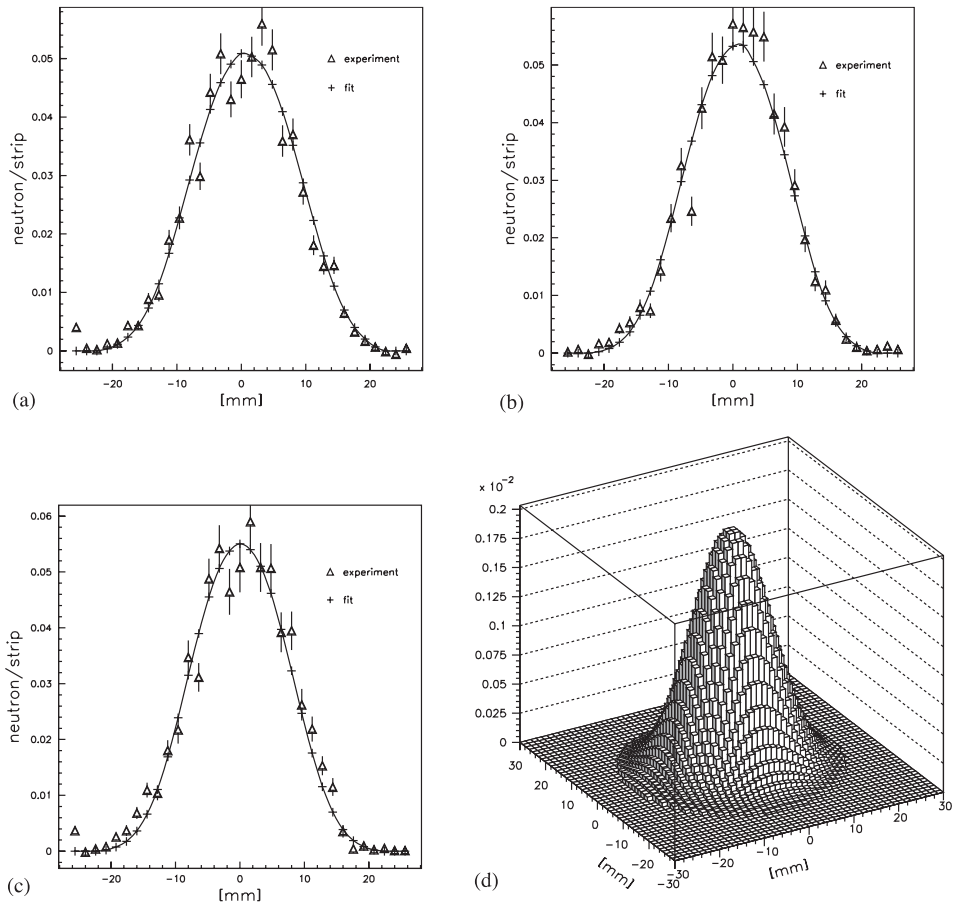


Fig. 10. Horizontal (a), vertical (b), 30° (c) experimental and analytic projected profiles between 100 keV and 1 MeV at 186 m and corresponding beam profile (d) for one bunch of $7 \times 10^{12}$ protons.

J Pancin et al. (The n_TOF Collaboration), NIMA, 524, 102 (2004)

# Micromegas (micro-mesh gaseous structure) detector

Parallel plate avalanche gaseous detector consisting of two regions:
the **conversion** and the **narrow amplification region**

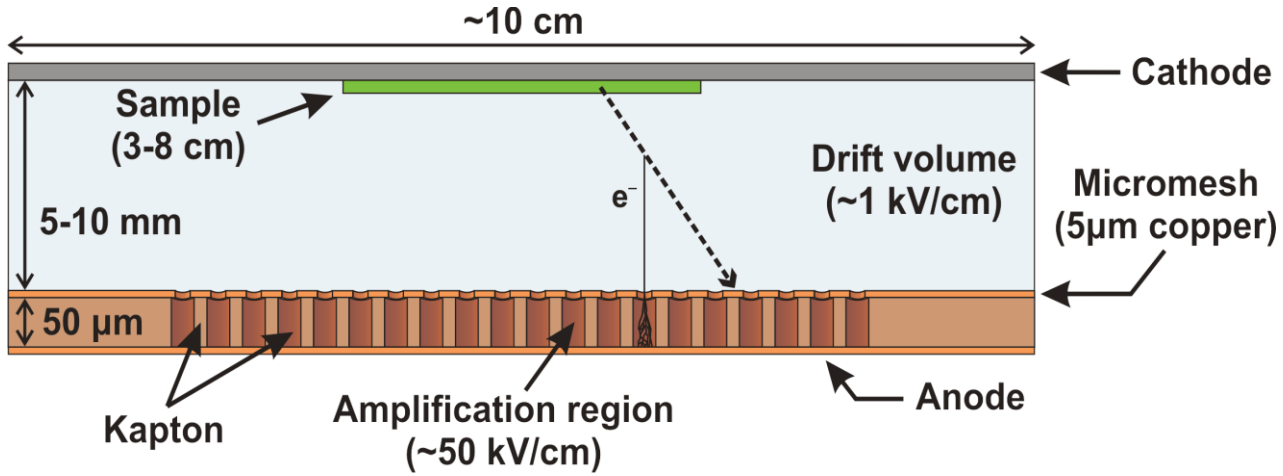


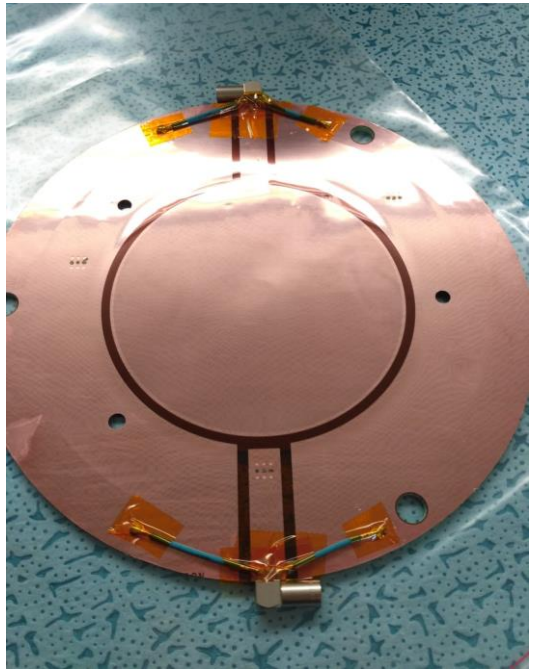

Mesh


Anode

**Advantages-Characteristics:**

- Minimal material (almost ”transparent” for neutrons)
- High detection efficiency (100% in fission studies)
- Radiation durability - important when highly radioactive samples (e.g. actinides) are used
- Fast response & time resolution

**Used (and to be used in):**

- (n,f) and (n,cp) reaction studies

# The n_TOF neutron beam profile with XY Micromegas detectors

From the CERN Axion Solar Telescope (CAST)

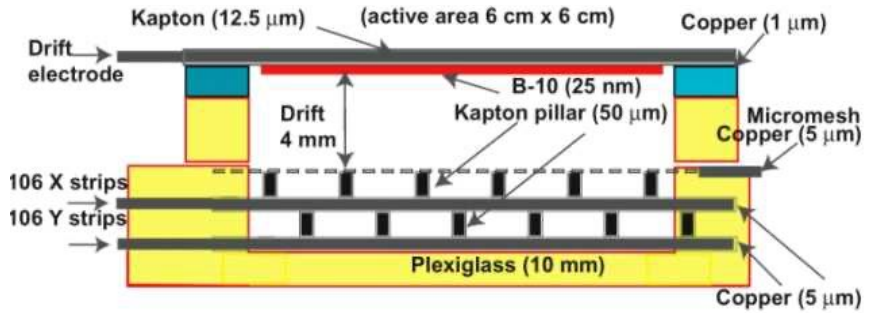


Fig. 1. (Color online) Schematic view of the X-Y MicroMegas "bulk" principle.

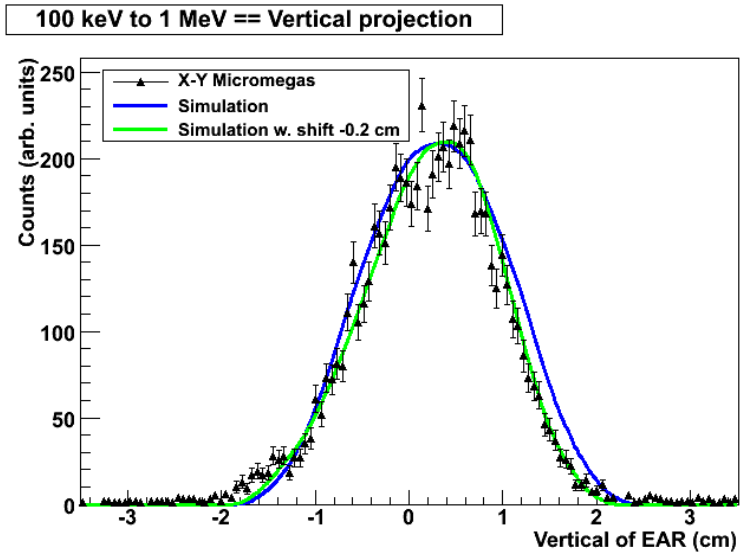


Fig. 6. (Color online) Vertical neutron beam profile at 185 m from the Lead spallation target for neutron energy between 100 keV and 1 MeV.

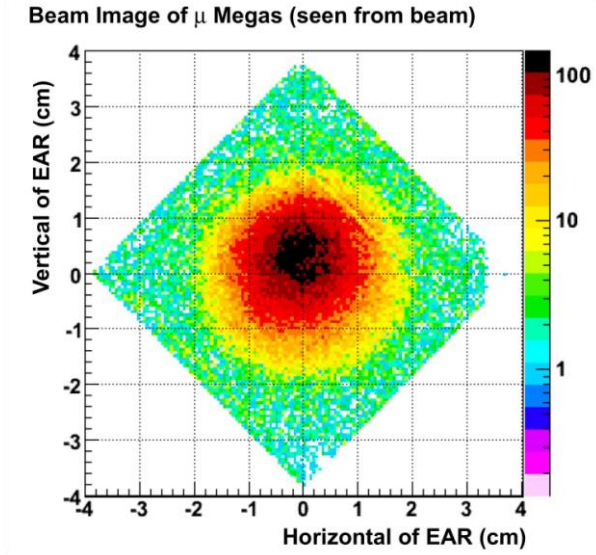


Fig. 5. (Color online) Neutron beam image at 185 m from the spallation target (EAR is the n_TOF Experimental Area).

S Andriamonje et al. (The n_TOF Collaboration), Journal of the Korean Physical Society **59**, 1601 (2011)

# TIMEPIX as beam monitor at n_TOF

2-Quad Timepix has been used for beam alignment and will be used for flux measurement in Phase-2021

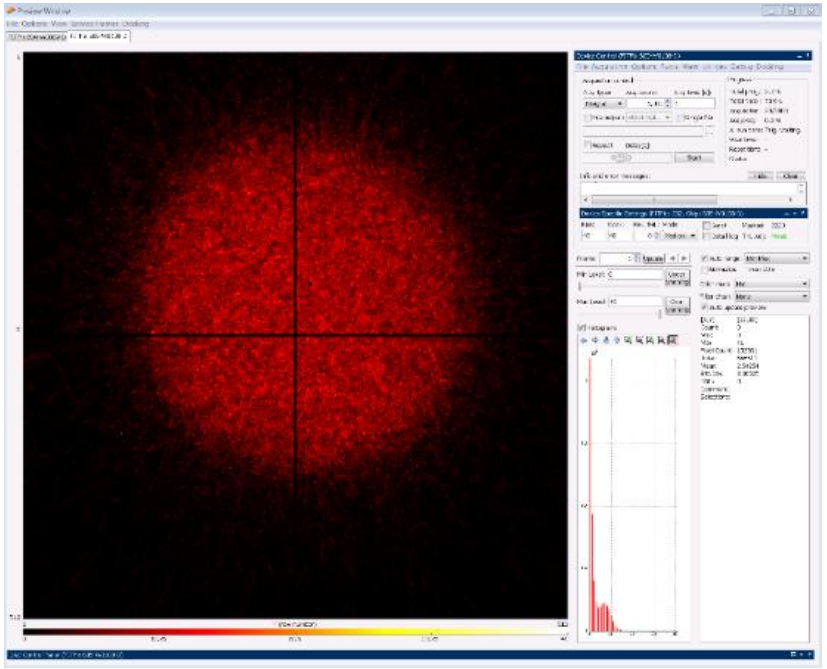

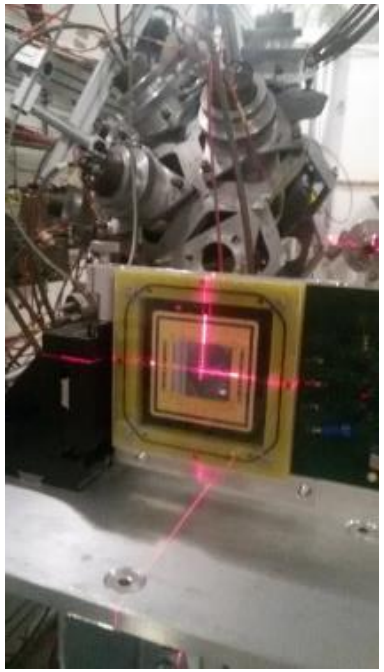

EAR1

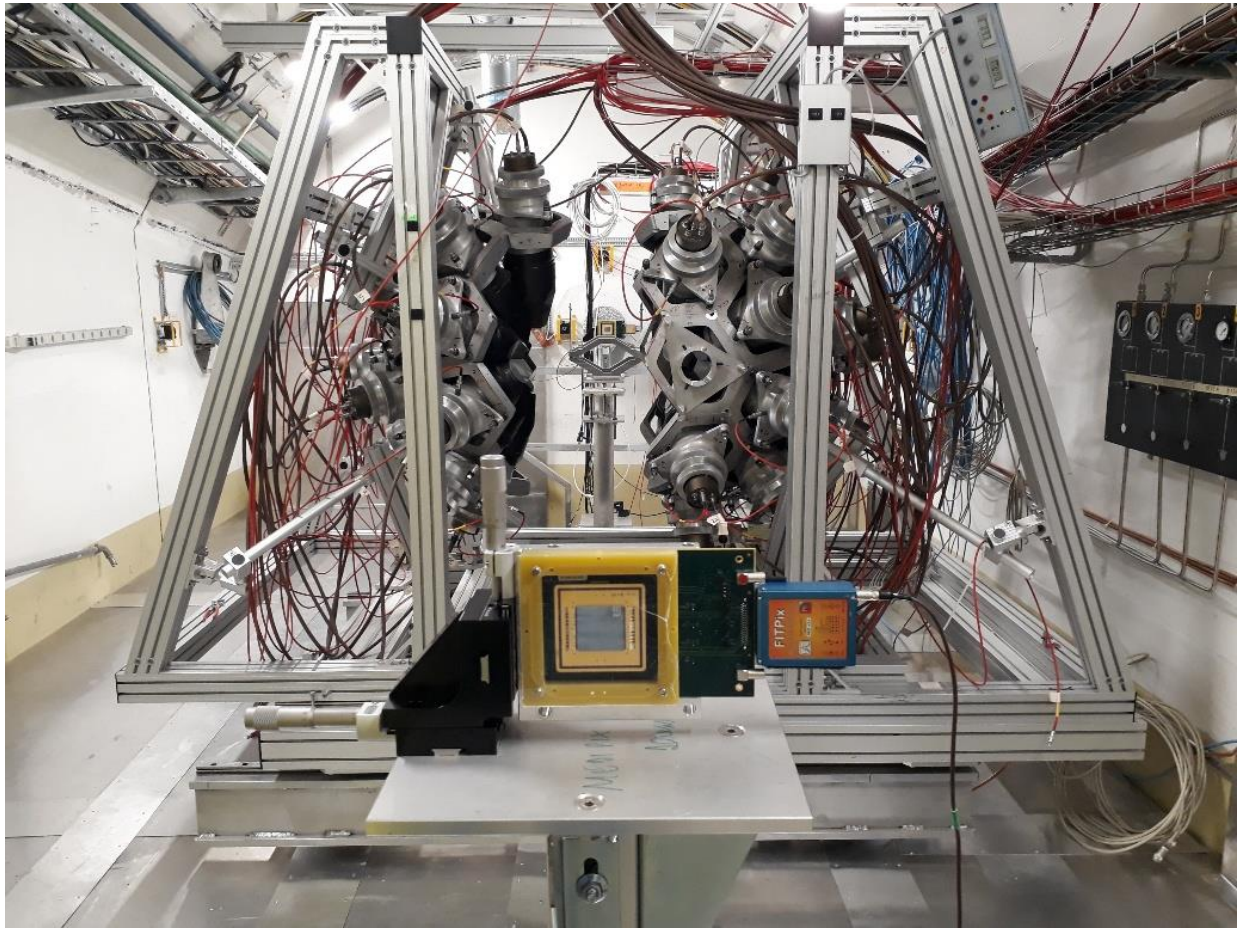

# What we really do at n_TOF

1. Nuclear astrophysics

2. Advanced nuclear technologies

3. Basic nuclear science & applications

# Big bang nucleosynthesis

**time:** **0.5 s – 200 s**

thermal equilibrium $n_n/n_p = e^{-Q/kT}$ up to T ~ 10 GK

~ 1/7 at T ~ 1 GK

**time:** **200 s – a few min**

nucleosynthesis of d, $^{3}$He, $^{4}$He and $^{6,7}$Li

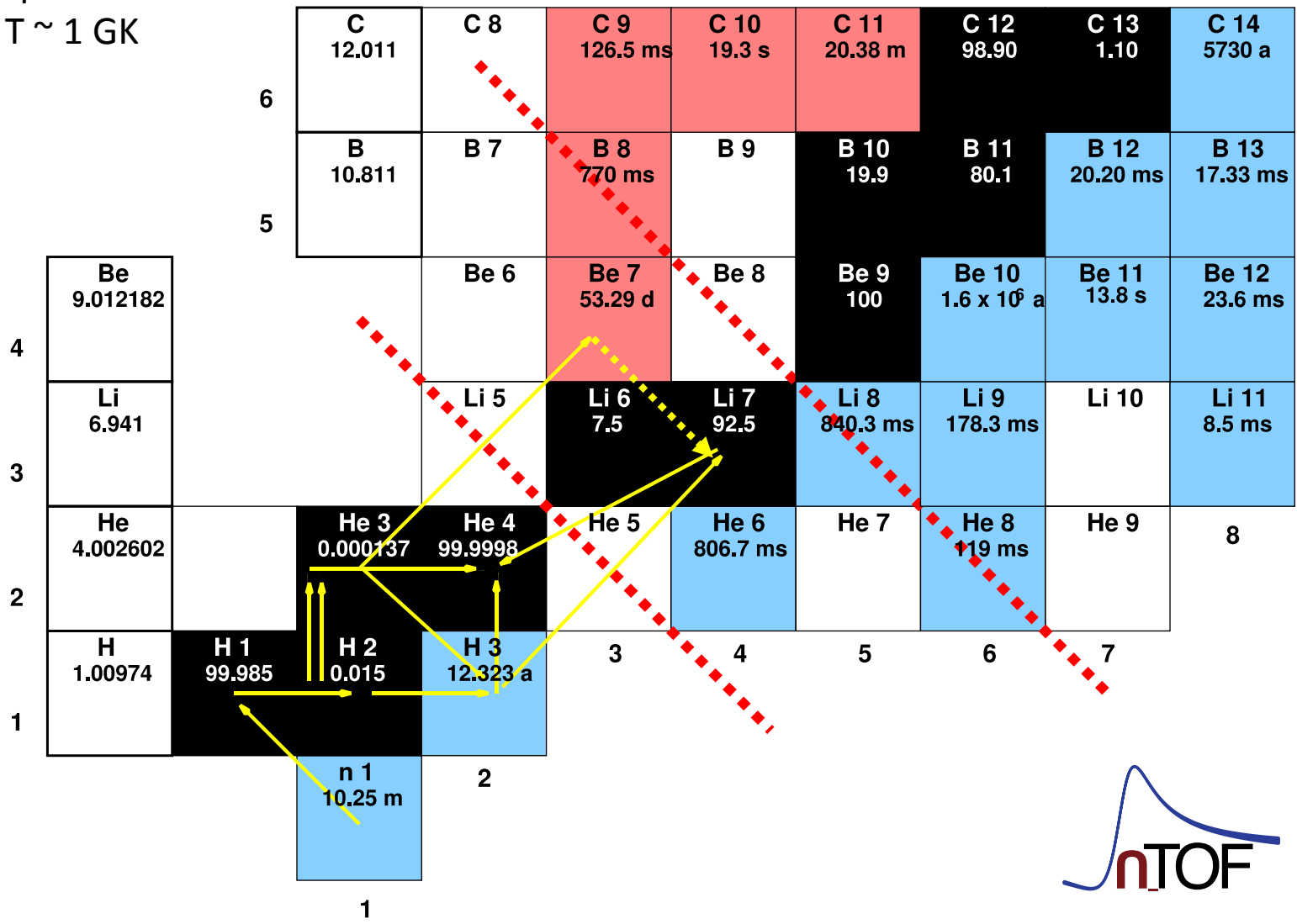

# Big bang nucleosynthesis

$^4He$

$Y_p = 0.245 \pm 0.004$

not measurable in stars, emission lines from gaseous nebulae in dwarf galaxies, with low metallicity

$^2H$

$D/H = (2.53 \pm 0.04) \times 10^{-5}$

from quasar absorption lines (nearly unprocessed gas)

$^3He$

Difficult to measure in unevolved objects + uncertain chemical evolution
less useful as an observational test

$^7Li$

$^7Li/H=(1.6 \pm 0.3) \times 10^{-10}$

from metal-poor stars in the Galactic halo
constant Li/H as function of metal content
interpreted as primordial

# Metal-poor stars

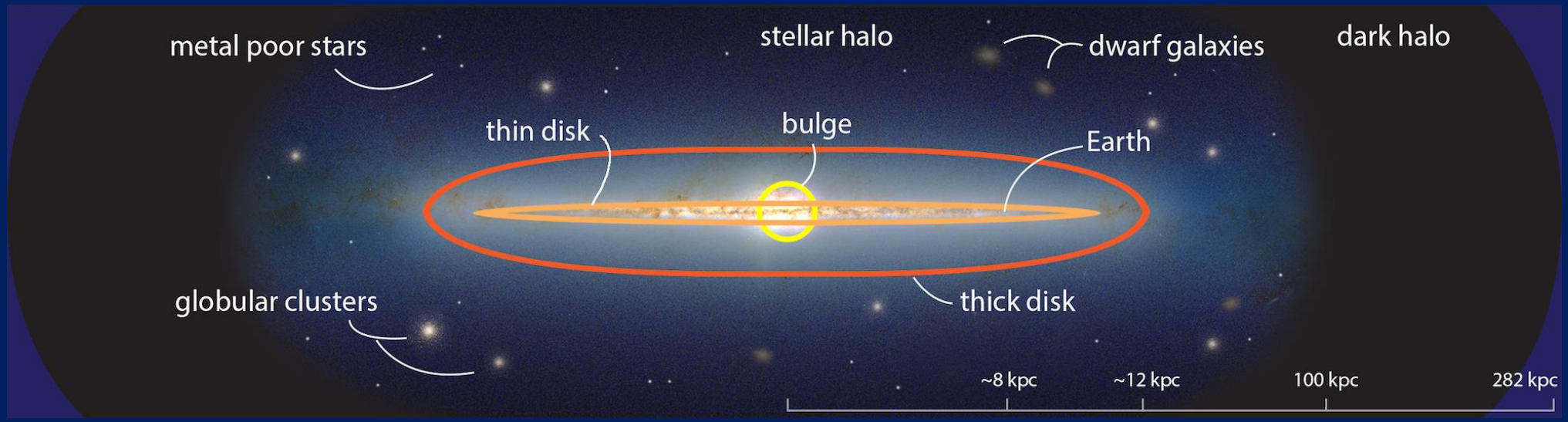


1 kpc = 3 x $10^{19}$ m = 3260 light-years

# Big bang nucleosynthesis: CLiP

Best value from observations:
[Li/H] = 1.6 $\pm$ 0.3

Expected from CMB analysis and standard BBN

[Li/H] = 4.45 $\pm$ 0.05

Expected from standard BBN
$Y_p$ and D abundance concordance

3.9 $\leq$ [Li/H] $\leq$ 5.3

[ ] : $10^{-10}$

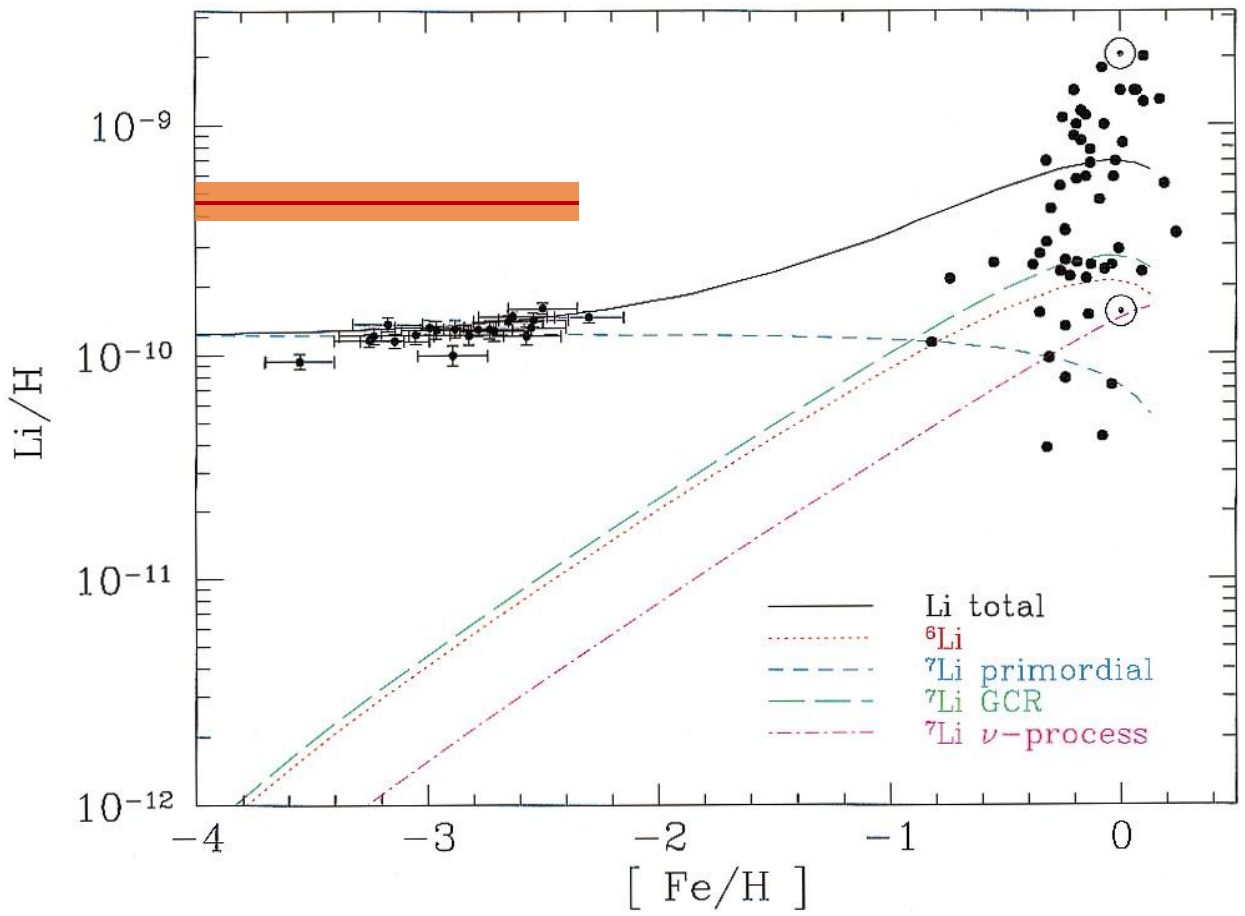


Contributions to the total predicted lithium abundance from the adopted GCE model of Fields & Olive (1999a, 1999b), compared with low metallicity stars (RNB) and high-metallicity stars (Lambert, Heath, & Edvardsson 1991). The solid curve is the sum of all components.

S G Ryan et al. ApJ 530 (2000) L57

BD Fields et al., PDG Review (2016)

# Big bang nucleosynthesis: CLiP

**time:** **0.5 s – 200 s**

thermal equilibrium $n_n/n_p = e^{-Q/kT}$ up to T ~ 10 GK

~ 1/7 at T ~ 1 GK

**time:** **200 s – a few min**

nucleosynthesis of d, $^{3}$He, $^{4}$He and $^{6,7}$Li

## $^{7}$Be(n,p)

L A Damone et al. (The n_TOF Collaboration)
Phys. Rev. Lett. **121** (2018) 042701

## $^{7}$Be(n,$\alpha$)

M Barbagallo et al. (The n_TOF Collaboration)
Phys. Rev. Lett. **117** (2016) 152701

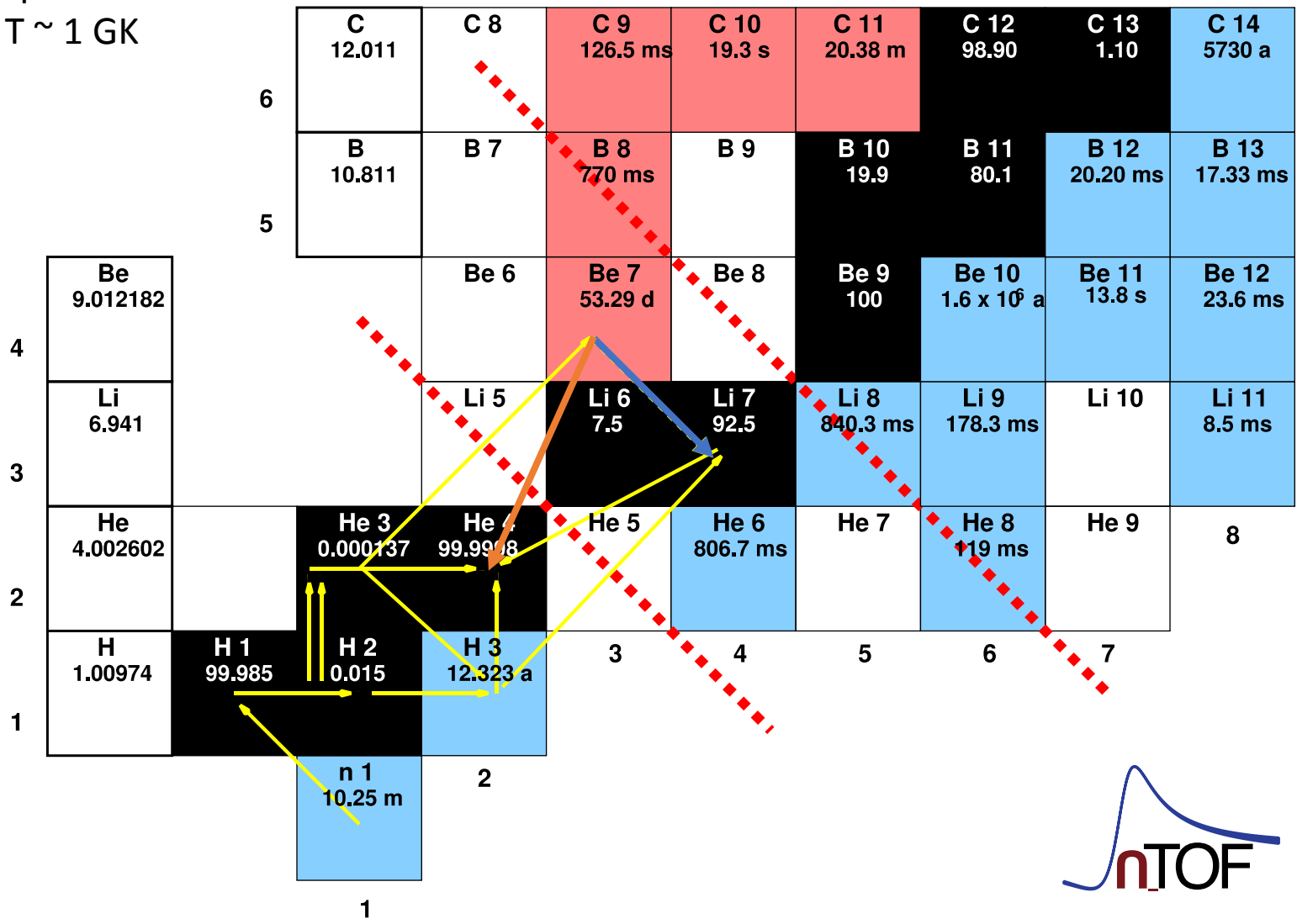

# $^{7}Be(n,\alpha)^{4}He$

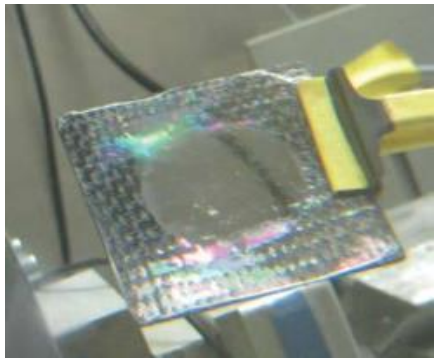

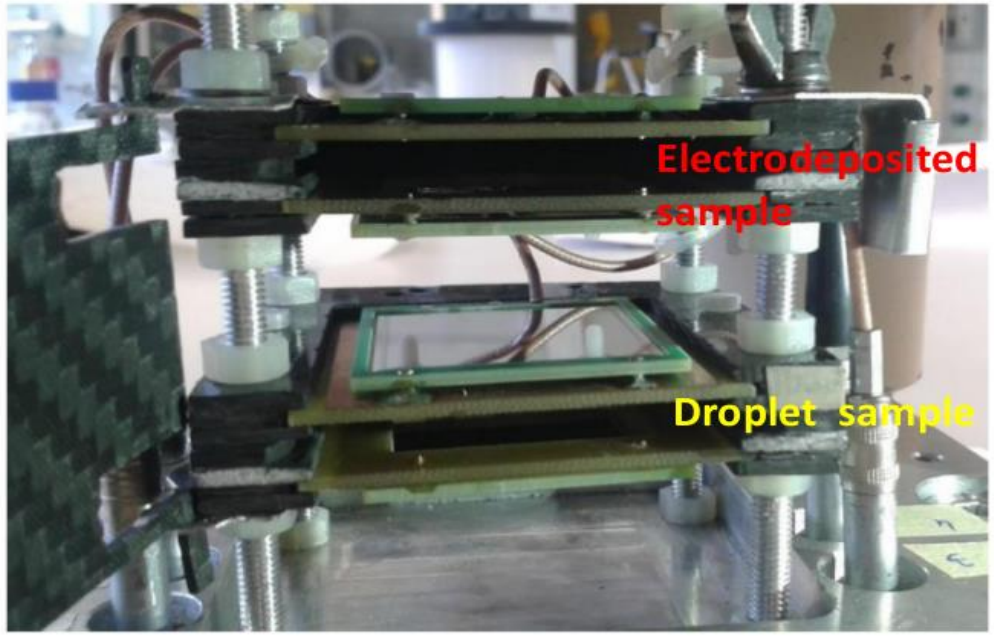


Silicon detectors insterted directly into the neutron beam
3x3 $cm^2$ active area, 140 µm thickness
Two samples with ~18 GBq activity each (~1.4 µg of $^{7}Be$)

L. Cosentino et al. (n_TOF Collaboration), NIM A 830 (2016) 197-205

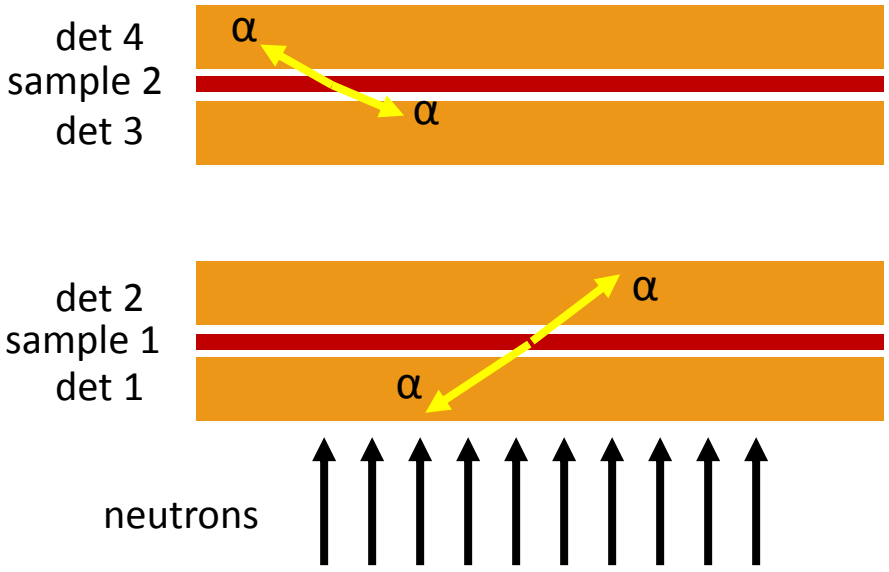


Strong rejection of BG events due to tof,
low duty-cycle, coincidence signals for:

- protons from the (n,p) channel
- γ from $^{7}Be$ activity
- $n+^{7}Li \rightarrow {}^{8}Li\ (\beta^{-})\ 840\ ms \rightarrow {}^{8}Be^{*} \rightarrow 2\alpha$

# $^{7}Be(n,\alpha)^{4}He$

**PSI hot-cell**

Two samples with ~18 GBq activity each (~1.4 µg of $^{7}Be$)

- electrodeposition on a 5-µm-thick Al foil
- droplet deposition on a 0.6-µm-thick low-density polyethylene foil
- Both $^{7}Be$ samples were prepared at PSI, starting from a 200 GBq solution extracted from the spallation target of the SINQ source, as $Be(NO_3)_2$ solution


E. Maugeri *et al.* (The n_TOF Collaboration), Nucl. Instr. and Meth. A **889** (2018) 138
M. Barbagallo *et al.* (The n_TOF Collaboration), Nucl. Instr. and Meth. A **887** (2018) 27-3

# $^{7}Be(n,p)^{4}He$

A three-step experiment:

- Extraction of 200 GBq from water cooling of SINQ spallation source at PSI
- Implantation of the 30 keV (~45 nA) $^{7}Be$ beam on suited backing using **ISOLDE-GPS separator and RILIS**
- Measurement at n_TOF-EAR2 using a silicon telescope (20 and 300 mm, 5x5 $cm^2$ strip device)

**PSI hot-cell**

**ISOLDE - GLM**

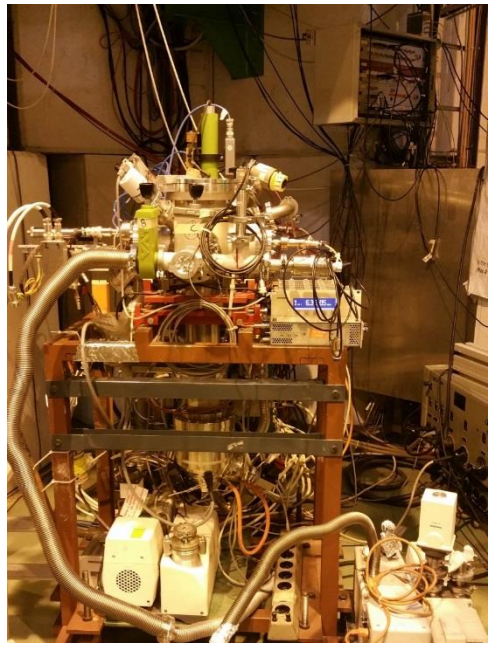

**n_TOF EAR2**

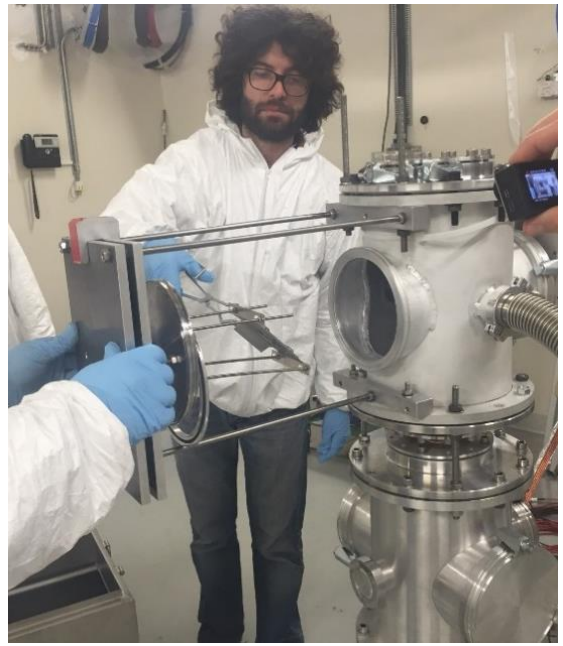

E. Maugeri *et al.* (The n_TOF Collaboration), Nucl. Instr. and Meth. A **889** (2018) 138
M. Barbagallo *et al.* (The n_TOF Collaboration), Nucl. Instr. and Meth. A **887** (2018) 27-3

# $^{7}Be(n,p)^{4}He$

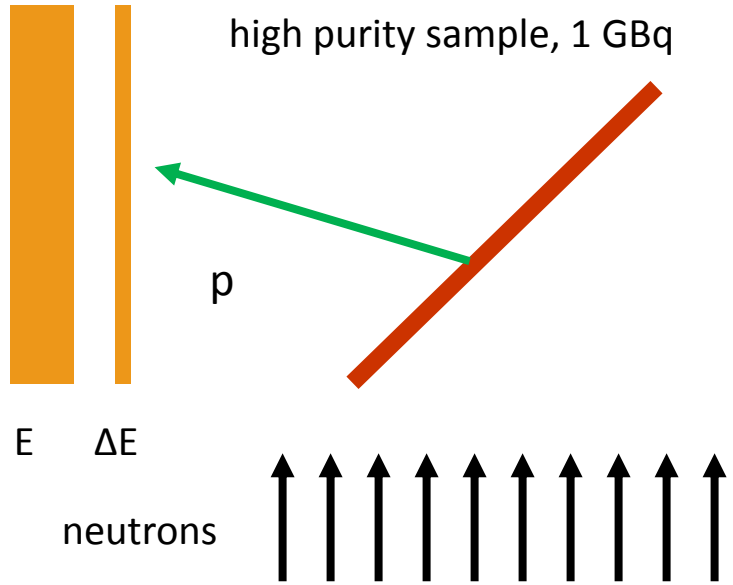


Silicon telescope from Lodz Uni. 20 $\mu$m and 300 $\mu$m thickness for $\Delta$E-E detectors
Detection and identification of protons of 1 and 1.4 MeV

L A Damone et al. (The n_TOF Collaboration)
Phys. Rev. Lett. **121** (2018) 042701

## Results

The new estimate of the $^{7}Be$ destruction rate based on the new results yield a decrease of the predicted cosmological Lithium abundance, but **insufficient to provide a viable solution to the CLiP**

The two n_TOF measurements can finally rule out neutron-induced reactions, and possibly Nuclear Physics, as a potential explanation of the CLiP, leaving all alternative physics and astronomical scenarios still open

# Stellar nucleosynthesis

# The s-process

The lifetime of a nucleus against (n,$\gamma$) is:

$$\tau_{n,\gamma} = \frac{1}{N_n \langle \sigma_{n,\gamma}\, v \rangle_{kT}}$$

For $kT \sim 30\ keV$ and $\sigma_{n,\gamma} \sim 100\ mb$ it is

$$\tau_{n,\gamma} \sim \frac{10^9}{N_n} \text{ years}$$

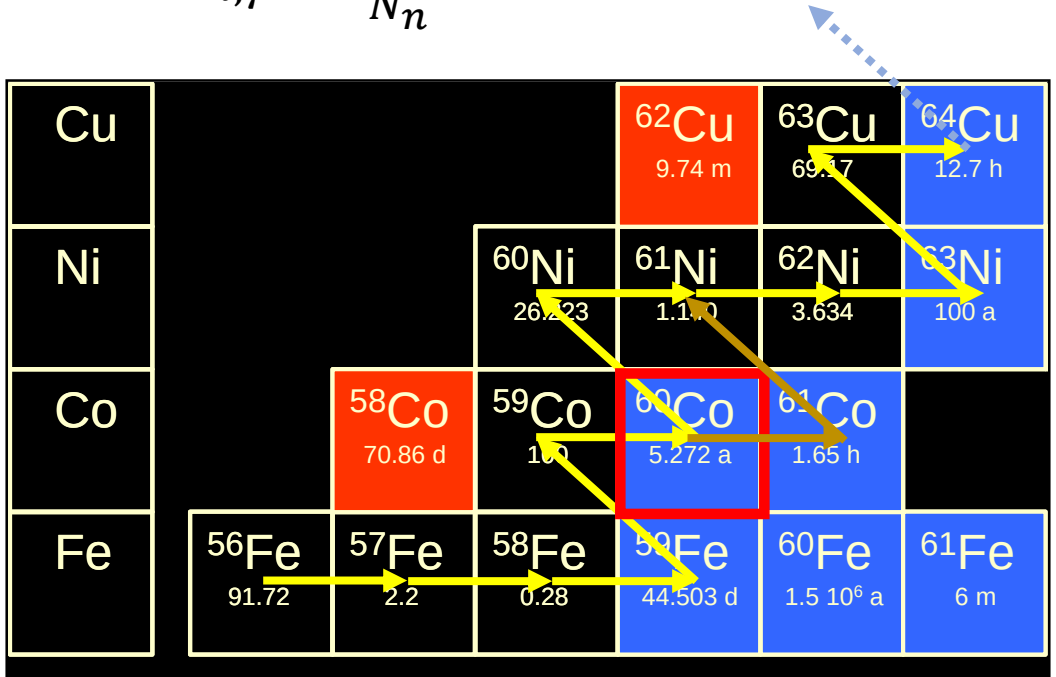


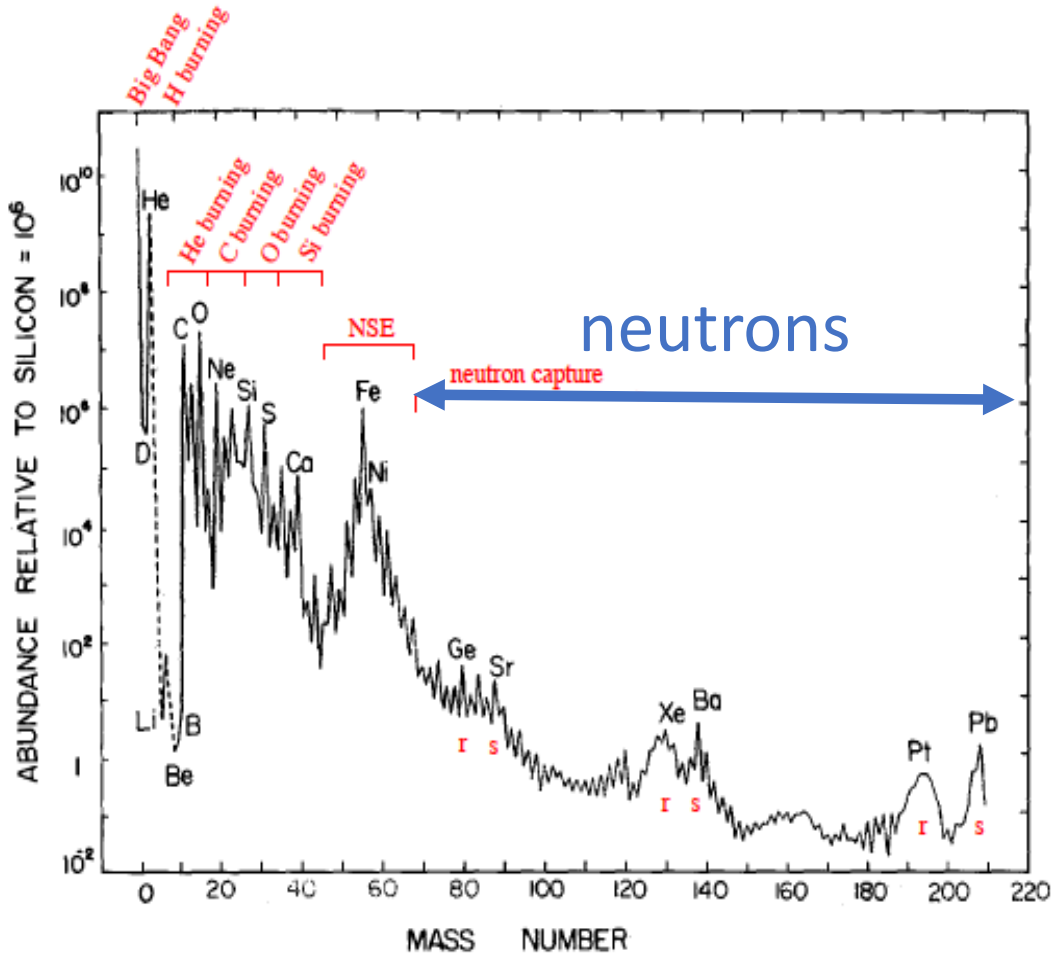


Figure 1.1: The 'local galactic' abundance distribution of nuclear species, as a function of mass number $A$. The abundances are given relative to the Si abundance which is set to $10^6$. Peaks due to the $r$- and $s$-process are indicated. It is the main aim of this course to provide an understanding of this figure. Adapted from Cameron (1982).

# The s-process

$$\langle \sigma_{n,\gamma} \rangle_{kT} \times N_A = \text{const.}$$

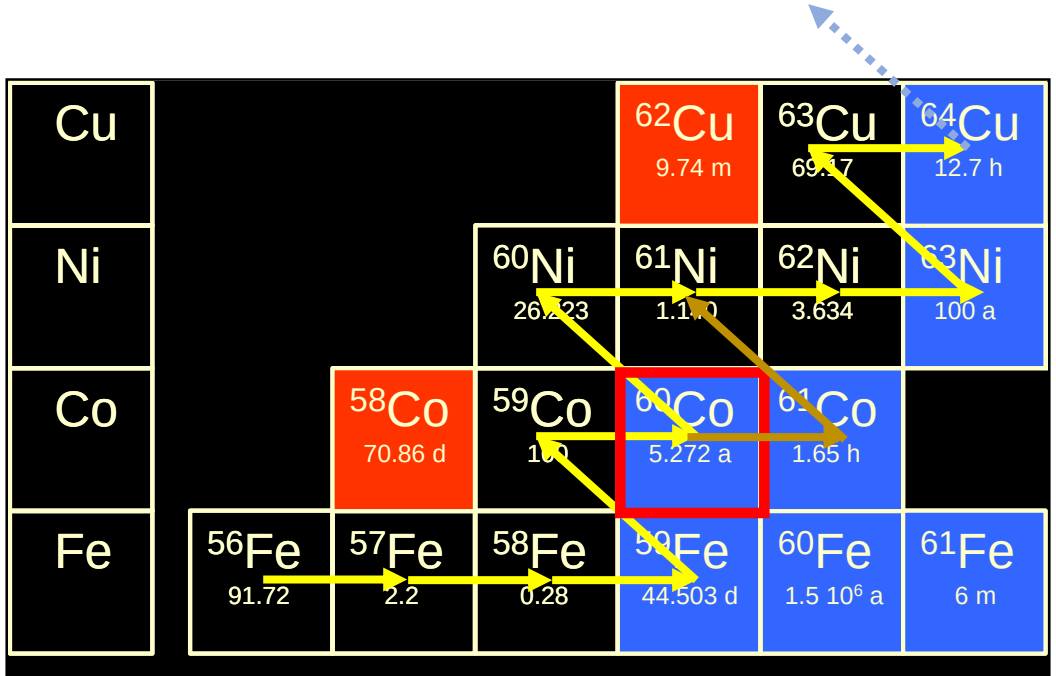


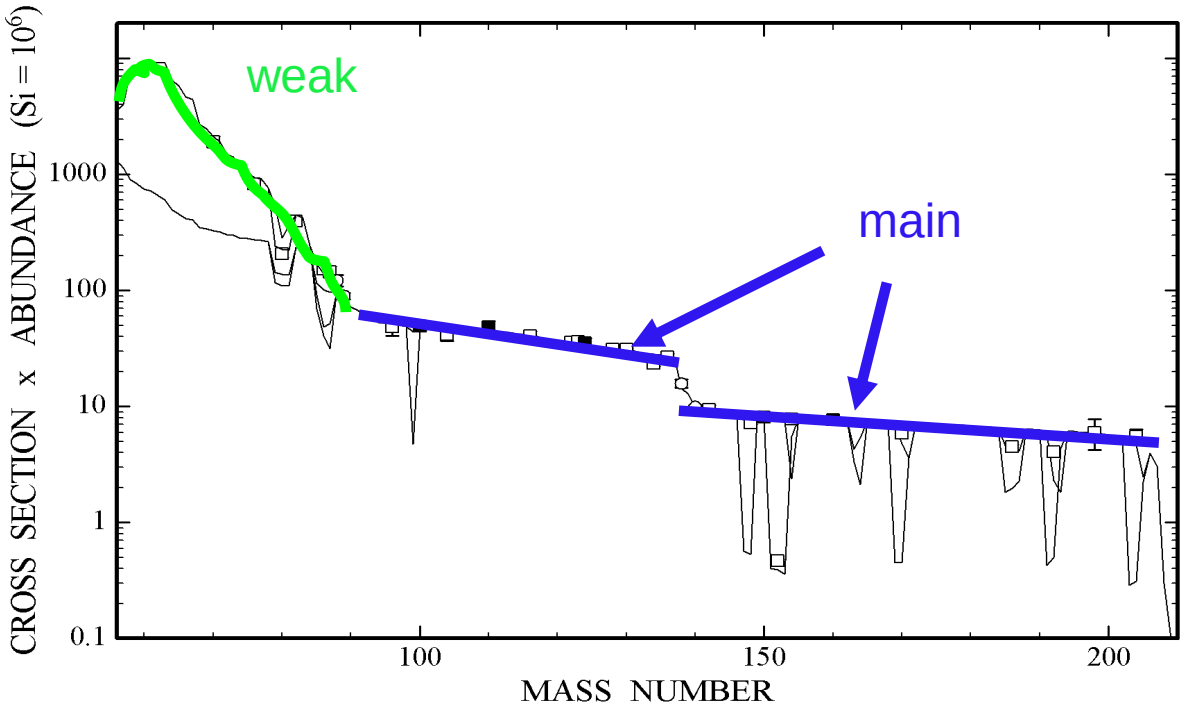


F Käppeler (Prog. Part. Nucl. Phys. 43, 1999)

# The $C_6D_6$ Total Energy Detectors (TED): (n,$\gamma$)

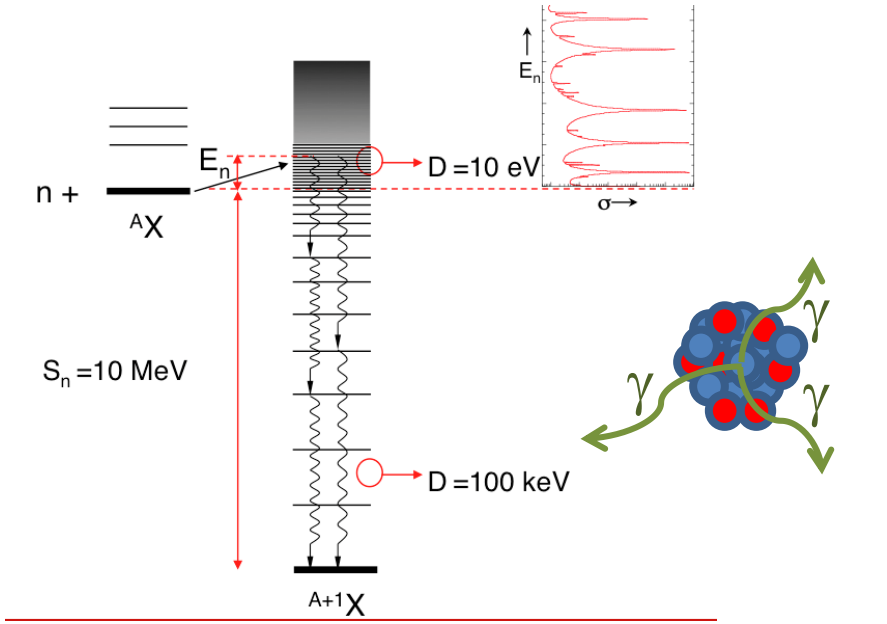


**Efficiency to detect a cascade UNKNOWN: depends on the cascade path**

# The $C_6D_6$ Total Energy Detectors (TED): (n,$\gamma$)

**TED: Based in two principles**

- **Condition I : Low efficiency detectors** $\varepsilon_{\gamma i}<<1$

  Detecting a cascade: $\varepsilon_c=1-\Pi(1-\varepsilon_{\gamma i}) \approx \sum \varepsilon_{\gamma i}$

- **Condition II: The efficiency is proportional to $E_\gamma$**

$\varepsilon_{\gamma i} \propto E_{\gamma i}$

$$\varepsilon_c = k \sum_{i=1} E_{\gamma i} = kE_c$$

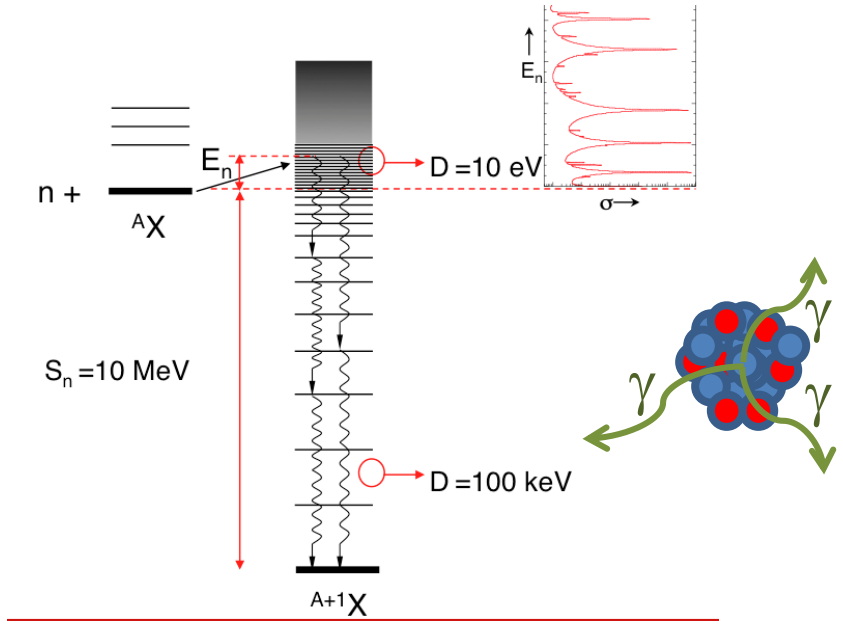


**Efficiency independent of the cascade path**

# The $C_6D_6$ Total Energy Detectors (TED): (n,$\gamma$)

**TED: Based in two principles**

- **Condition I : Low efficiency detectors** $\varepsilon_{\gamma i}<<1$

  Detecting a cascade: $\varepsilon_c=1-\prod(1-\varepsilon_{\gamma i}) \approx \sum \varepsilon_{\gamma i}$

- **Condition II: The efficiency is ~~proportional~~ to $E_\gamma$**

~~$\varepsilon_{\gamma i} \propto E_{\gamma i}$~~

~~$\varepsilon_c = k \sum_{i=1} E_{\gamma i} = kE_c$~~

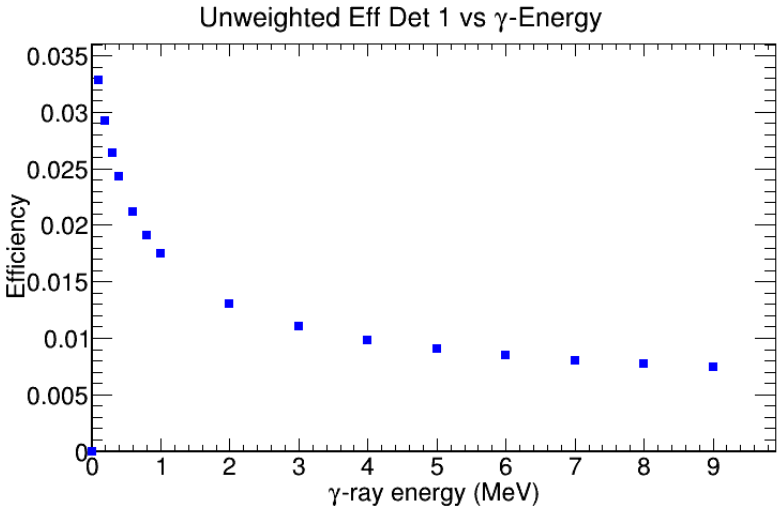


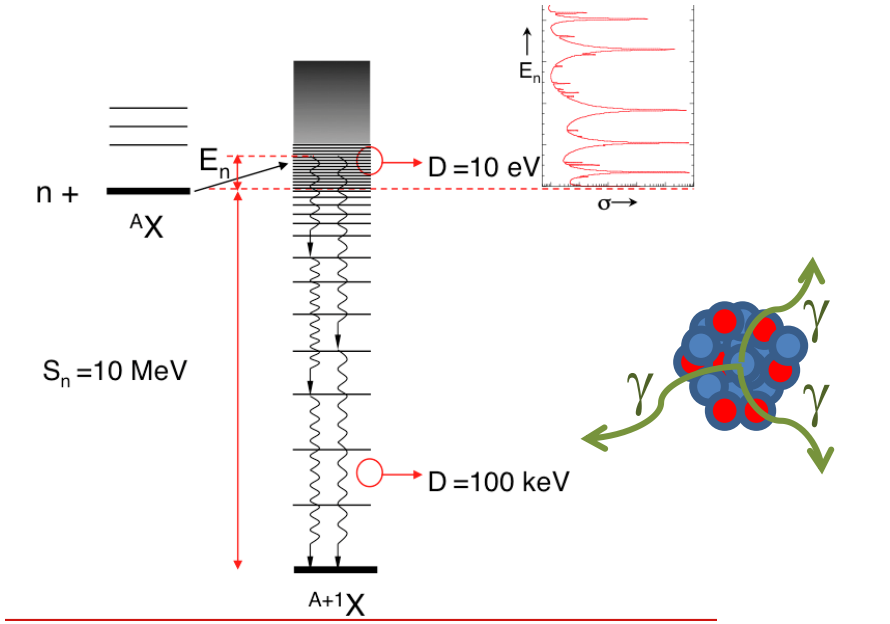


**Efficiency to detect a cascade UNKNOWN: depends on the cascade path**

# The $C_6D_6$ Total Energy Detectors (TED): (n,$\gamma$)

**TED: Based in two principles**

- **Condition I : Low efficiency detectors** $\varepsilon_{\gamma i}<<1$

  Detecting a cascade: $\varepsilon_c=1-\Pi(1-\varepsilon_{\gamma i}) \approx \sum \varepsilon_{\gamma i}$

- **Condition II: The efficiency is ~~proportional~~ to $E_\gamma$**

~~$\varepsilon_{\gamma i} \propto E_{\gamma i}$~~

~~$\varepsilon_c = k \sum_{i=1} E_{\gamma i} = kE_c$~~

**Solution: Give to each signal a amplitude-dependent weight: PHWT**

**After PHWT:**

$(\varepsilon_c)_{\text{Weighted}} = \sum_i E_{\gamma i} = E_c = S_n + E_n$

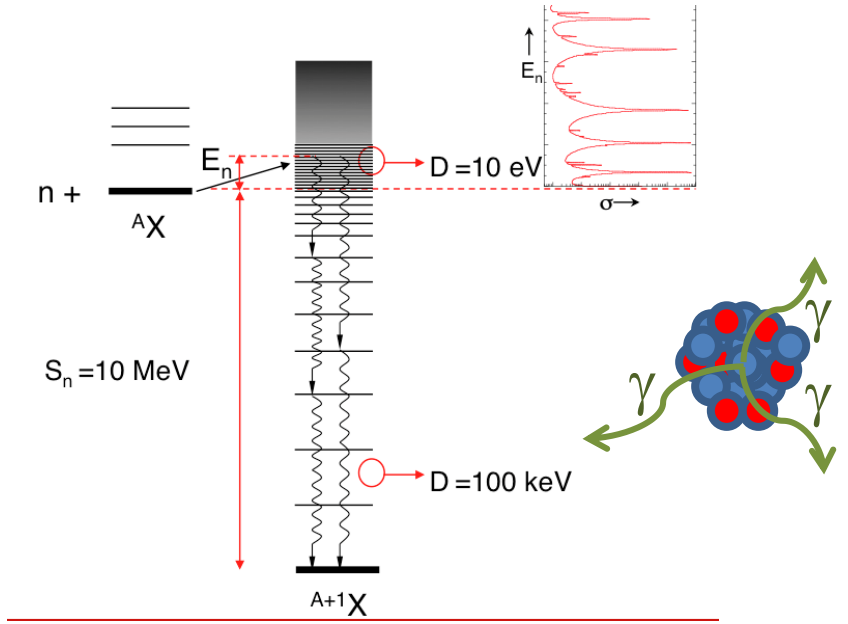


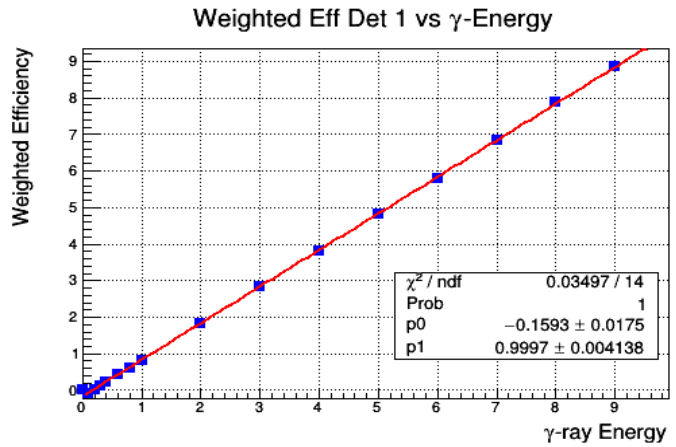

# The $C_6D_6$ Total Energy Detectors (TED): (n,$\gamma$)

**TED: Based in two principles**

- **Condition I : Low efficiency detectors** $\varepsilon_{\gamma i}<<1$

  Detecting a cascade: $\varepsilon_c=1-\Pi(1-\varepsilon_{\gamma i}) \approx \sum \varepsilon_{\gamma i}$

- **Condition II: The efficiency is proportional to $E_\gamma$**

$\varepsilon_{\gamma i} \propto E_{\gamma i}$

$$\varepsilon_c = k \sum_{i=1} E_{\gamma i} = kE_c$$

**Solution: Give to each signal a amplitude-dependent weight: PHWT**

**PHWT requires response of the detectors : MC simulations (Geant4)**


**4 x BICRON $C_6D_6$ scintillators 135º: in-beam γ-rays**

**Goal: Reach high $E_n$ (500 keV)**
- Low neutron sensitivity
- Fast (~10 ns)

R Plag et al., NIMA **496**, 425 (2003)

# Capture cross section measurements

- $^{151}$Sm(n,$\gamma$) – the first measurement at n_TOF
- $^{171}$Tm(n,$\gamma$) – the last measurement at n_TOF/EAR2

the full list is here: https://twiki.cern.ch/NTOFPublic/DataDissemination

# s-process branching at $^{151}$Sm

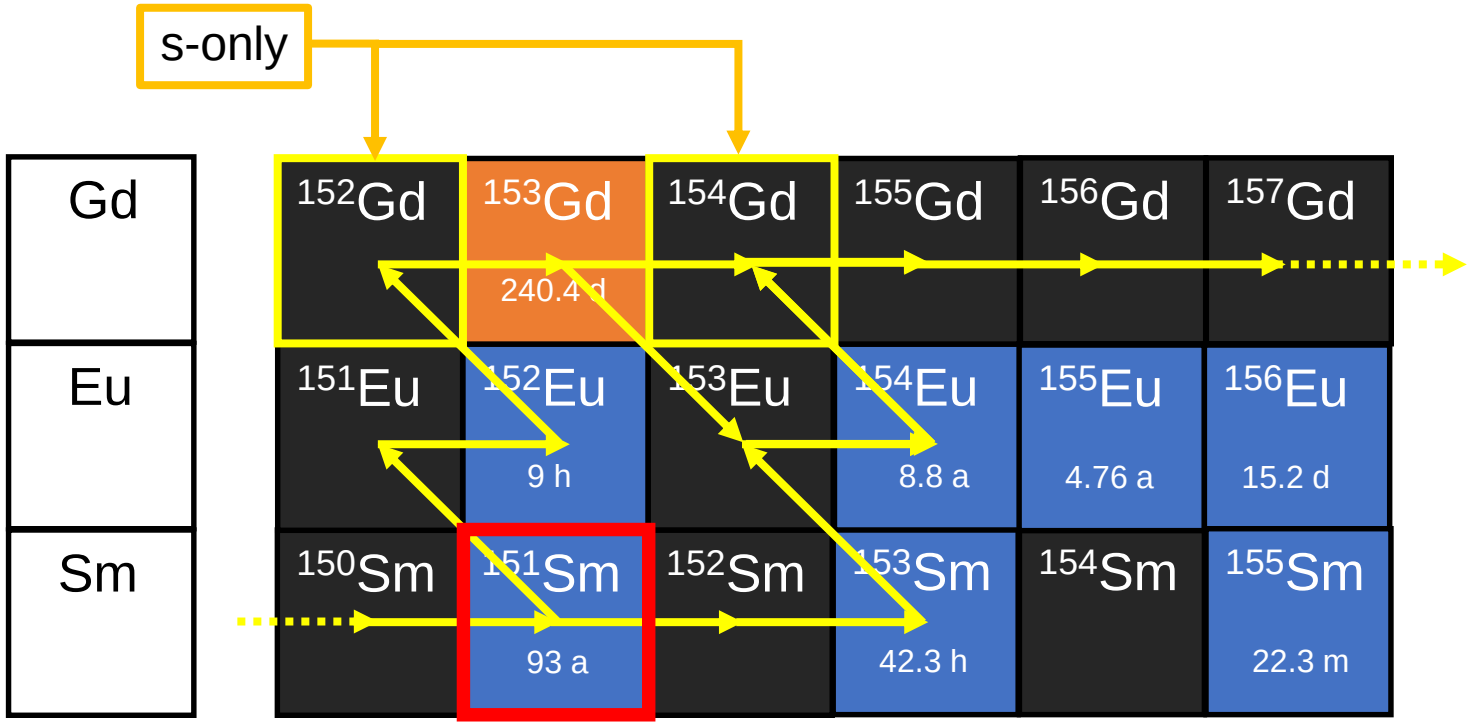


U Abbondanno *et al.* (The n_TOF Collaboration), Phys. Rev. Lett. **93** (2004), 161103

- branching isotope in the Sm-Eu-Gd region: test for low-mass TP-AGB
- branching ratio (capture/β-decay) provides infos on the thermodynamical conditions of the s-processing (if accurate capture rates are known!)

# $^{151}$Sm(n,$\gamma$) cross section results

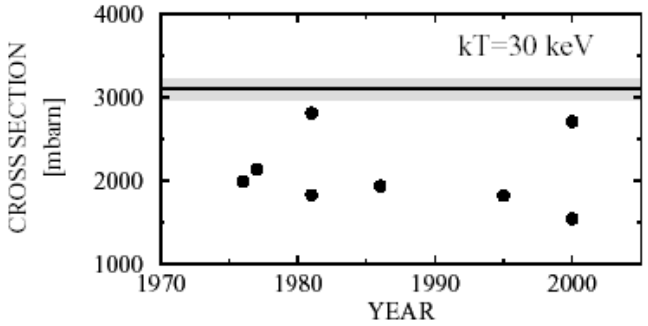


**MACS-30 = 3100 ± 160 mb**

$\langle D_0 \rangle$ = 1.48 ± 0.04 eV,
$S_0$ = (3.87 ± 0.20)×10$^{-4}$
$\langle \Gamma_\gamma \rangle$ = 108 ± 15 meV

U Abbondanno *et al.* (The n_TOF Collaboration), Phys. Rev. Lett. **93** (2004), 161103

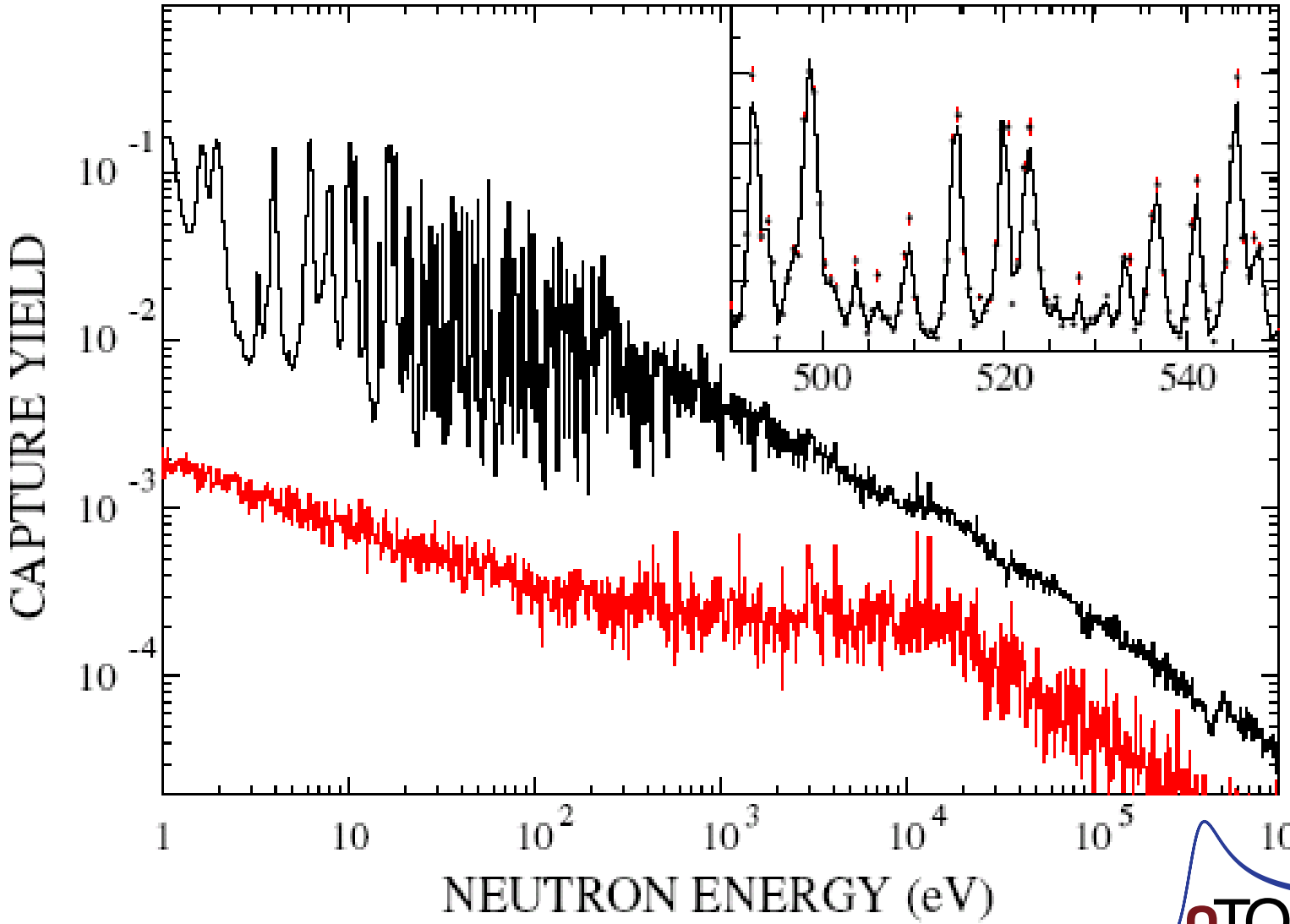


small samples

180 mg of $^{151}$Sm

**Neutron Capture on the *s*-Process Branching Point $^{171}$Tm via Time-of-Flight and Activation**

C. Guerrero,[1,2,*] S. Halfon,[4] N. L. Weissman,[4] A. Barak,[4] M. J. D. Bosnar,[21] A. Casanc M. A. Cortés-C Y. Eisen,[4] B. Fe A. Gawlik,[4] T. H. Harada,[32] T T. Katabuchi M. Krtička, D. Macina F. Matteucci,[4] S. Montesano I. Porras,[46] J. Pr A. Ryan,[20] M. A. Stamatopou G. Vannini,[25,38] stallo,[7,8] R. Dressler,[5] an,[5] D. Schumann,[5] icak,[14] J. Balibrea,[13] ieux,[19] J. Billowes,[20] ltt,[13] R. Cardella,[10] ,[15] G. Cortés,[23] Dupont,[19] I. Durán,[22] bel,[18] A. R. García,[13] yer,[14] F. Gunsing,[19,9] Kadi,[10] B. Kaizer,[4] oris,[37] A. Kriesel,[4] ile,[28] R. Losito,[10] Mastromarco,[15] grone,[25] M. Mirea,[30] ski,[11] L. Piersanti,[7] out,[47] C. Rubbia,[10] J. hev,[29] A. G. Smith,[20] anis,[37] S. Valenta,[17] rren,[20] M. Weigand,[18]

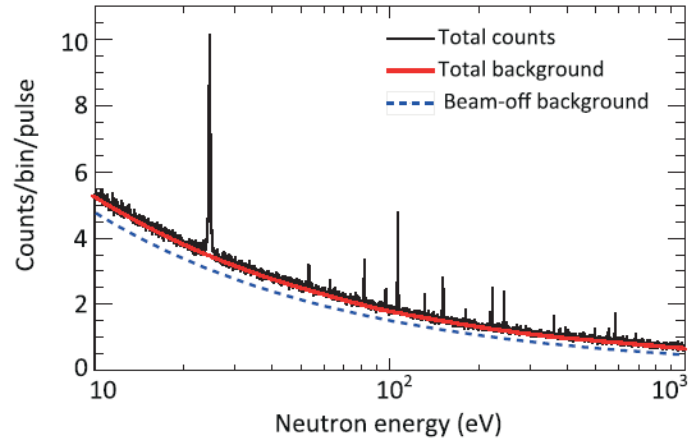


FIG. 2. Distribution of counts as function of the neutron energy during the $^{171}$Tm$(n,\gamma)$ experiment at *n*TOF. The dominant beam-off background from the activity of the sample does not prevent resolving the individual resonances (see inset).

# Nuclear Astrophysics at n_TOF

- origin of the heavy elements
  s-process nucleosynthesis in stars

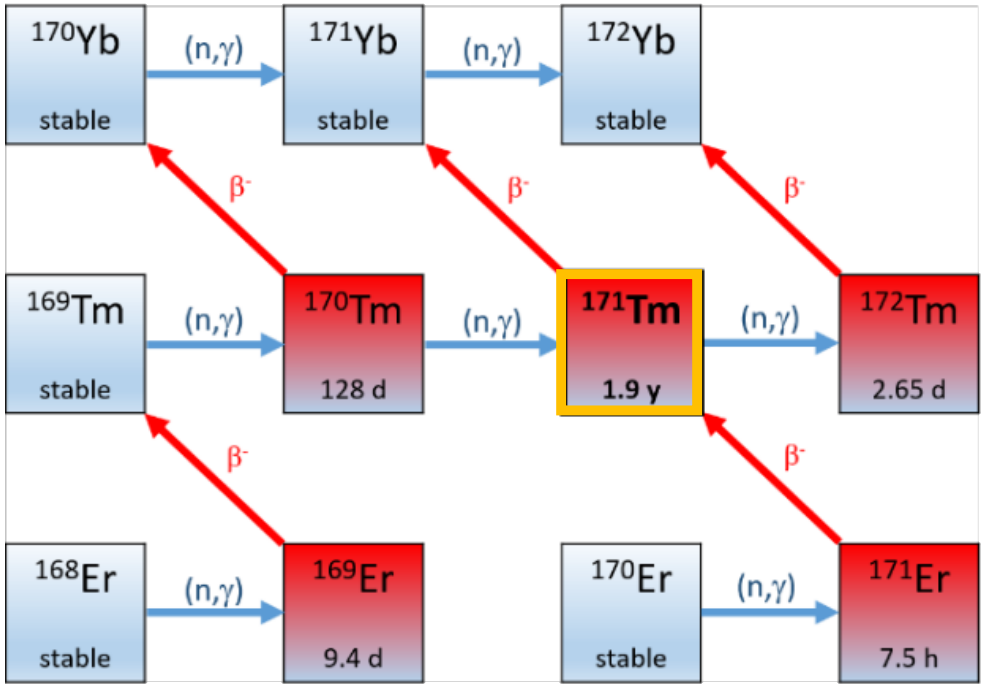


## $^{171}$Tm(n,$\gamma$)

| | |
|---|---|
| sample mass: | 3.13 mg, 1.10 x $10^{19}$ atoms |
| $t_{1/2}$ | 1.9 yr |
| activity | 126 GBq |

sample produced at ILL, Grenoble, France
separated at PSI, Villigen, Switzerland
measured at n_TOF and SARAF-LiLiT facility, Soreq NRC, Israel

C Guerrero et al. (The n_TOF Collaboration), Physical Review Letters **125**, 142701 (2020)

# Better MACS means more than just nuclear data

Reducing the uncertainty in the MACS is not only a question of better nuclear data: higher accuracy in the reaction rates opens the possibility to investigate new astrophysical scenarios

[nuclear clocks, constrains on the BBN, AGB modeling, nucleosynthesis conditions in explosive scenarios, others]

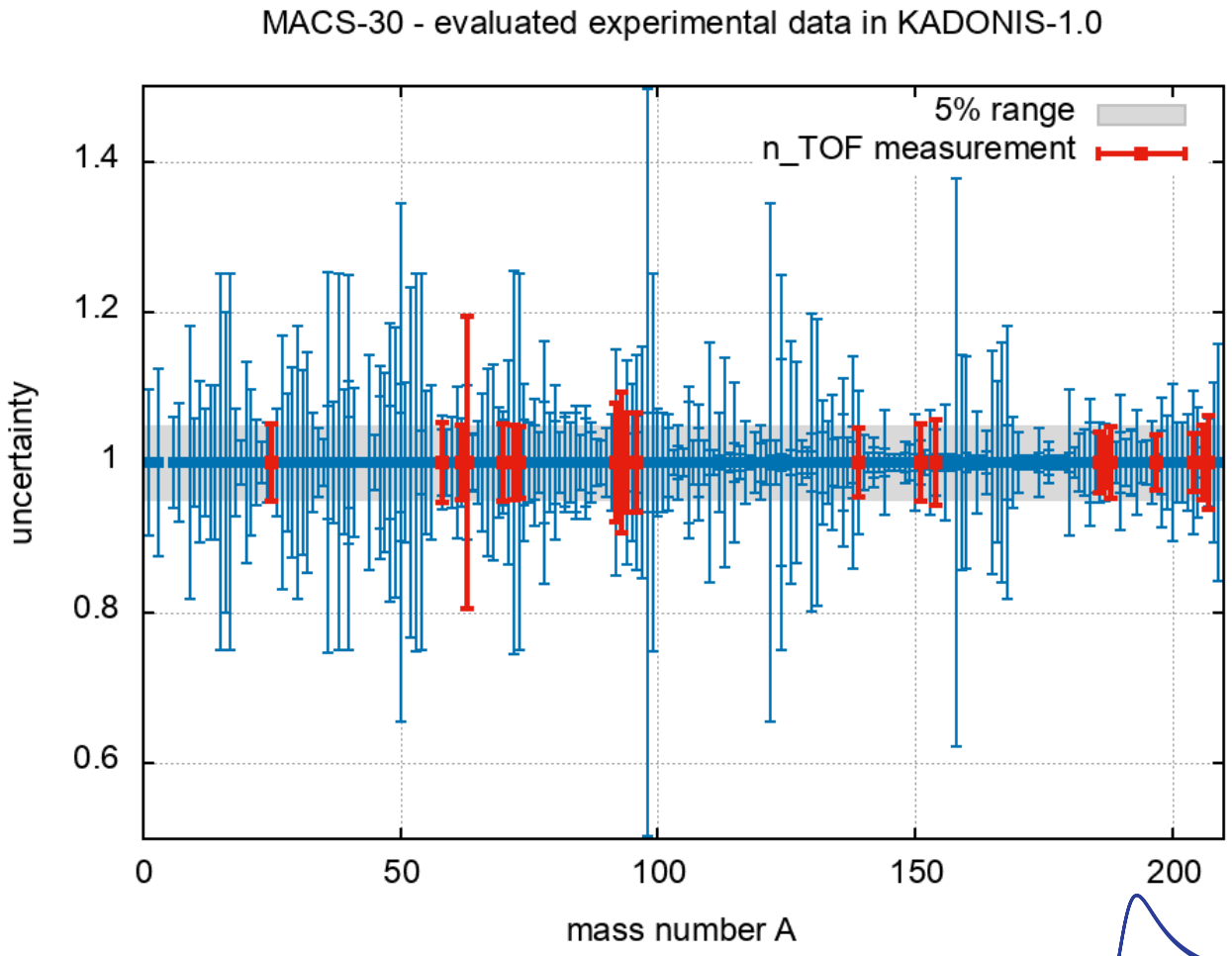


https://twiki.cern.ch/NTOFPublic/ListOfPublications

# Advanced Nuclear Technologies

"Several parameters, **particularly safety parameters** of reactors and other nuclear facilities, need to be known with a precision well below 0.1% resulting in **nuclear data precisions better than a few percent, sometimes better than 2%, and this is a serious challenge**. In other cases, the precision needed can range from 5 to 20% but the isotope or material to be measured is highly radioactive or very scarce raising a different but also important challenge."

cit. "SUPPLYING ACCURATE NUCLEAR DATA FOR ENERGY AND NON-ENERGY APPLICATIONS – SANDA"
EU H2020 Nuclear Data Project, started in September 2019 (4 years duration)

Significant contribution received from the different EURATOM programmes to the activities related to nuclear technologies, starting with FP5 (NTOF-ND-ADS) and followed by EUROTRANS/NUDATRA, ANDES, CHANDA and SANDA (H2020). Transnational access projects in H2020 (ARIEL and ERINDA) are also acknowledged.

CERN

HORIZON2020

European Commission

nTOF

# Neutron Induced Fission

# Parallel Plates Avalanche Counters

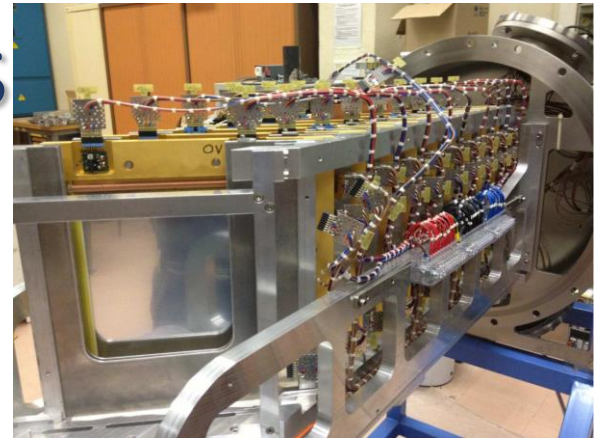

Each PPAC consists of 3 parallel plate electrodes:
- a central anode coated with gold  or aluminum
- 2 two stripped cathodes (2 mm wide) in orthogonal directions
    coated with gold or aluminum

1 PPAC detector: 10 PPACs + 9

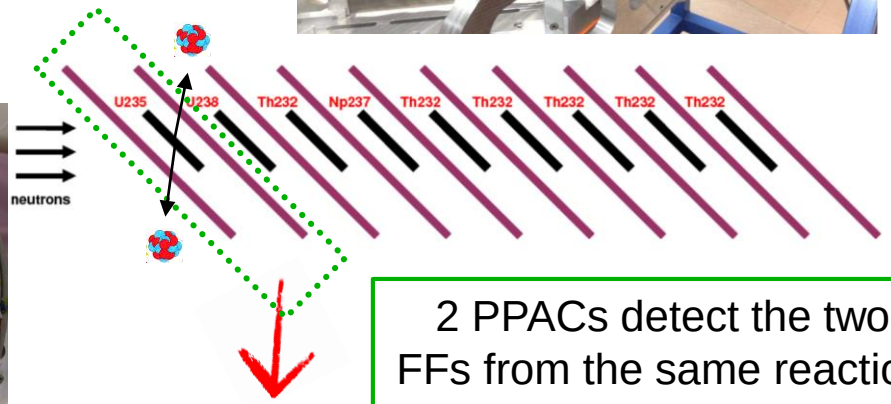


2 PPACs detect the two FFs from the same reaction in coincidence

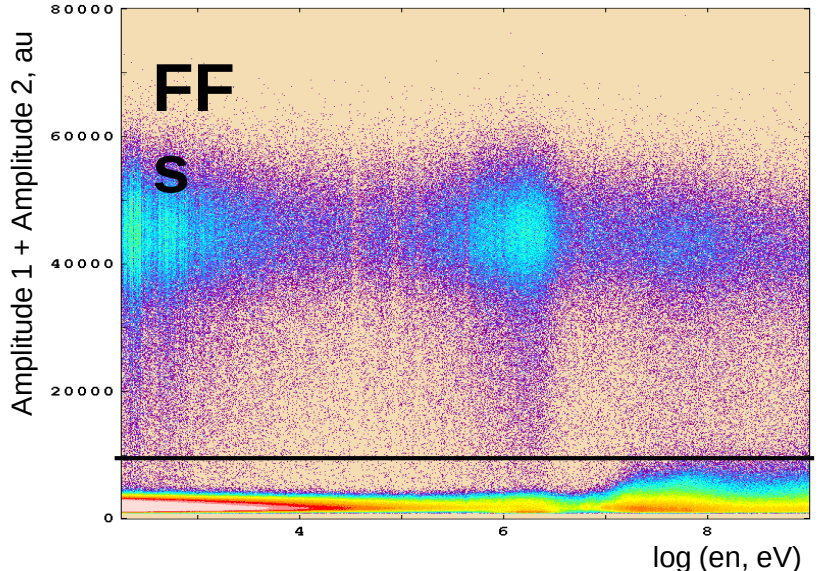


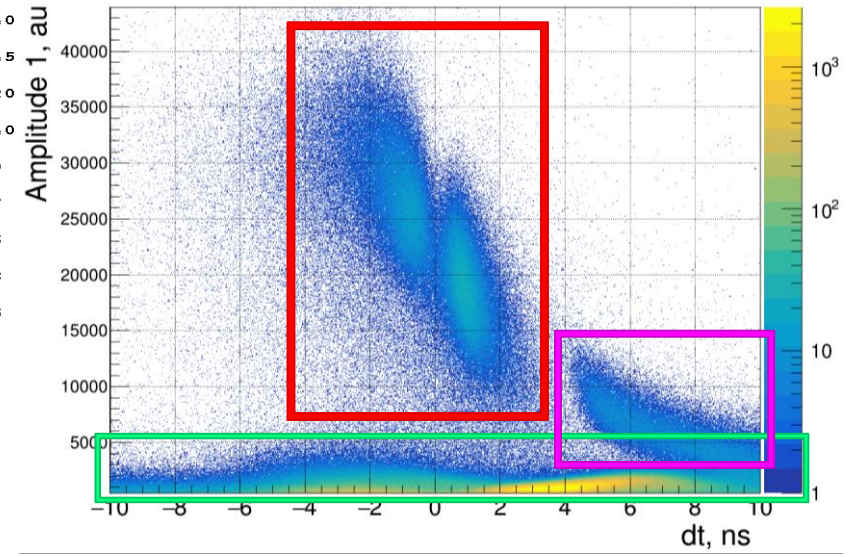


FF
s
FFs
from the 2nd sample
bk
g

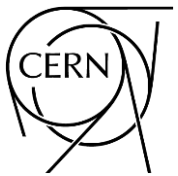


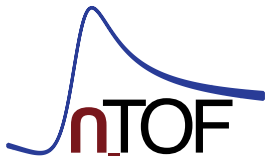

# Parallel Plates Avalanche Counters

The strips, which are read at both ends of the delay line, allow for

- a localisation of the FFs impact positions
- the reproduction of the hitting point of the neutrons in the sample

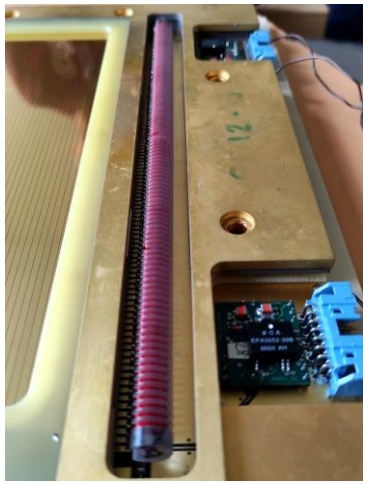

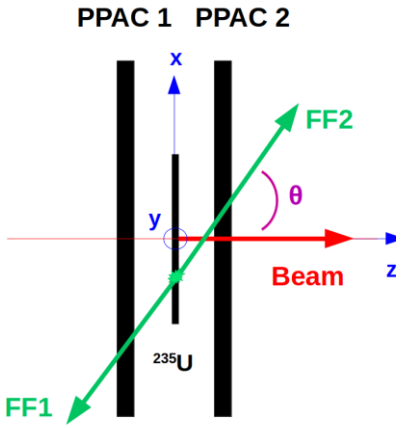


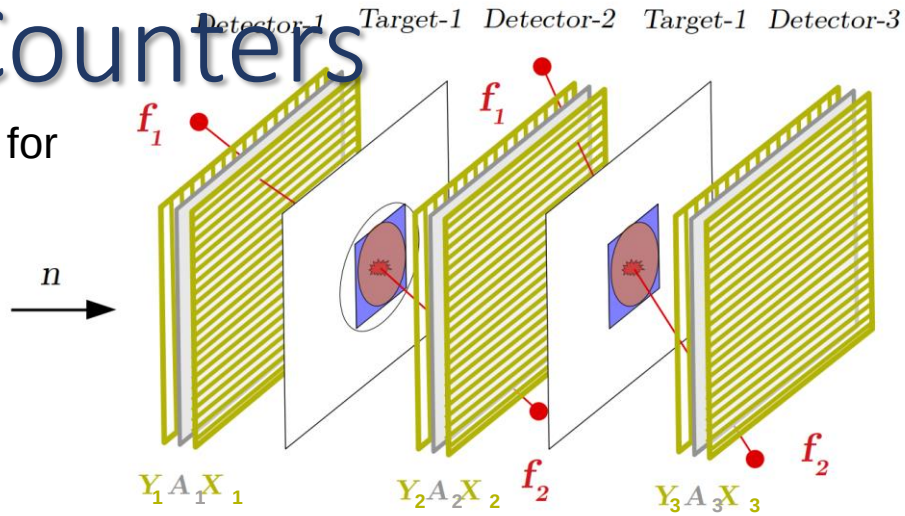


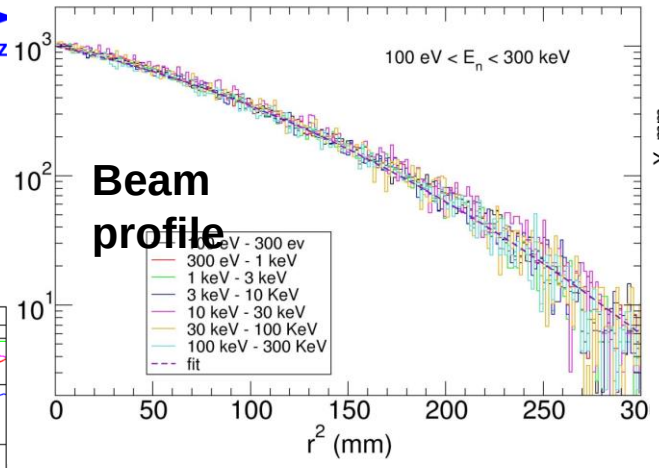


**Beam profile**

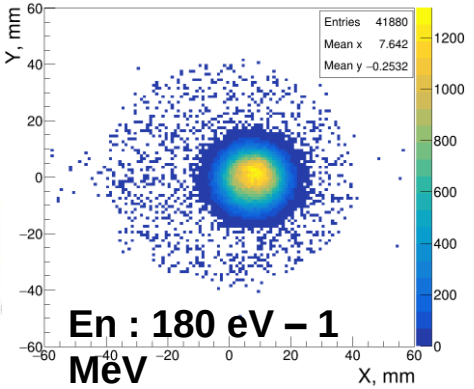


**En : 180 eV – 1 MeV**

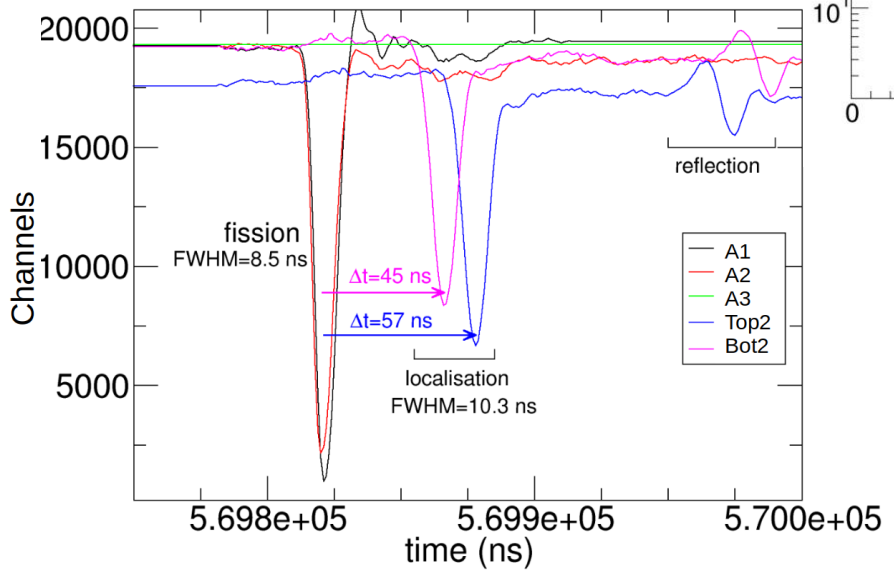


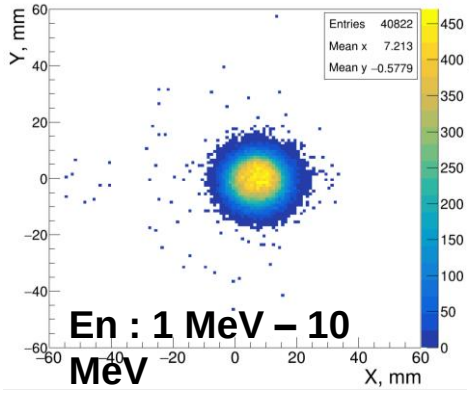


**En : 1 MeV – 10 MeV**

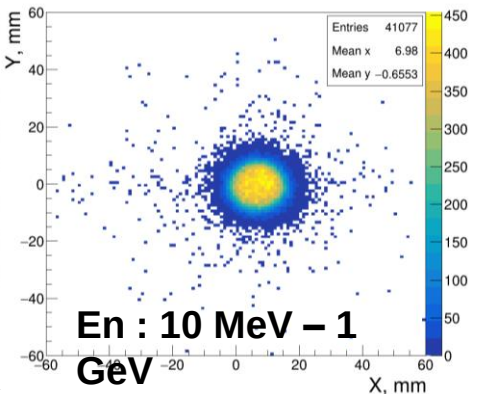


**En : 10 MeV – 1 GeV**

# Fission chamber

Parallel plate ionisation chamber for $^{235}$U(n,f) cross section measurement above 20 MeV

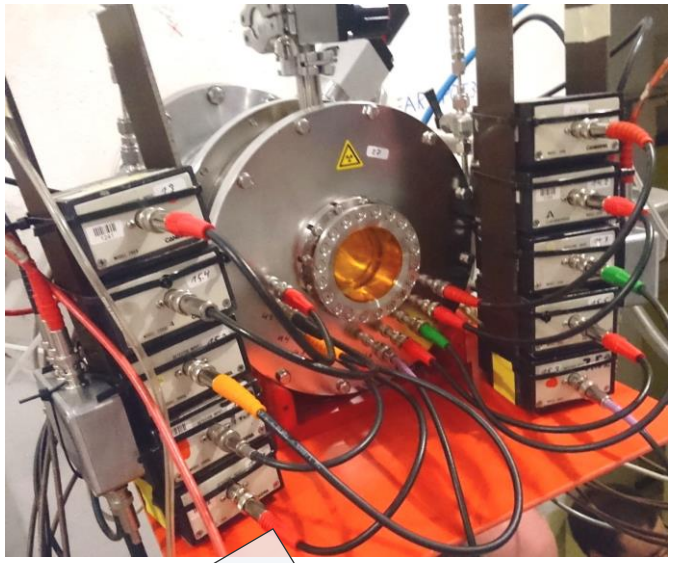

- 8× $^{235}$U samples (~32 mg, 99.93% enrichment)
- Thin sample backings/windows to reduce interaction with gamma-flash
- Separate read-outs for each sample
- Electronic interference reduced by baseline subtraction
- Fragment detection efficiency about 95%

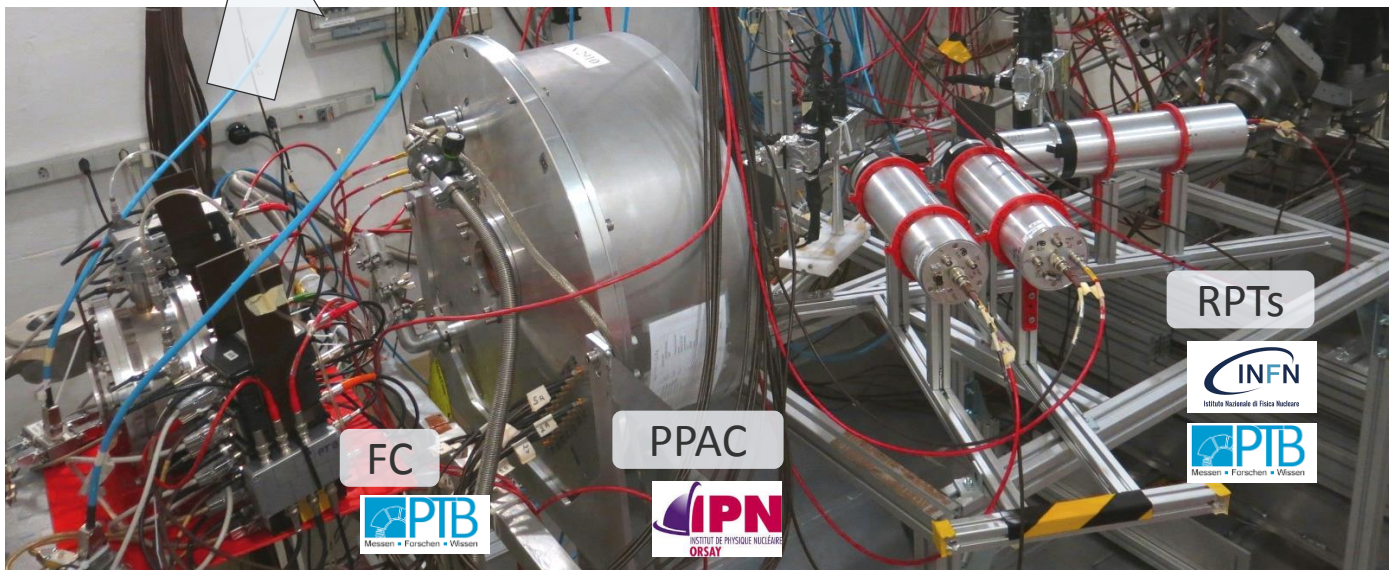


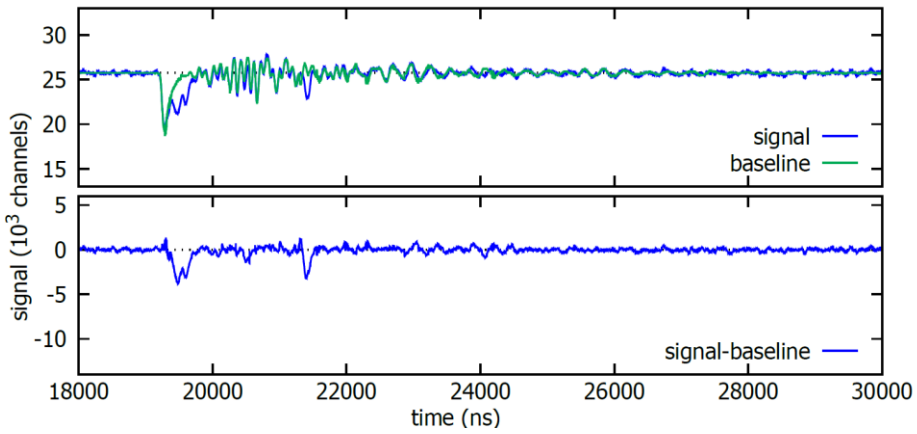


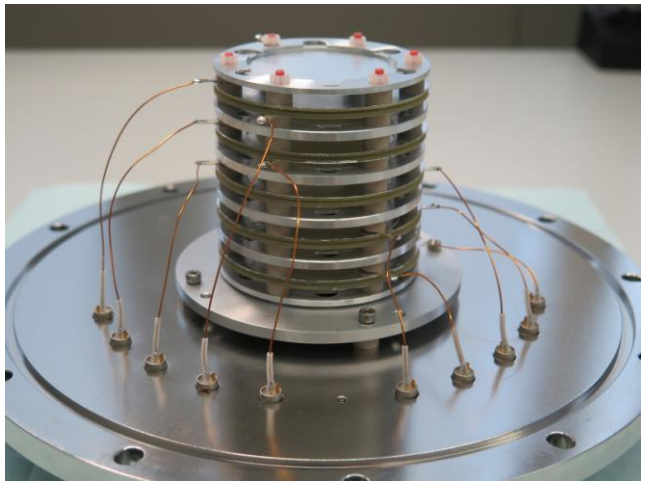

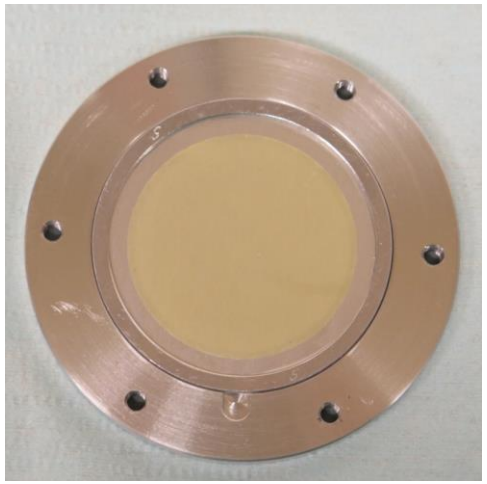

# $^{234}$U(n,f) for the $^{232}$Th/$^{233}$U cycle

Half-life: **2.45x10$^5$ y**
**EAR-1**

Mass: 27 mg (2 samples)
Activity: **3.1 MBq** (per sample)
**Detector: PPAC perpendicular**

Mass: ~35 mg (7 samples)
Activity: **~1 MBq** (per sample)
**Detector: FIC**

- High resolution and high accuracy n_TOF data (4-5% uncertainty), **up to 1 GeV**

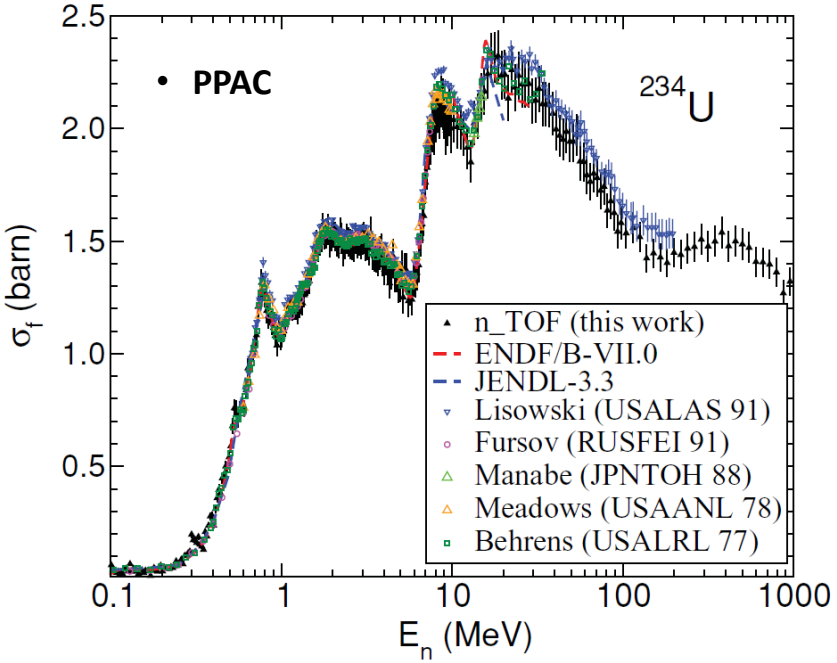


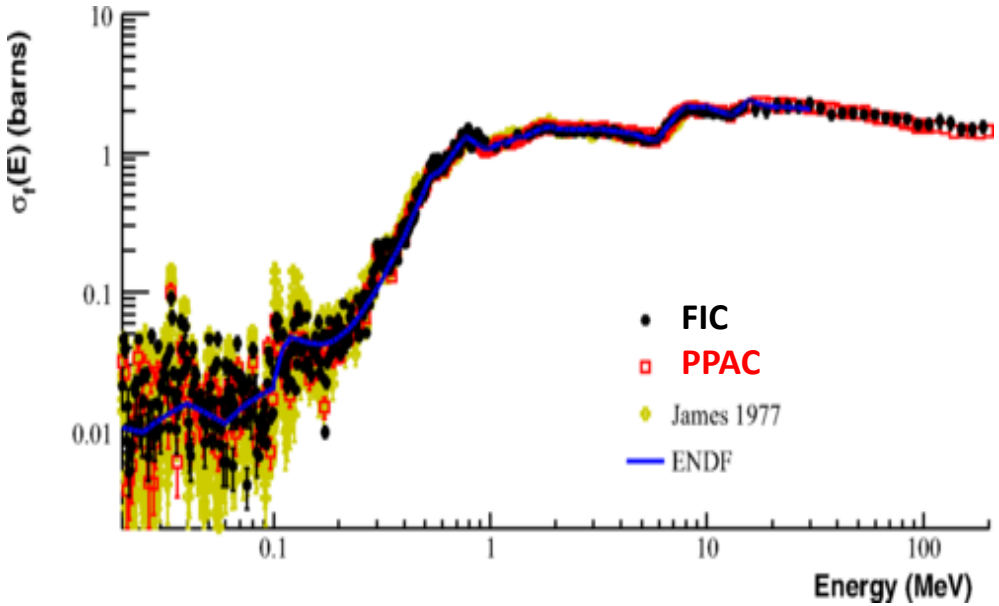


=> Good agreement between PPAC and FIC


C. Paradela *et al.* (The n_TOF Collaboration), Phys. Rev. C **82**, 034601 (2010)
D. Karadimos *et al.* (The n_TOF Collaboration), Phys. Rev. C **89**, 044606 (2014)

# $^{235}$U(n,f) for energies up to 500 MeV

Fission detectors

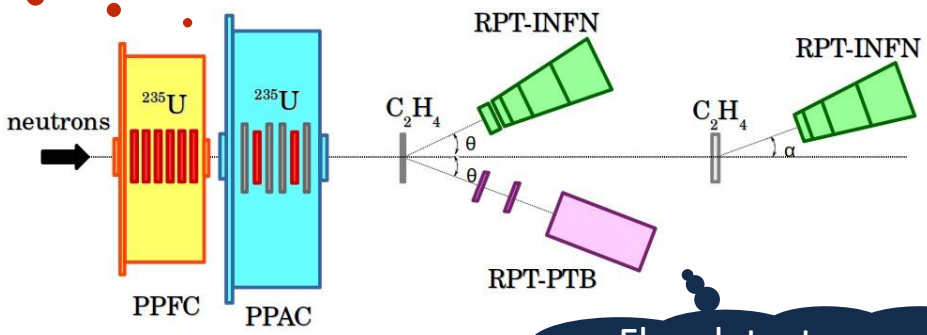


Flux detectors
**n-p scattering**

# $^{235}$U(n,f) for energies up to 500 MeV

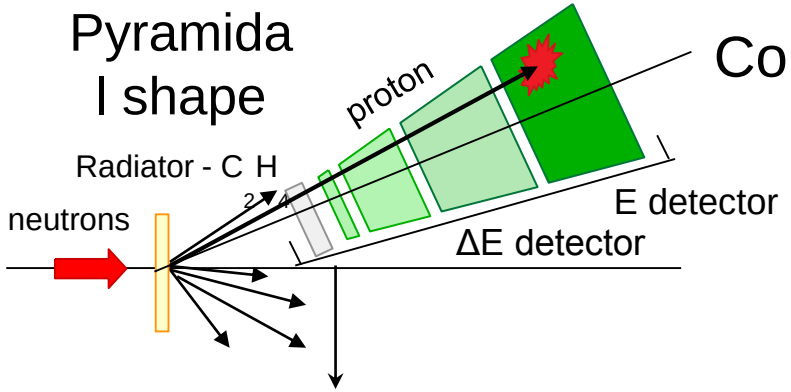


Coincidence + ΔE-E

$\Delta E \cdot E \propto k \cdot z^2 \cdot M$

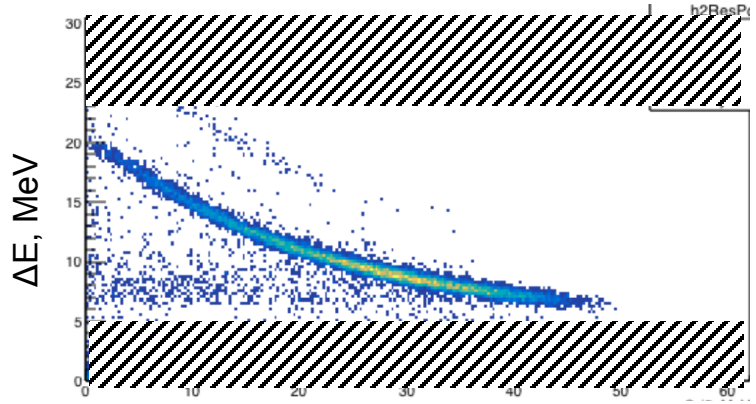


2 silicon detectors 300 μm thick
4 plastic scintillators (thickness)
5 mm, 30 mm 60 mm and 60 mm

$C_2H_4$

n + H → n + p

n+H → n + p

n+C → $^{9}$Be + α, $^{11}$B + d, $^{12}$B + p, $^{10}$B + t, ...

⇨ **Recoil Proton Telescope**

The main requirement for reaching 1 GeV: **γ-flash response**

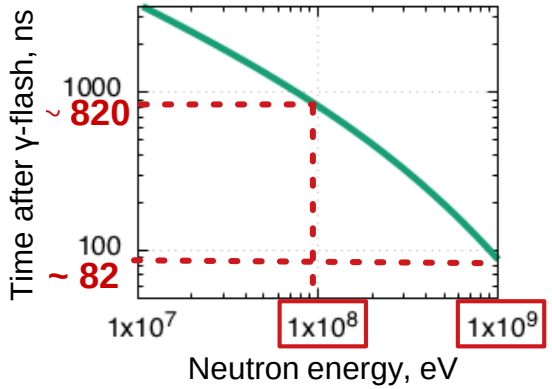


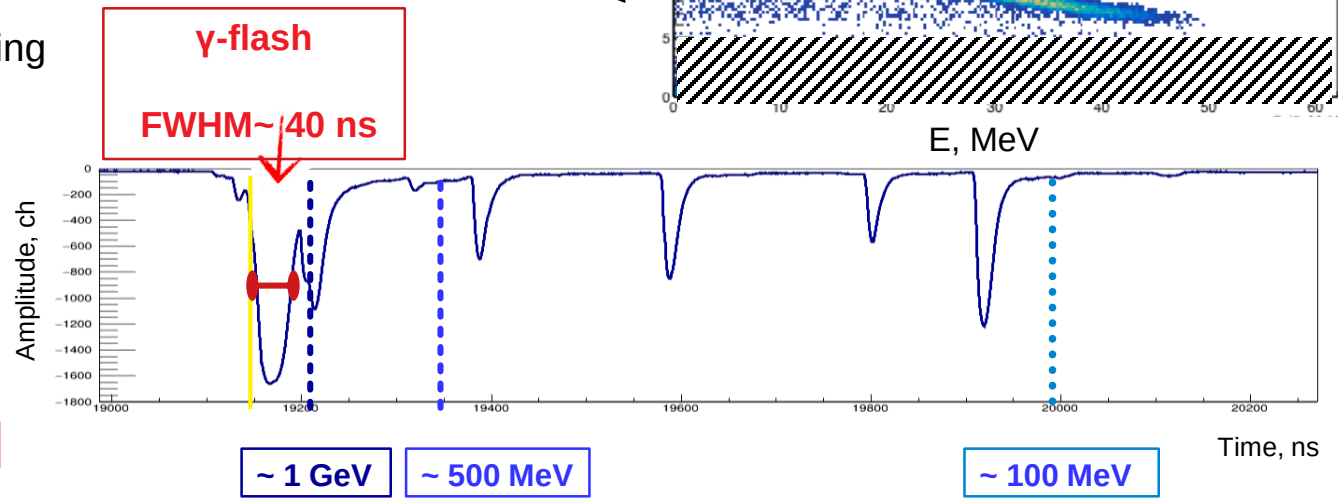

# Recoil Proton Telescope

$$\phi_n = \frac{N_p/\varepsilon}{n_H \left(d\sigma_{np}/d\Omega\right) \Delta\Omega}$$

For measuring the neutron flux above 20 MeV

- Neutron detection via $^1$H(n,p)
- PE sample in beam
- Recoil proton detectors at an angle (25°), in air
- Optimised for the energy range from 20 to 150 MeV

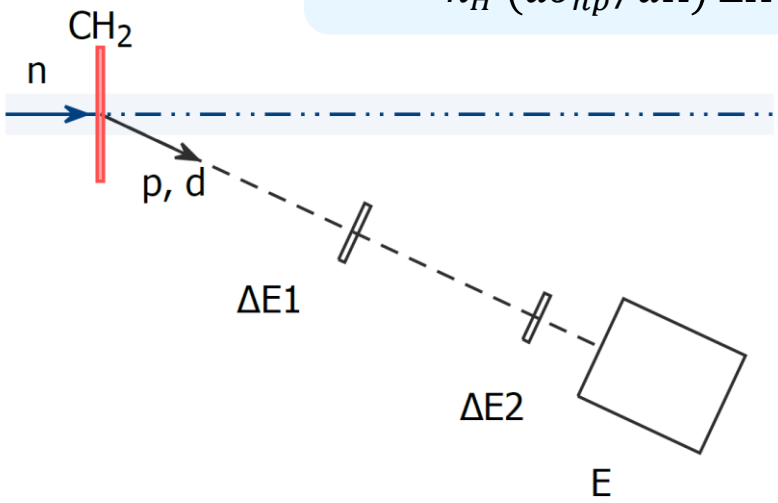


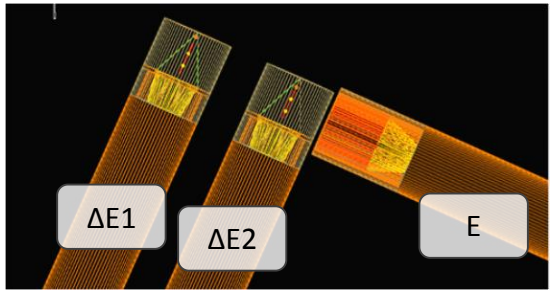


Specifications:

- plastic scintillators (EJ-204)
- triple stage (ΔE1, ΔE2, E) for suppression of random coincidences
- solid angle defined by ΔE2
- particle identification via ΔE2-E, for fully-stopped particles
- different configurations: thickness of PE radiator and ΔE-detectors optimised for different energy ranges

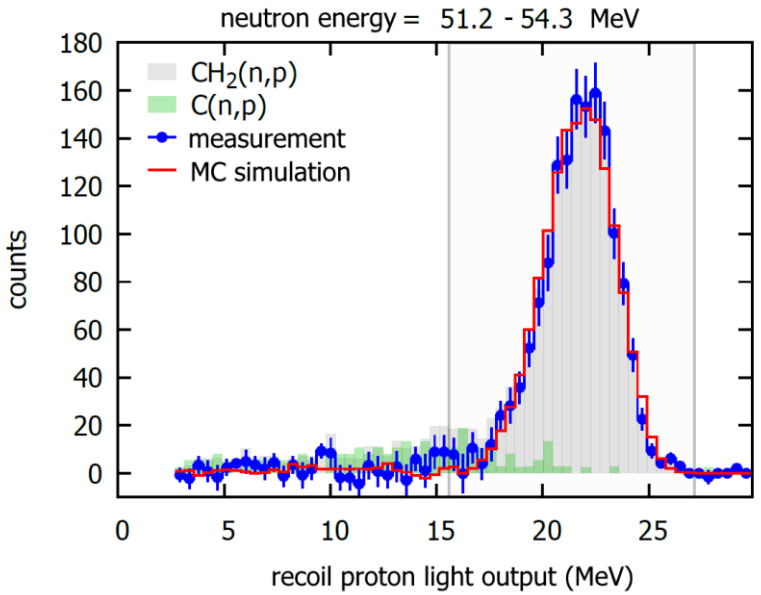


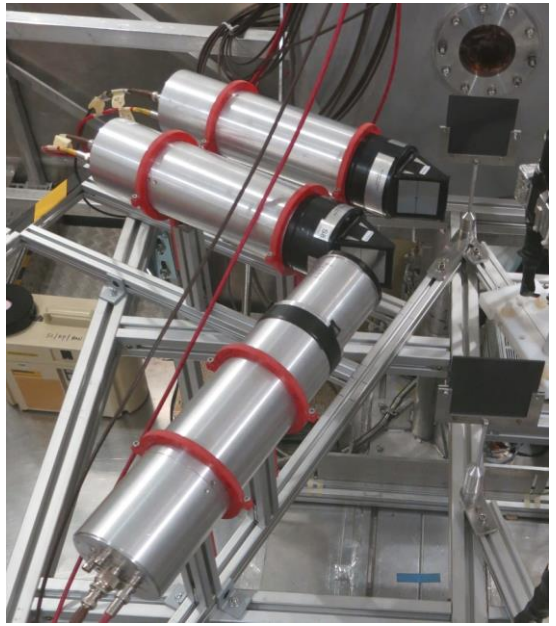

# $^{235}$U(n,f) for energies up to 500 MeV

Fission detectors

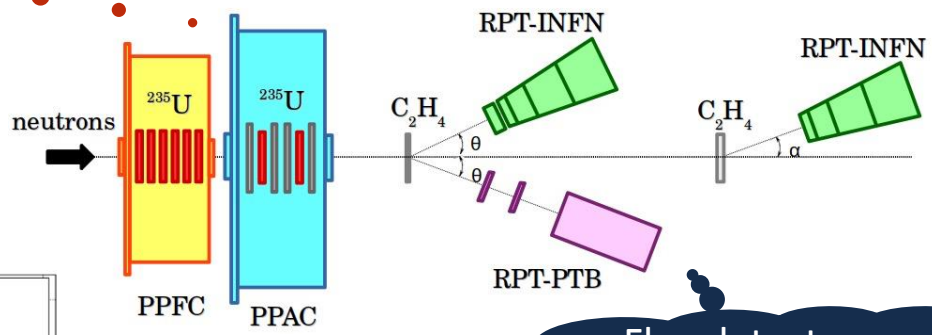


Flux detectors
**n-p scattering**

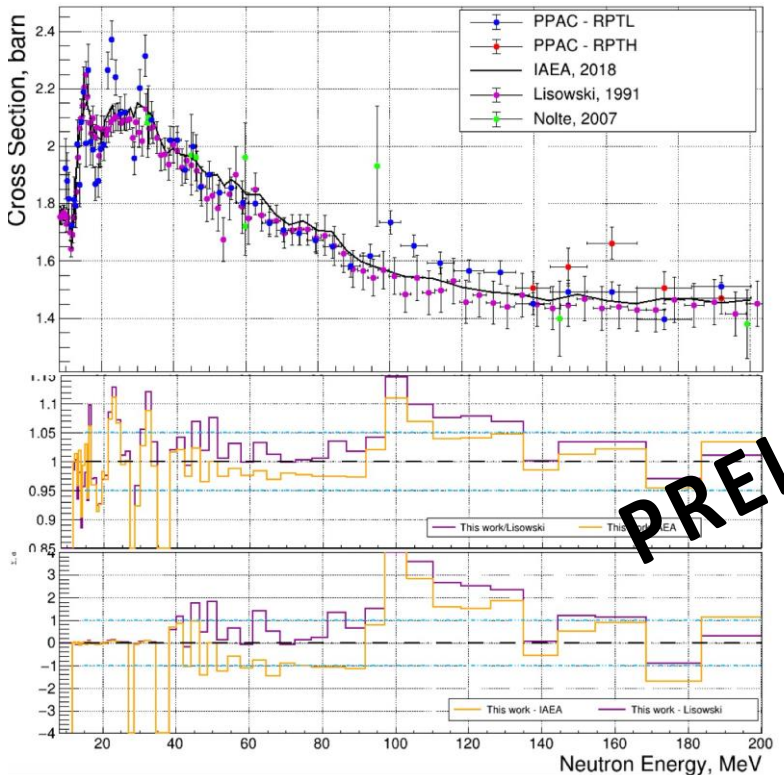


PRELIMINARY

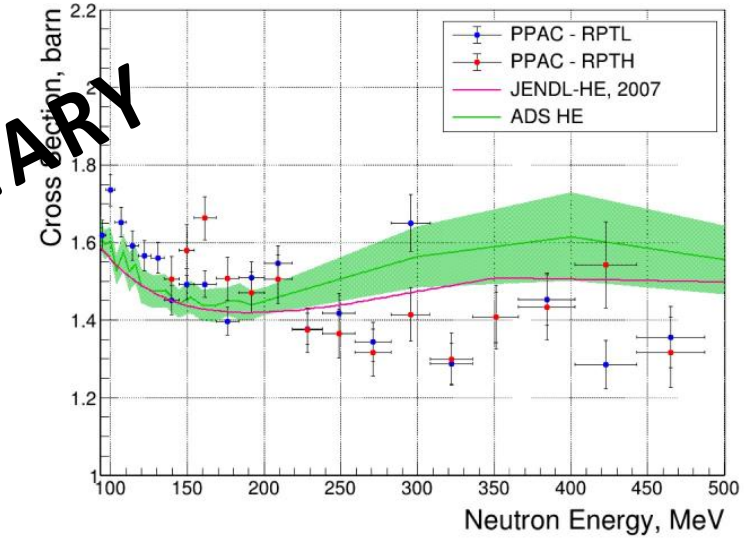

# The n_TOF Total Absorption Calorimeter (TAC)


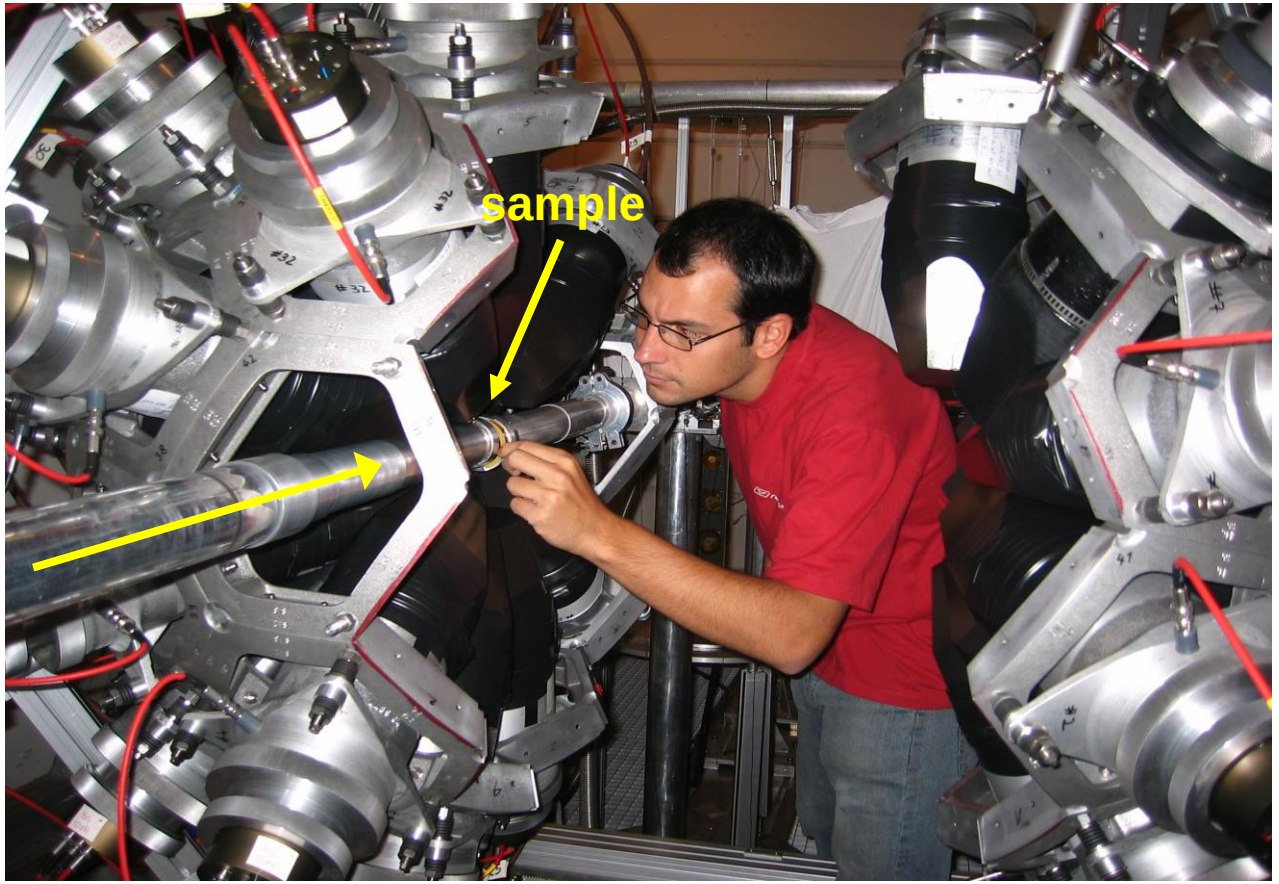

# The n_TOF Total Absorption Calorimeter (TAC)

**Segmented 4π array of 40 $BaF_2$ crystals**

- 95% solid angle (20/50 cm inner/outer diameter)
- Absorber to reduce neutron sensitivity
- Combined capture and fission detection

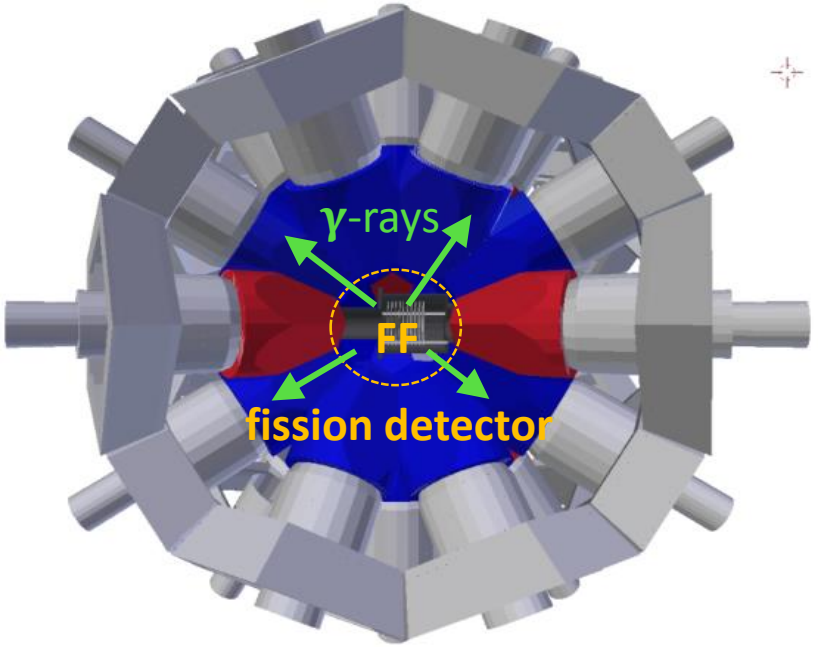


**Ideal for σ(n,γ) measurements of small-mass and radioactive samples**

- High geometrical & intrinsic efficiency
- Powerful background rejection via coincidence analysis
- $^{233, 234, 235, 238}U$, $^{237}Np$, $^{240}P$, $^{241}Am$, $^{243}Am$, $^{244}Cm$

Physics output in addition to cross sections:

- γ-ray strength functions
- capture/fission events discrimination

**Very accurate efficiency determination based on Geant4 Monte Carlo simulations**

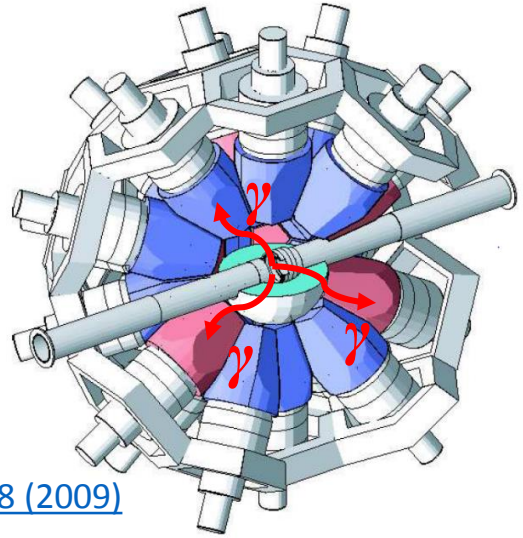


C. Guerrero et al., Nucl. Inst. and Meth. A 608 (2009)

$^{88}Y$ spectra

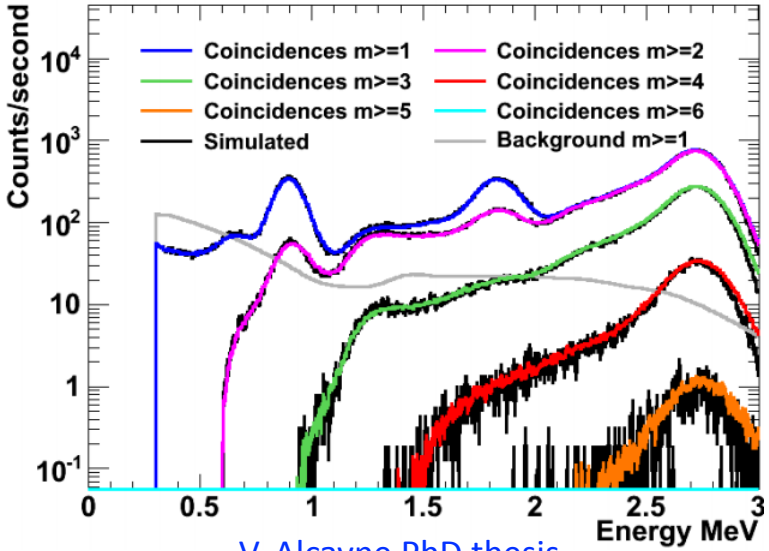


V. Alcayne PhD thesis

# The n_TOF Total Absorption Calorimeter (TAC)

$^{237}$Np(n,$\gamma$)

half-life: 2.1 Myr

C. Guerrero et al. (n_TOF Collaboration)
Phys. Rev. C 85, 044616 (2012)

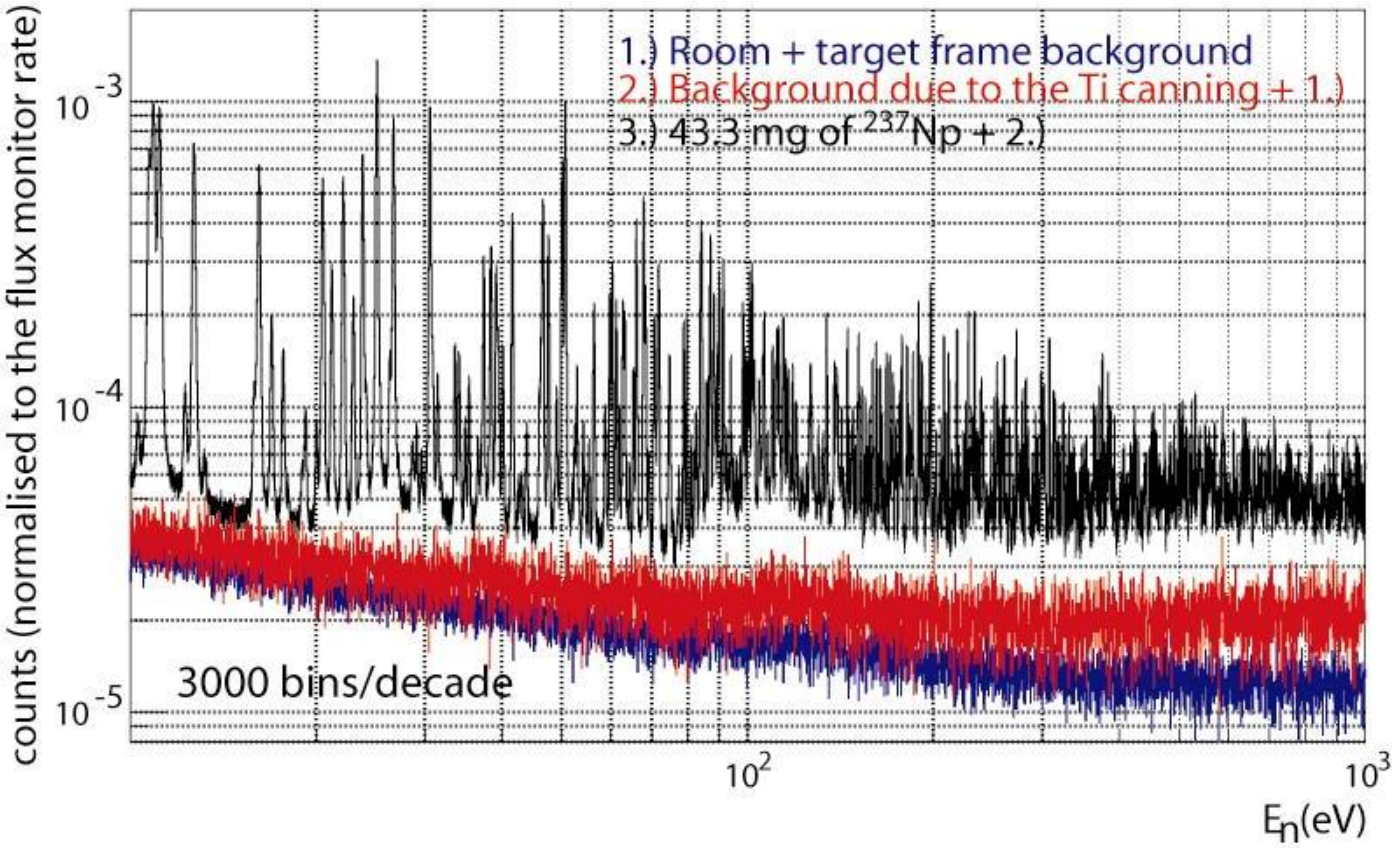


CERN

European Commission

nTOF

# TAC and the Fission Tagging Chamber

- Compact – cylindrical chamber Ø9 cm × 12 cm
- Simple ionization cells – minimum material in beam
  - 14 cathodes/deposits (10 µm Al each) readout from 8 anodes (20 µm Al each)
- Fast signals (34 ns FWHM) for high α-count rates (>1 MBq per anode)
  - Fast ionizing gas $CF_4$ @ 1.1 bar
  - Dedicated electronics (CEA/DAM/DIF)
  - 3 mm gap @ 1.4 kV/cm
- Used for $^{233}U(n,\gamma)$ fission tagging (+ TAC)
  - Tagging efficiency of 89.6(1)% @ Amp > 0.076 V

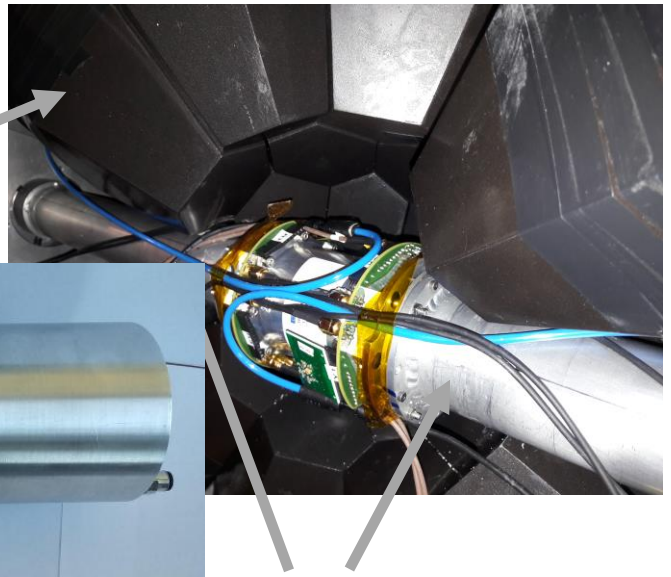


Chamber with electronics and gas supply mounted in the TAC

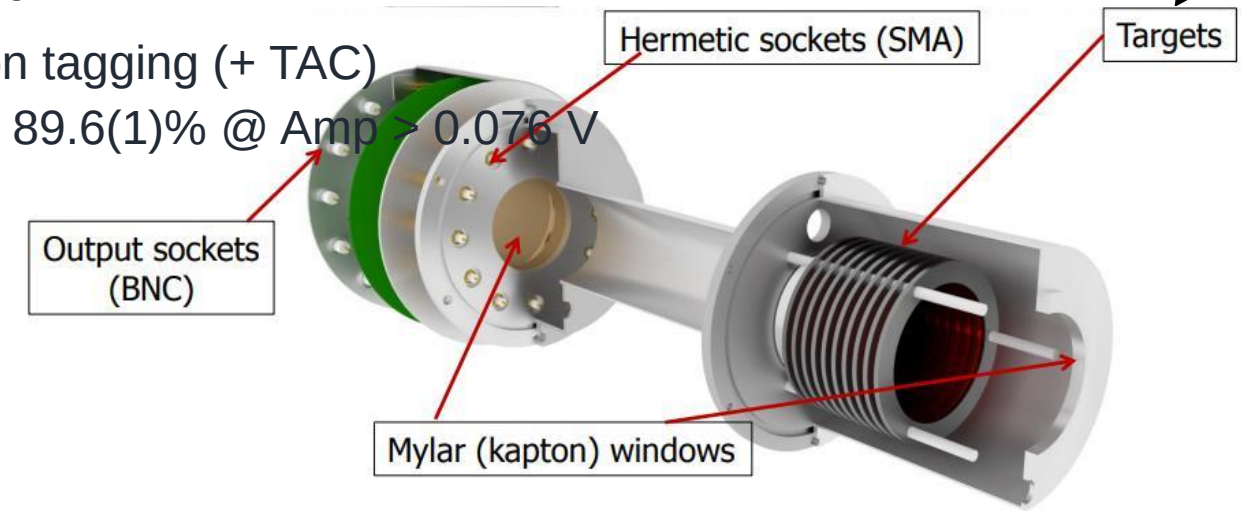


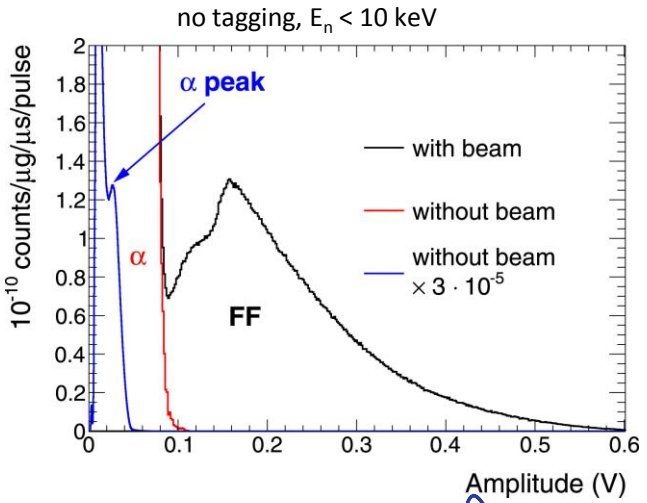


To be used in a $^{239}Pu(n,\gamma)$ and (n,f) measurement


J. Balibrea et al., Physical review C 102, 4 (2020) 044615
M. Bacak et al., Nucl. Int. and Meth. A 969 (2020) 163981

# Additional detection systems for a wide range of applications

# STEFF @ n_TOF

## Spectrometer for Exotic Fission Fragments

**Main axis (arms one and two)**

- Secondary electron timing detectors for FF time-of-flight measurements:
  - MCP start detector
  - MWPC stop detector (10 mbar isobutane)
- Ionization chambers (100 mbar isobutane)
  - Solid angle ~ 0.03 sr
  - 15 segments

**Secondary axes (arms three and four)**

- Secondary MCP electron timing detectors for FFs
- Ionization chambers (100 mbar isobutane)
  - Solid angle ~0.03 sr

**Scintillators**

- Array of NaI and $LaBr_3$ detectors
- NaI high efficiency, $LaBr_3$ low deadtime

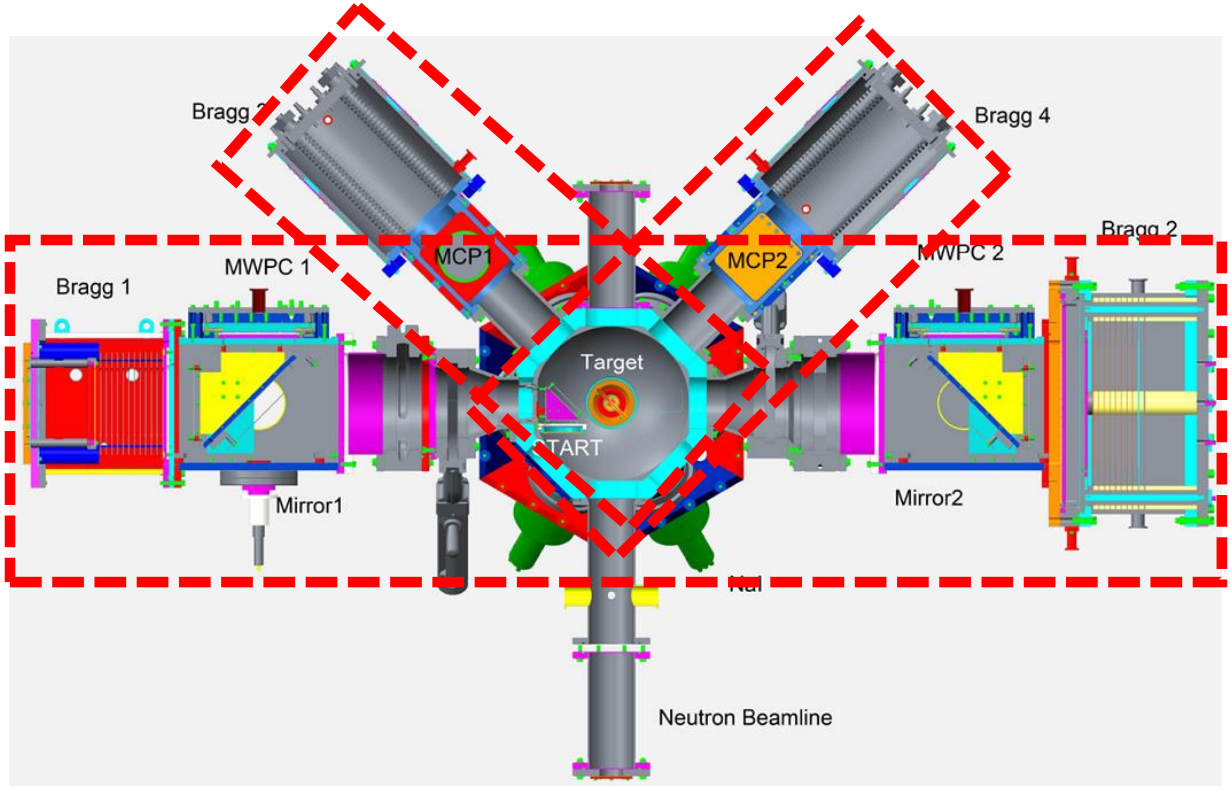


# Prompt fission γ-ray measurements with STEFF: $^{235}$U and $^{239}$Pu – EAR2

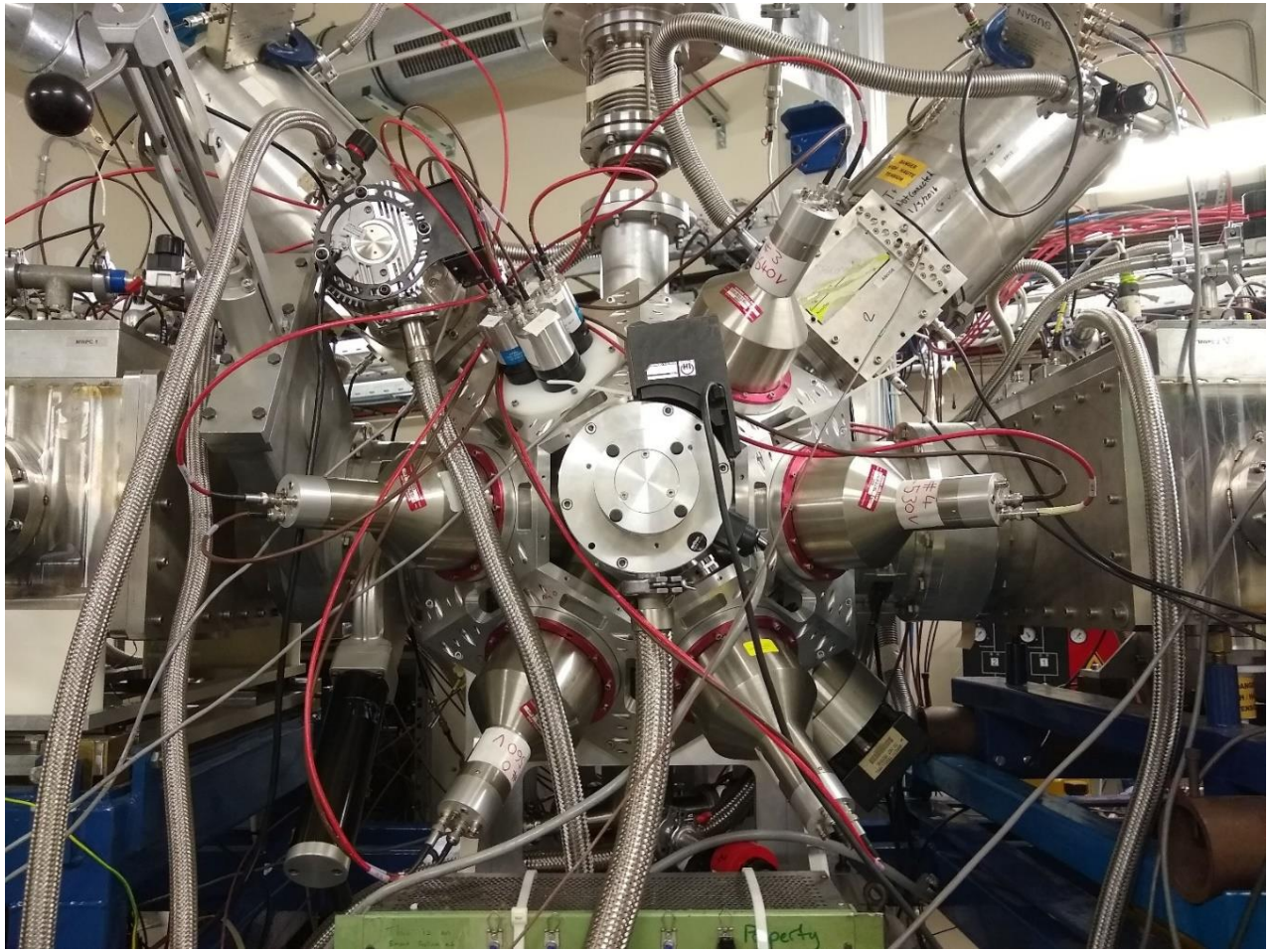

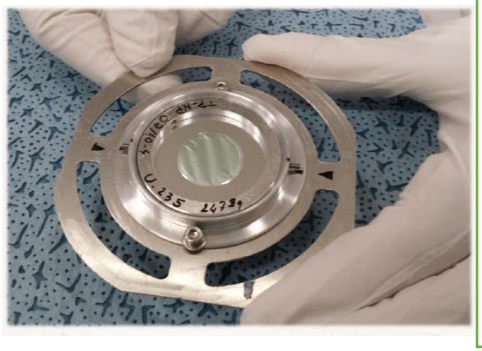

**2015:**
- 21 days of beam
- Small collimator
- **300 µg/cm$^2$ $^{235}$U target, 0.1 µm Al & 1.5 µm mylar backing**

**2016:**
- 30 days of beam
- Large collimator
- **100 µg/cm$^2$ $^{235}$U target, 0.7 µm Al backing**

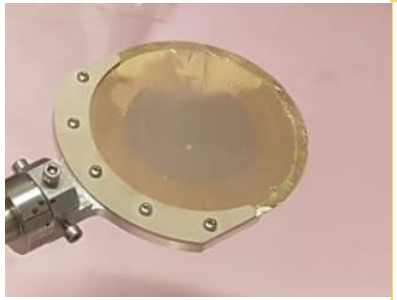

**2018:**
- 45 days of beam
- Small collimator
- 30 µg/cm$^2$ $^{239}$Pu Campaign, 30 µg/cm$^2$ polymide backing

# STEFF – Digital Signal Processing

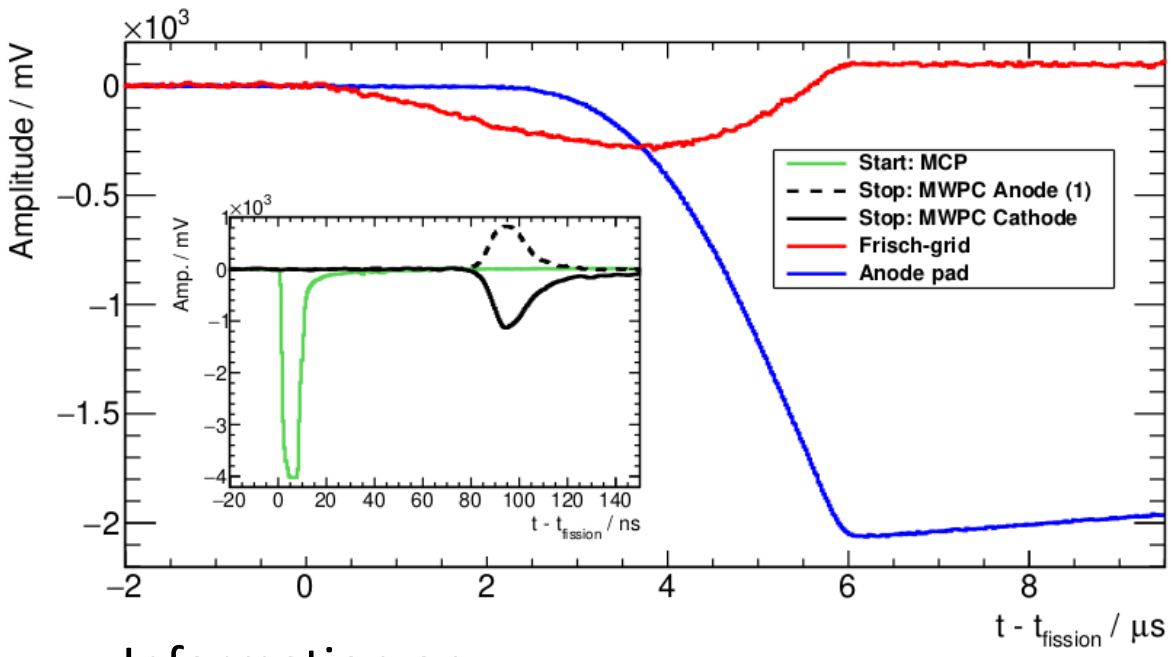


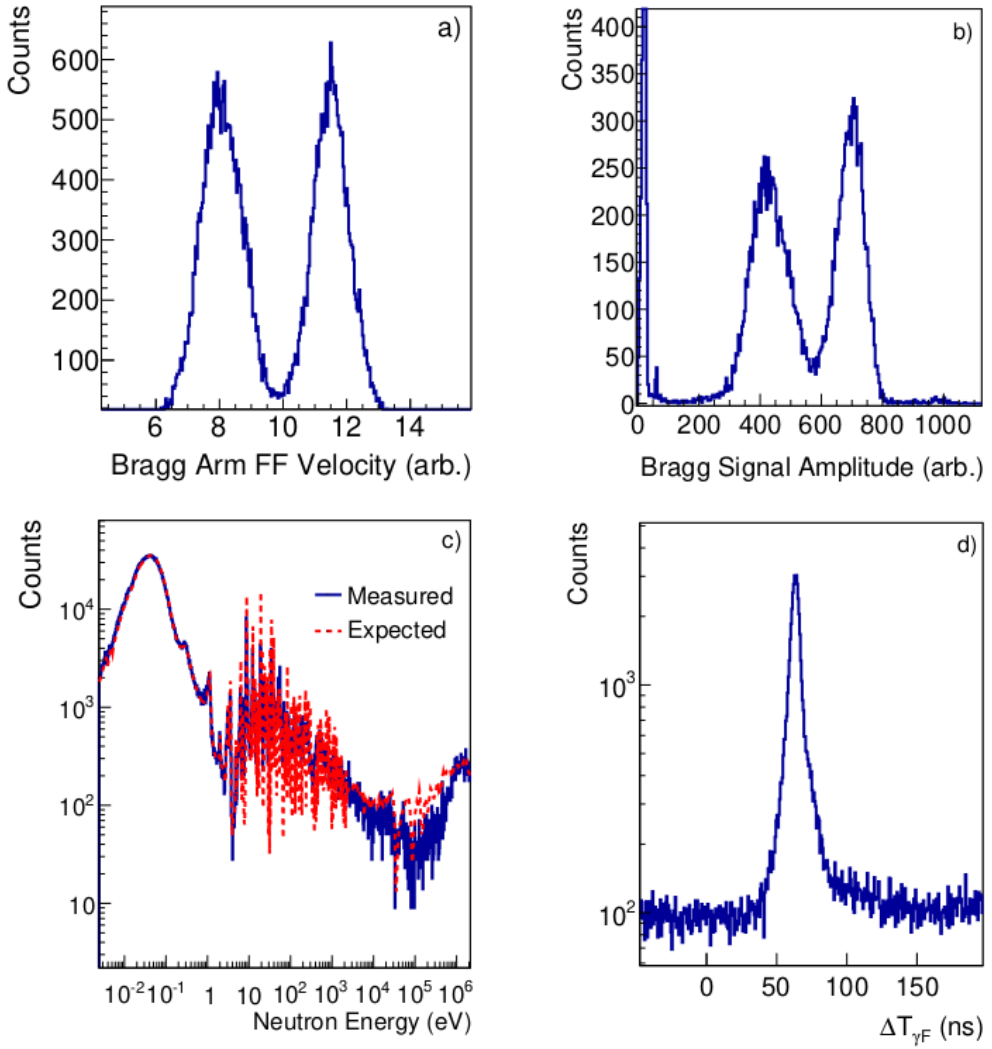


Information on:

- Prompt Fission Gammas (energy and multiplicity)
- Fragment Z yields
- Fragment A yields
- Prompt neutron emission  multiplicity (Nubar)

# Under development

# HYMNS: High-sensitivitY Measurements of key stellar Nucleo-Synthesis reactions
# i-TED: Total Energy Detector with gamma-ray imaging capability

European Research Council

HYMNS

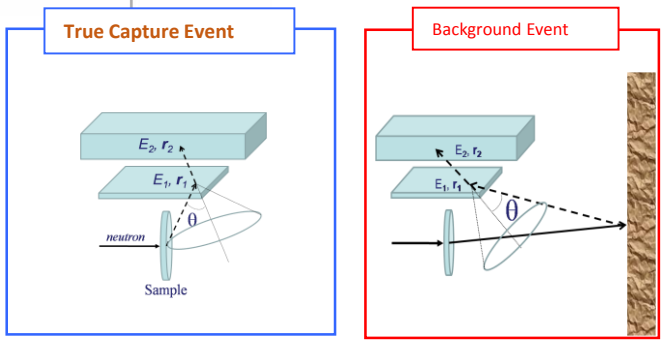


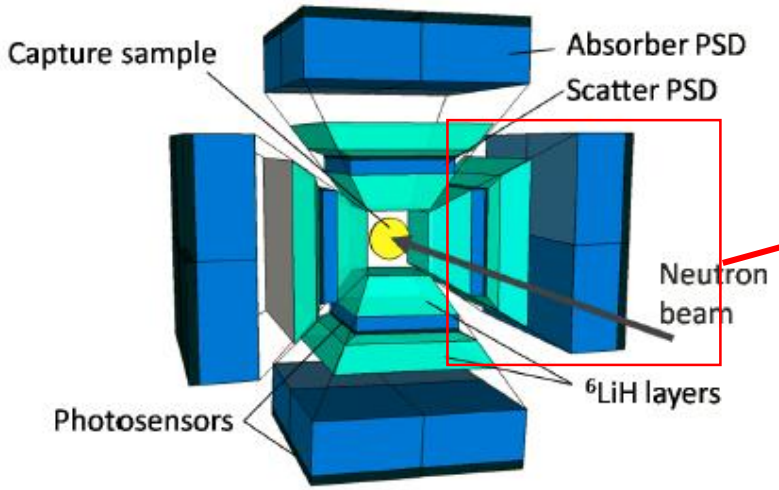


i-TED Module:

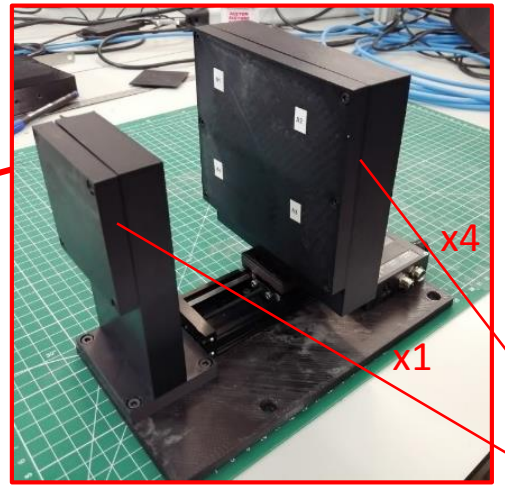


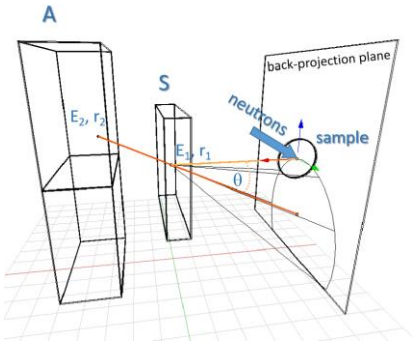


→Full i-TED = 4S+4A= **500 cm²** of PSDs

→ Readout: **1280 channels / pixels**

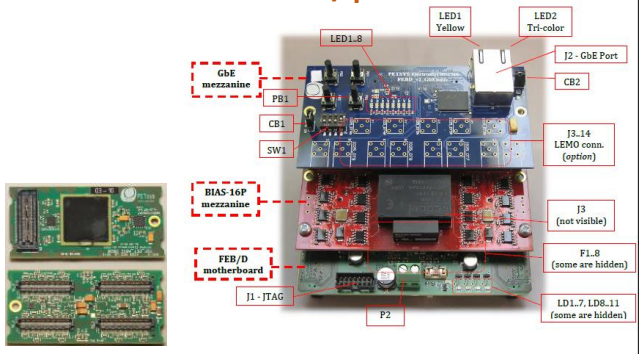


PETsys Electronics S.A. (Customized)

R.Bugalho et al., JINST_079P_0918

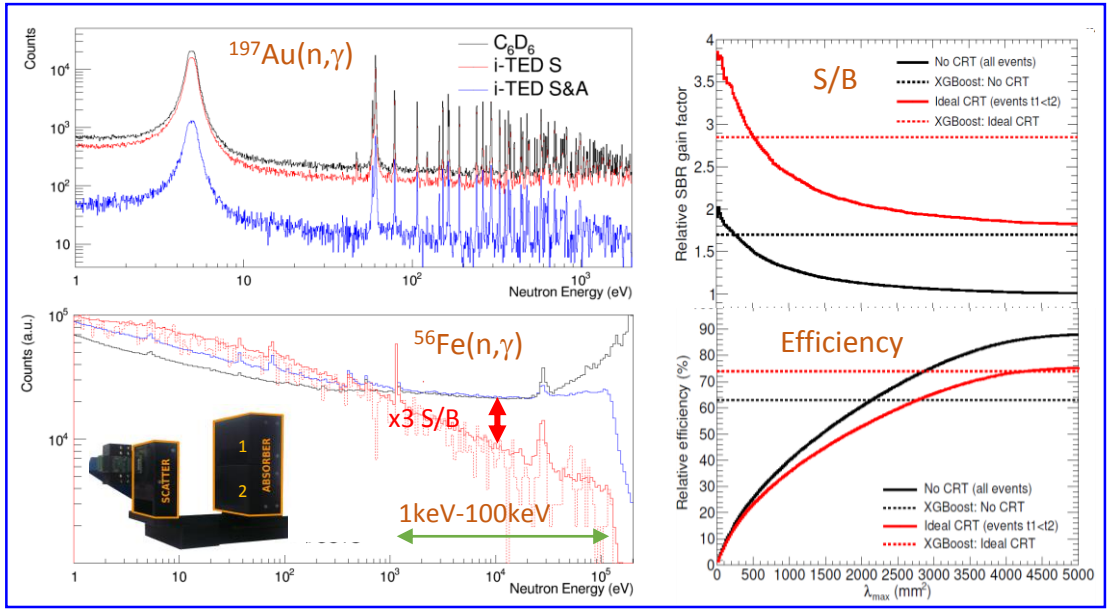


PSDs: 15 mm (S) and 25 mm (A)

Largest commercially available LaCl3 50x50mm²

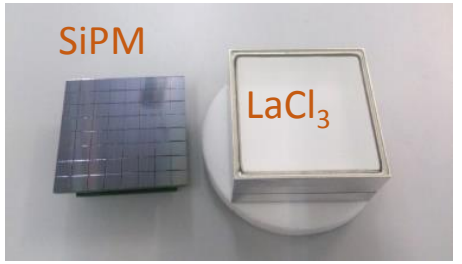


→ # pixels= 8x8y = 64 ch

→ pixel size = **6x6 mm²**

→ area = 5x5 cm² = 25 cm²


C. Domingo-Pardo, Nucl. Instr. Meth. A 825 (2016)

V. Babiano et al., Nucl. Instr. Meth. A 953 (2020)

V. Babiano, J. Lerendegui, et al., EPJ-A (2021) 57:197

Patent PCT/ES2016/070916 "Focusable Compton Camera", 21/12/2016 - WO 2017/109256 Al

Patent PCT/ES2021/070342 "A dual gamma-ray and neutron imaging device" (May 13th, 2021)



Acknowledgments: ERC-CoG Agreement Nr. 681740 (HYMNS)

# The $C_6D_6$ segmented Total Energy Detector sTED

**The superb characteristics of EAR's at n_TOF pose a number of challenges for σ(n,γ) measurements**

- **flash:** large energy deposition by ultra-relativistic particles
- **high counting rates**

**Solution/mitigation:**

a segmented total energy detector (**sTED)**

- Physical segmentation reduces the large energy deposition due to the flash and lowers the counting rate in each detector
- Smaller readout devices: PMTs and or, SiPMs with lower mass compared to PMTs (smaller volume for mitigating the interaction of the flash with the device itself)


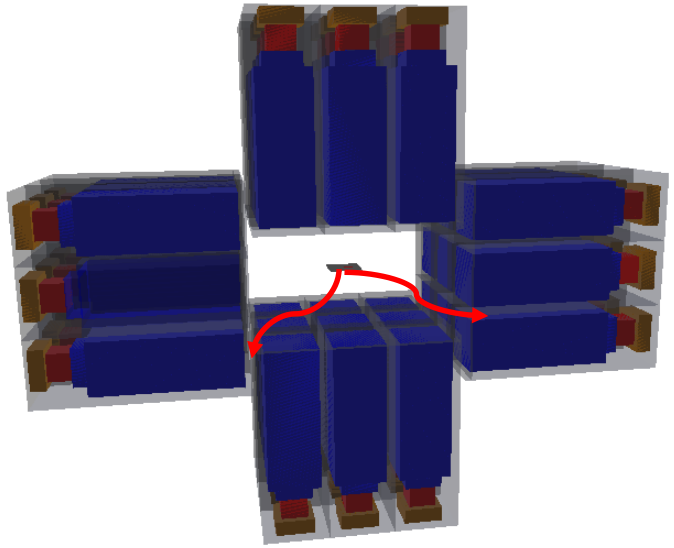

Work funded by the Spanish Ministry of Science, grant PGC2018-096717-B-C21 + **H2020 SANDA project**.

# HPGe with the n_TOF switcher

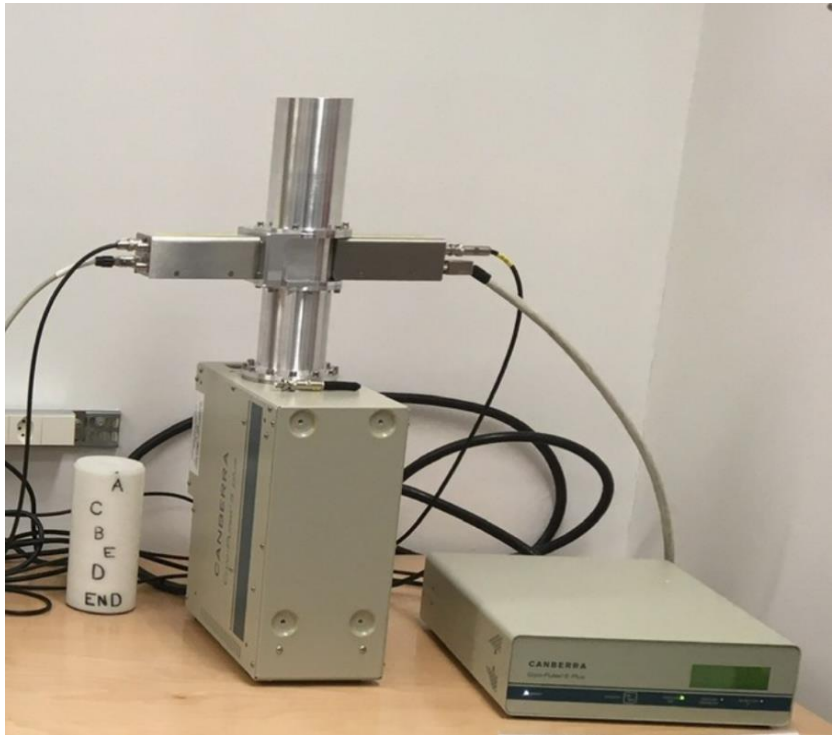


**Advantages - Characteristics**

- Excellent energy resolution (~2.2 keV @ 1.3 MeV)
- Excellent time resolution
- Electronic cooling system
- Det. 1 – rel. efficiency 26%
- Det. 2 – rel efficiency 55% (to be delivered in November)
- Both HPGe's are equipped with "n_TOF switcher"

**To be used in**

- NEAR Activation measurements
- (n,inl) reaction studies

A special designed "switcher circuit" gated by PS trigger is grounding the induced excessive charge from "g-flash" for 200-300 ns.
**Saturation** of the detector **is avoided**!

# Transparent nGEM for beam monitoring of fast neutrons

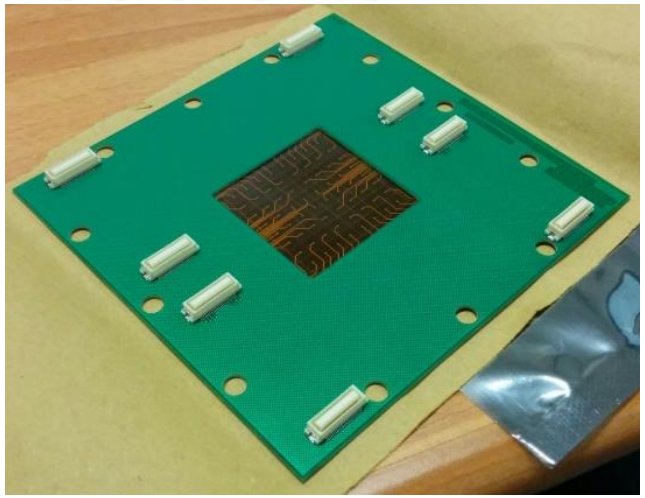

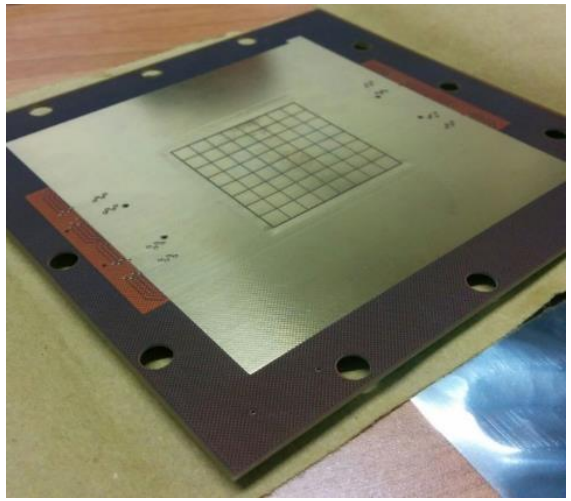

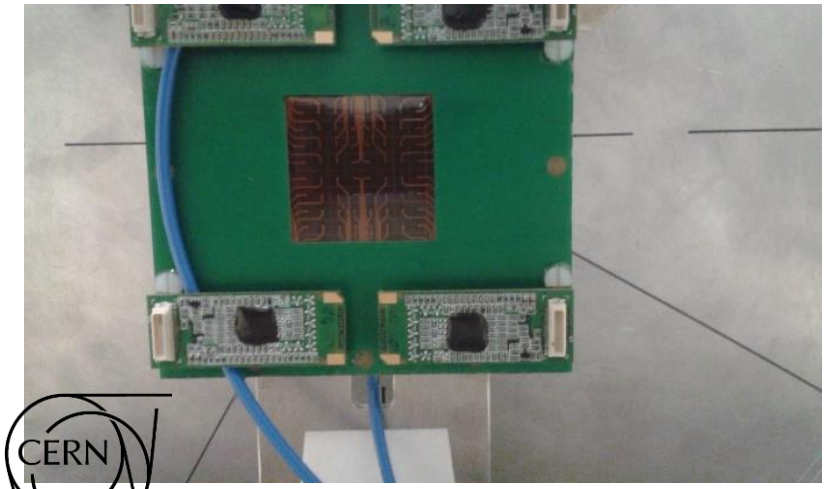

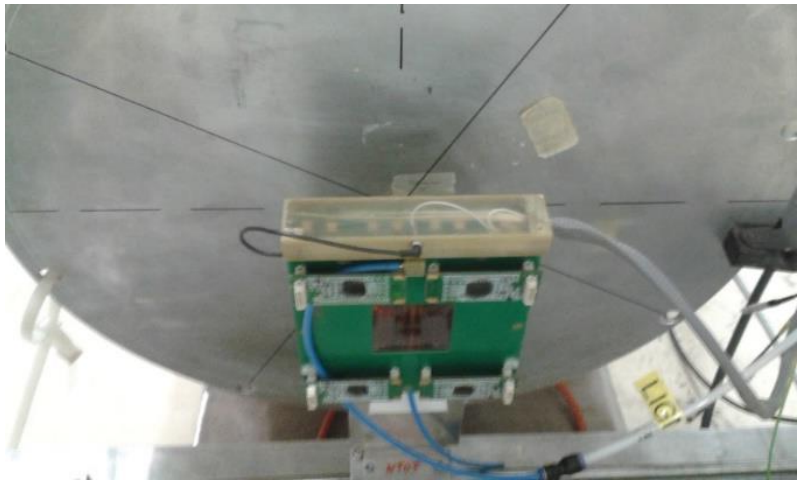

Low material budget

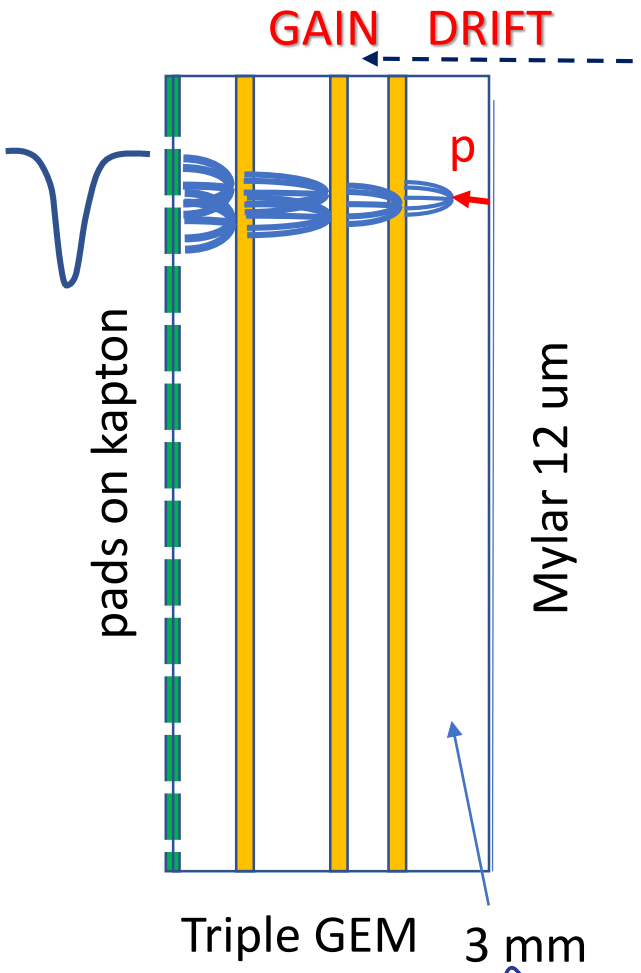


CERN

INFN LNF
Istituto Nazionale di Fisica Nucleare

nTOF

# The NEAR Station

# n_TOF Target-III

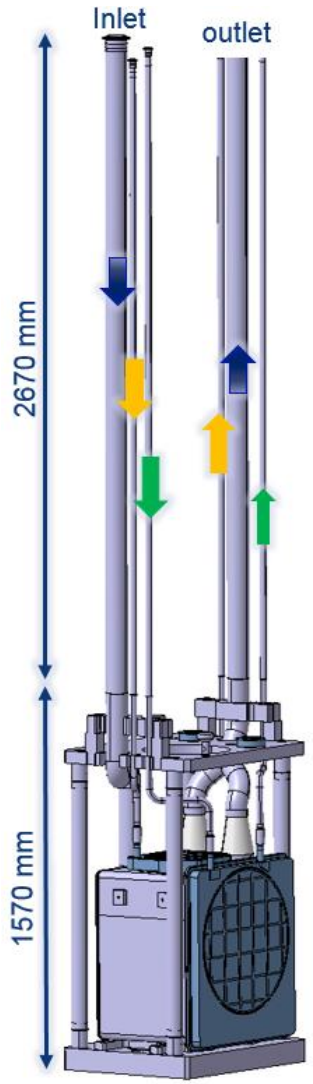


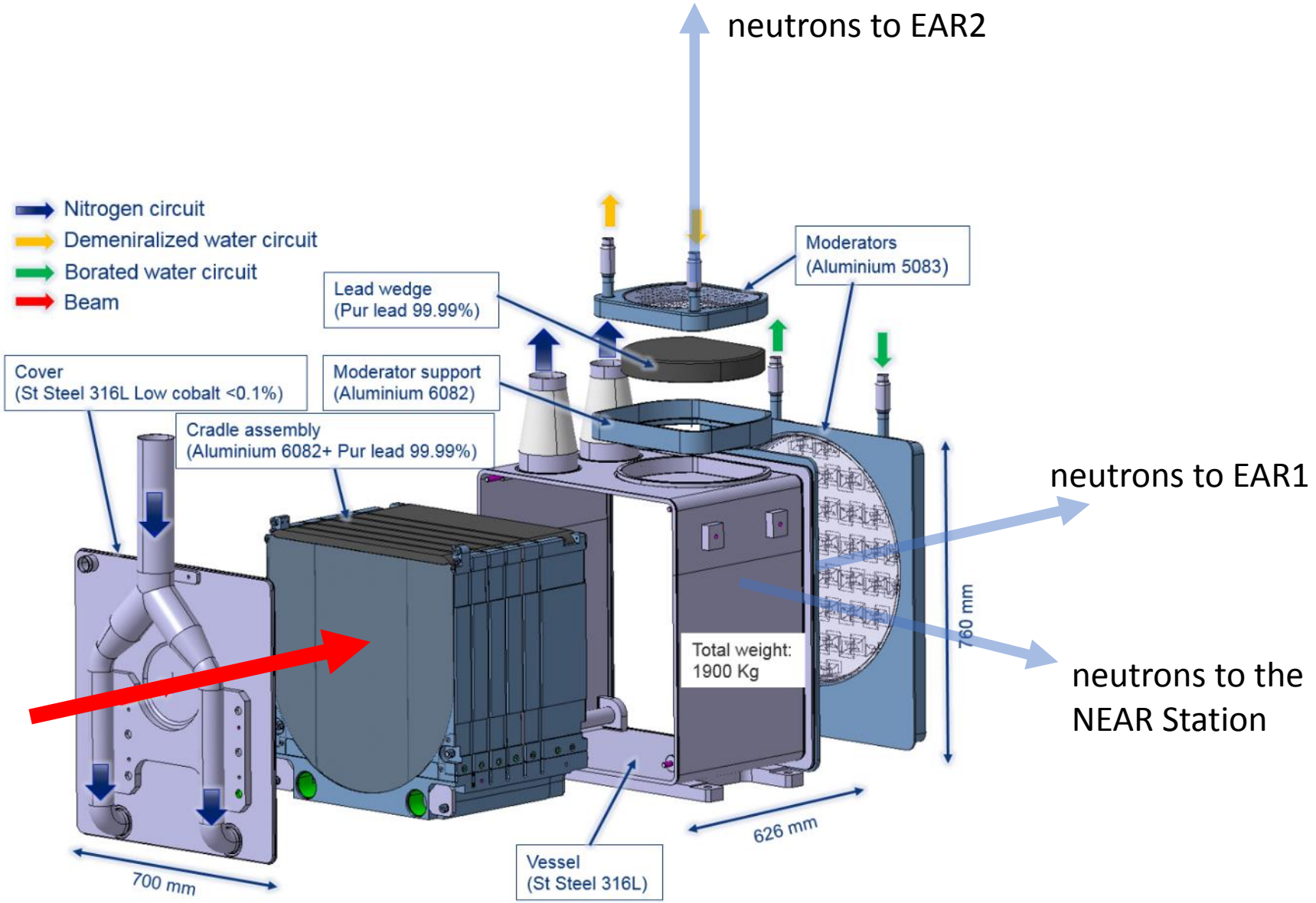

# The NEAR Station

during the design studies of the new shielding around the target station the opportunity for a new near-target experimental area  appeared (NEAR station)

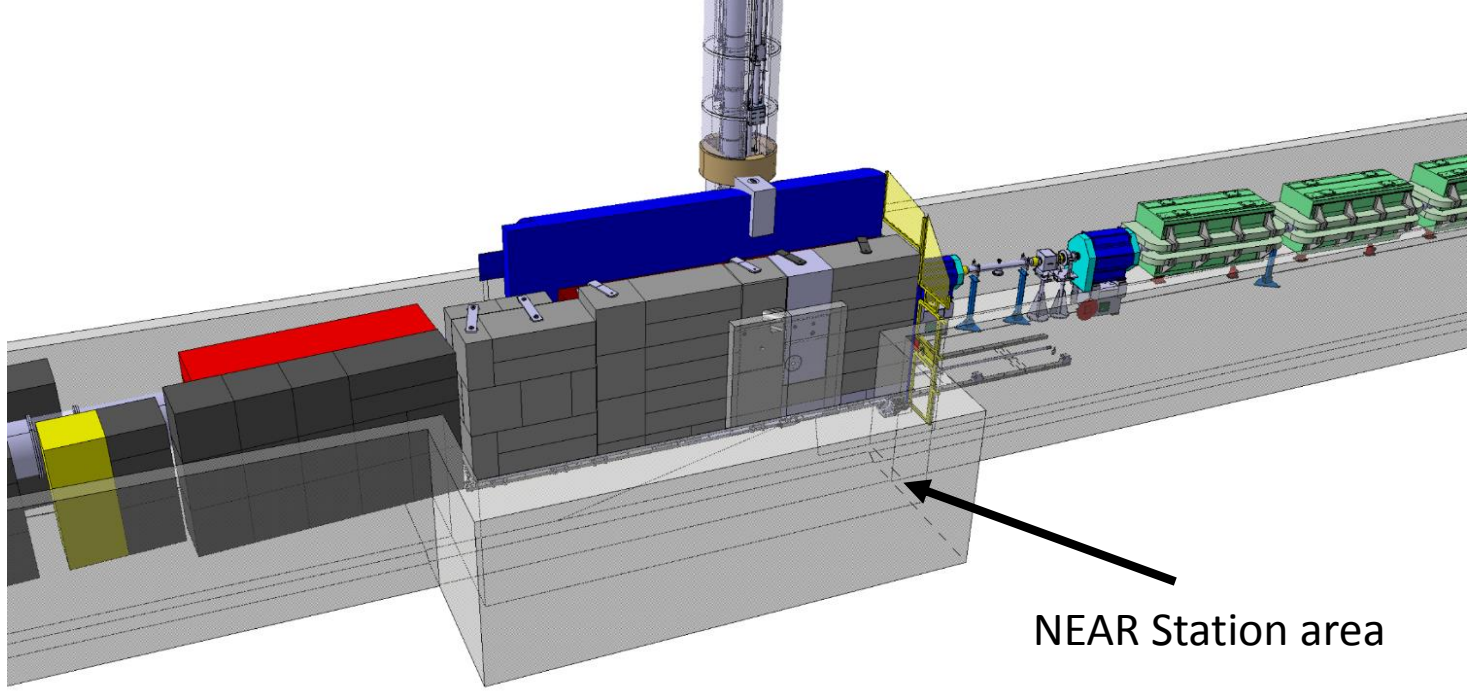


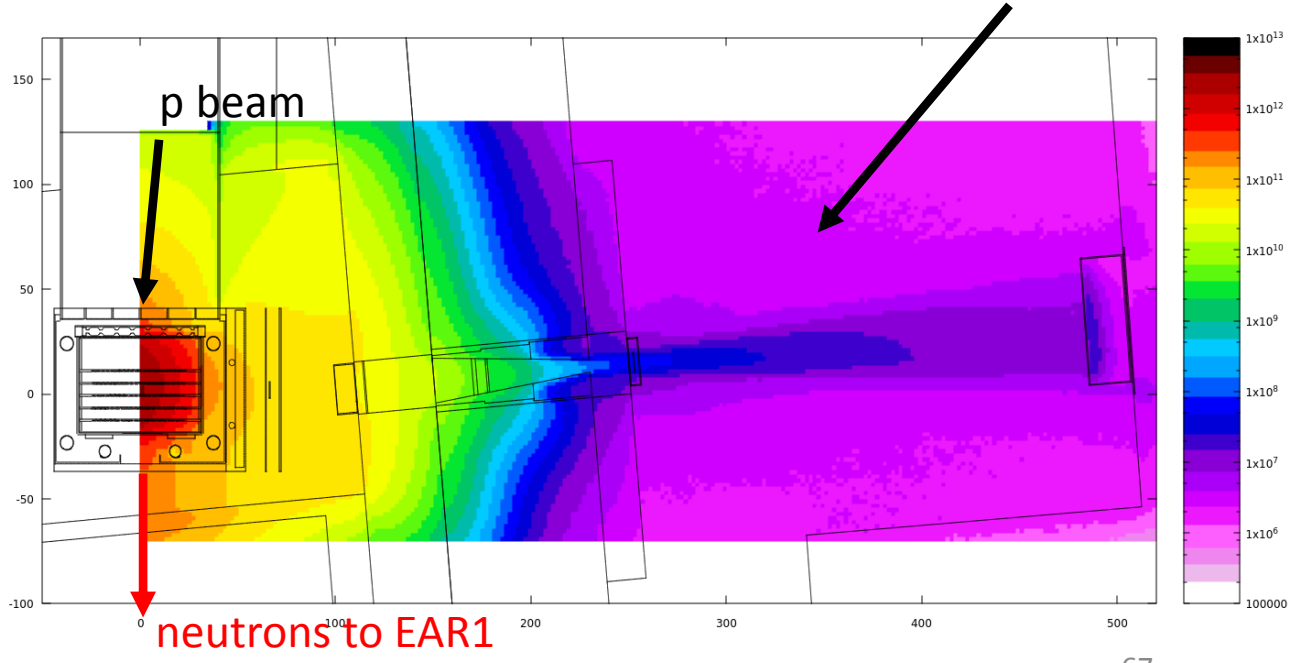


simulations by M Barbagallo

# The NEAR Station

example of simulations of the neutron beam in the NEAR area in comparison to the new ChipIr facility at ISIS(*)

(*)D Chiesa et al., NIMA 902 (2018) 14

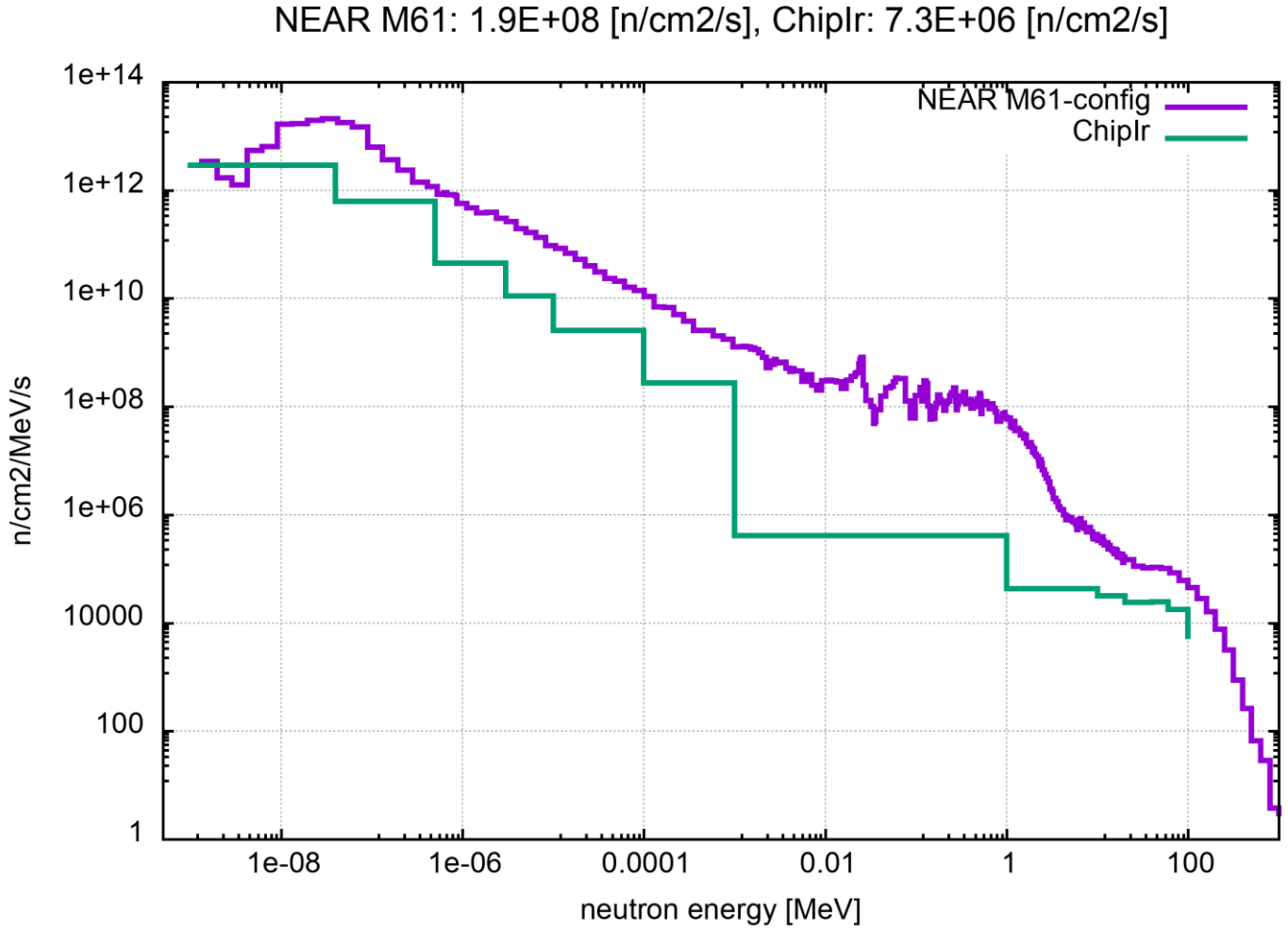


simulations by V Vlachoudis & M Barbagallo

# The NEAR Station

simulations by V Vlachoudis & M Barbagallo

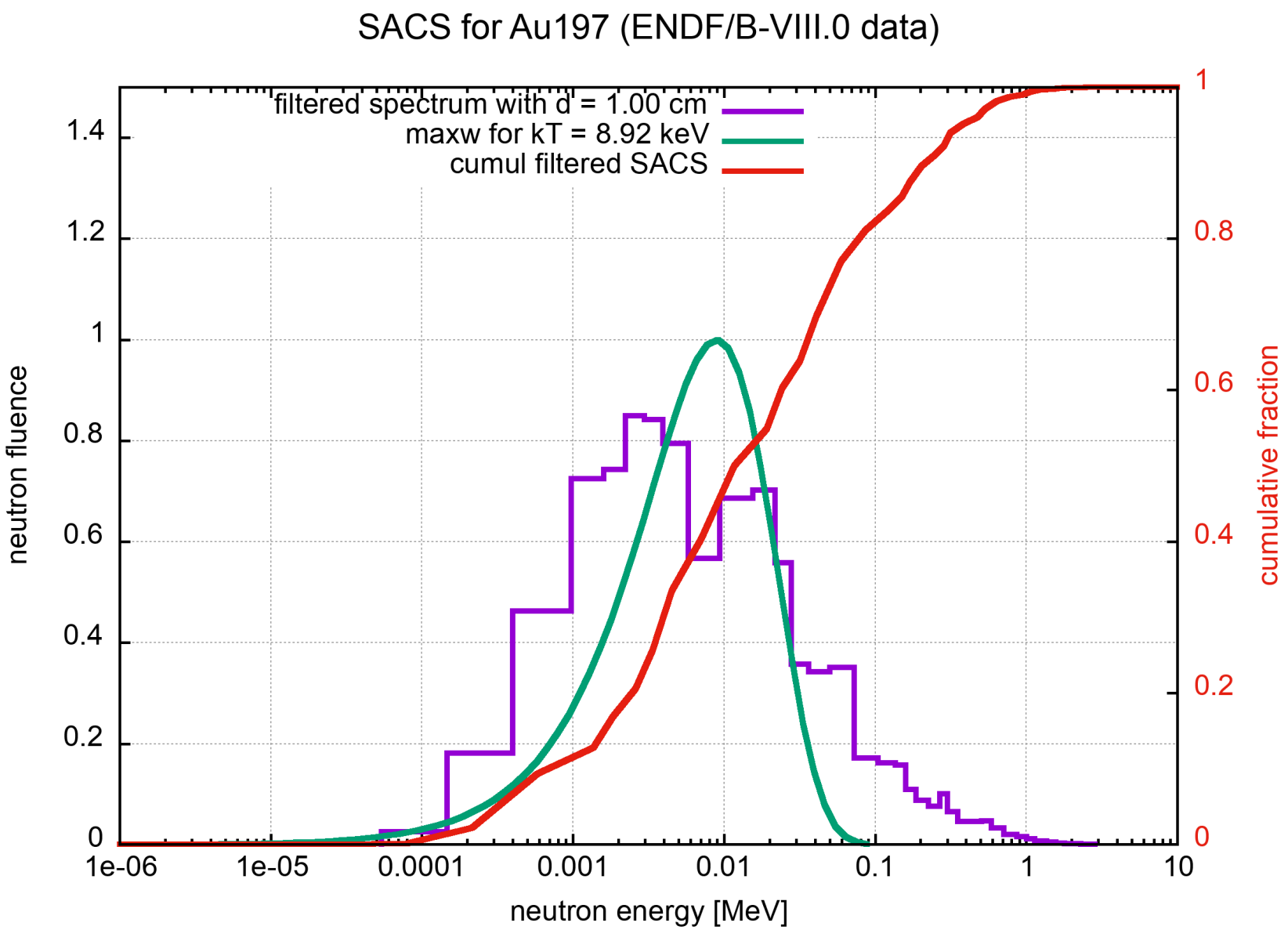

# The NEAR Station

simulations by V Vlachoudis & M Barbagallo

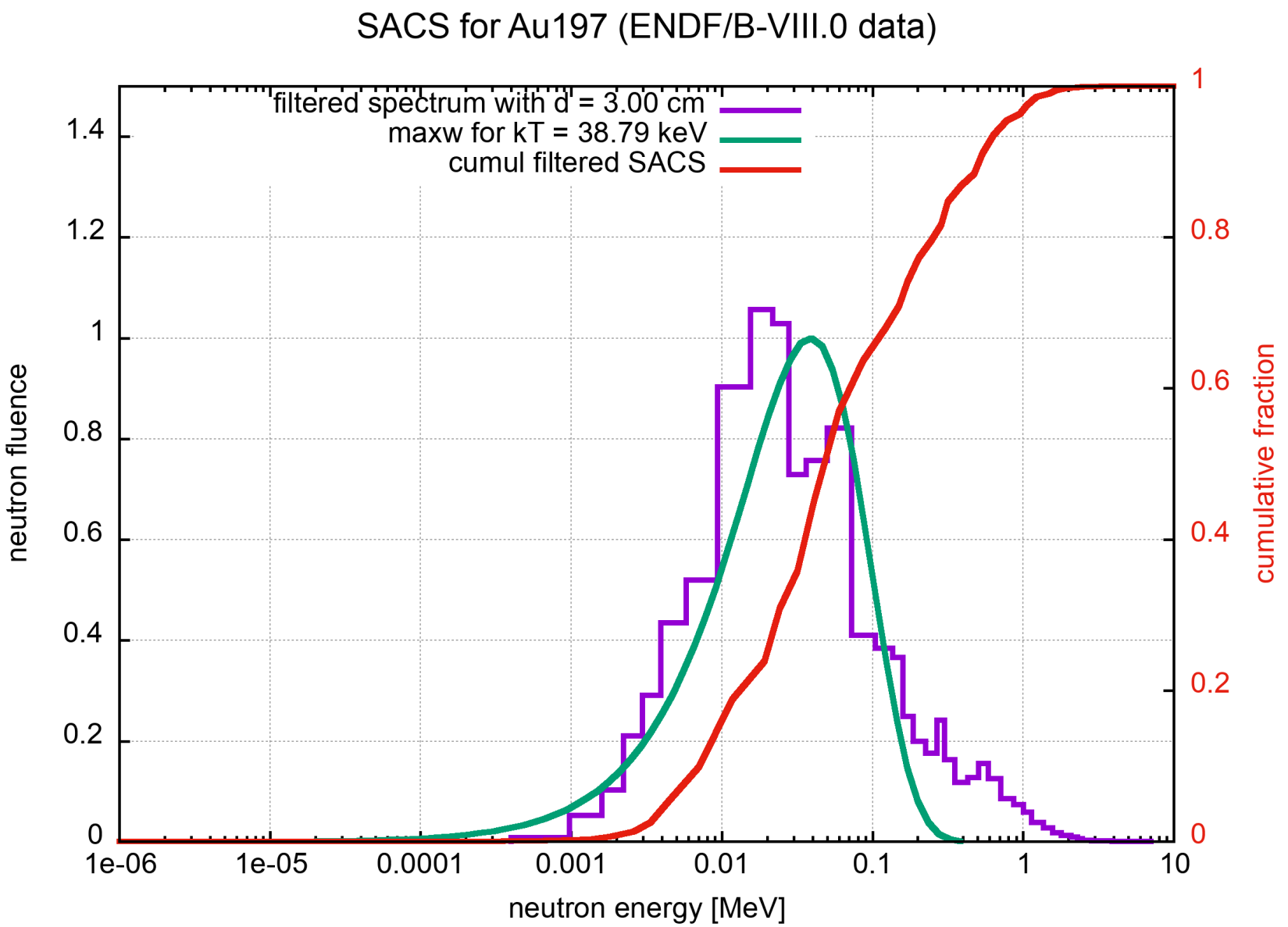

# The NEAR Station

1. Measurements of MACS by activation for nuclear astrophysics
2. Fusion-related measurements (cross sections, not irradiation)
3. Measurements of decay rates of long-lived isotopes
4. Irradiation of non-metallic materials + SEE (R2M & R2E projects)

contact: ntof-nearwg@cern.ch

# The NEAR Station

courtesy of Oliver Aberle (CERN)

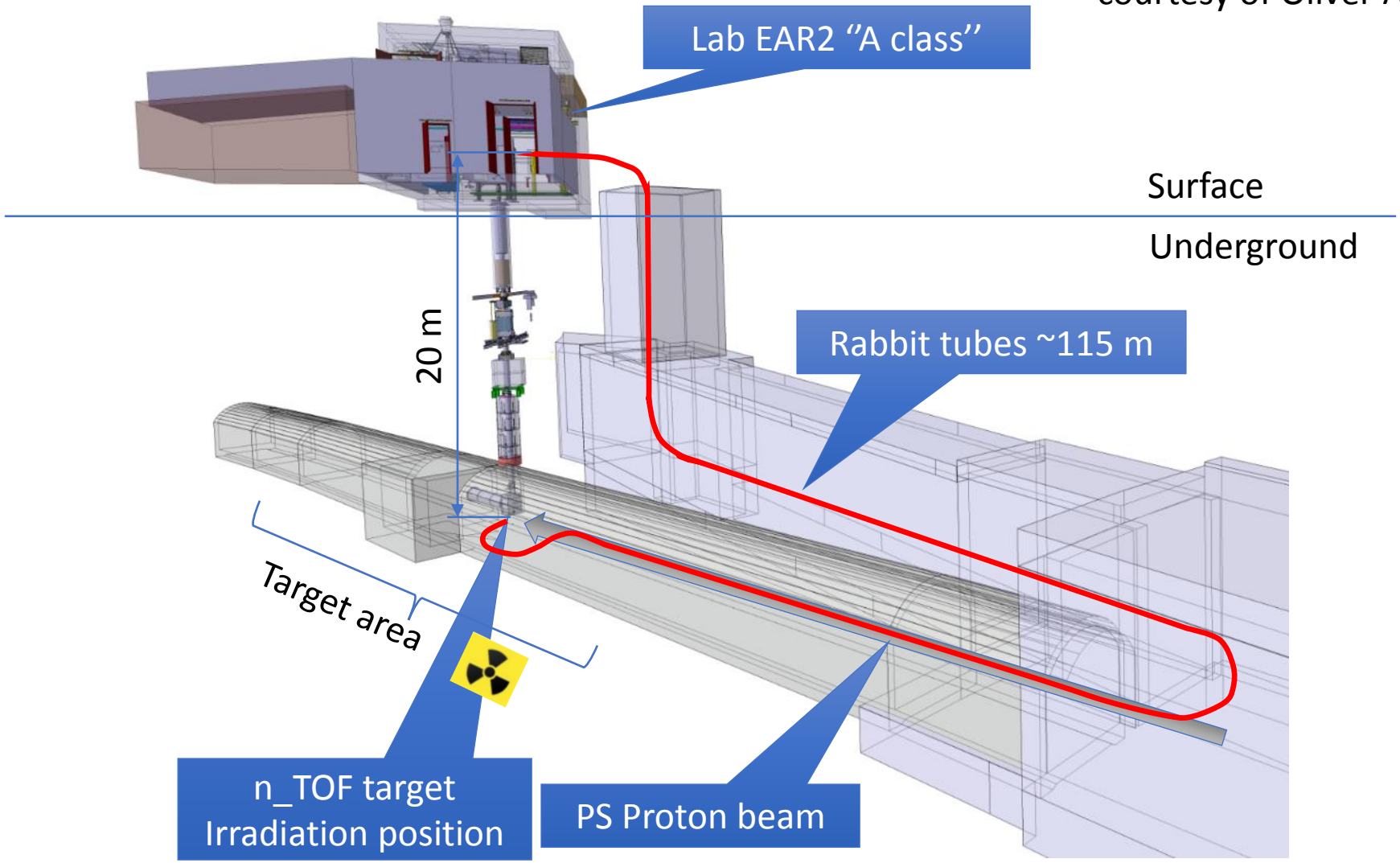

# The NEAR Station

courtesy of Oliver Aberle (CERN)

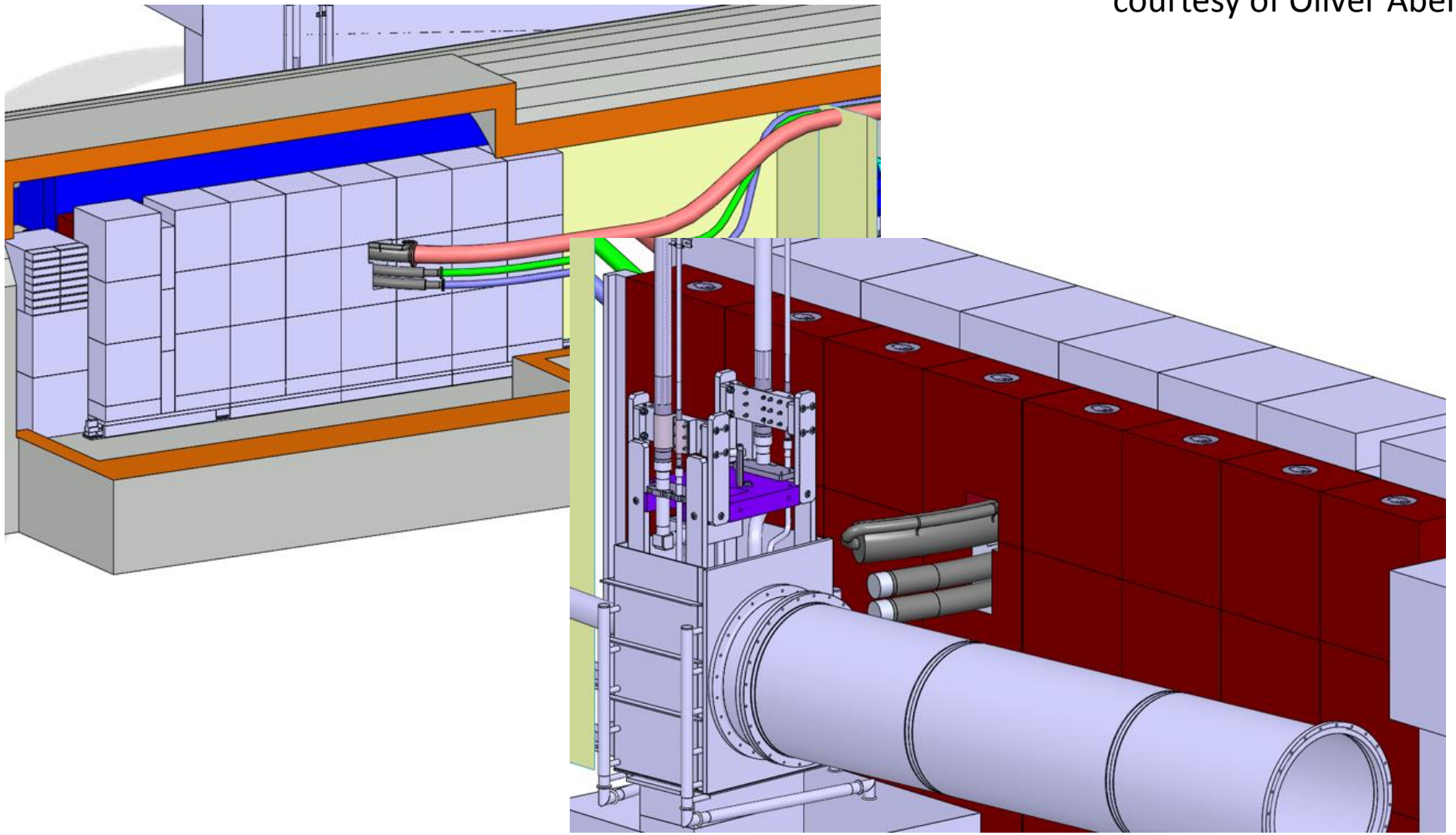

# Phase-2021: new proposals

| reaction | field of interest | note |
|---|---|---|
| $^{94,95,96}$Mo(n,$\gamma$) | – s-process AGB stars, SiC grains<br>– fp, fuel alloys | stable samples (*) |
| $^{94}$Nb(n,$\gamma$) | – anomalies in pre-solar grains<br>– strong contributor to the long-term radiotoxicity among fp | radioactive sample<br>$t_{1/2}$ = 20 ka |
| $^{79}$Se(n,$\gamma$) | – s-process thermometer<br>– strong contributor to the long-term radiotoxicity among fp | radioactive sample<br>$t_{1/2}$ = 300 ka |
| $^{50,53}$Cr(n,$\gamma$) | – criticality safety (major element in stainless steel) | stable samples |
| $^{40}$K(n,p)<br>$^{40}$K(n,$\alpha$) | – radiogenic heating in earth-like exoplanets (destruction vs production mechanisms) | ~ stable samples |

continue…

(*) part of a EU H2020 nuclear data project

# Phase-2021: new proposals

| reaction | field of interest | note |
|---|---|---|
| $^{239}$Pu(n,$\gamma$) and $\alpha$-ratio | – advanced nuclear technologies | radioactive sample $t_{1/2}$ = 24.1 ka (*) |
| n + d → p + 2n | – nn scattering length | basic nuclear physics application |
| $^{243}$Am(n,f) | – contributes to production of $^{239}$Pu (by $\alpha$ + $\beta^-$ decays) | radioactive sample $t_{1/2}$ = 7364 a |

(*) part of a EU H2020 nuclear data project

# Future

**Explored**

Cosmochronology (nuclear clocks) : Re/Os clock

BBN : the cosmological lithium problem (CLiP)

**Planned**

NN-scattering length : charge-symmetry breaking in QCD

**To be explored**

X17 ($n+^{3}He$, $n+^{7}Be$) : dark photons/fifth force (?)

# The n_TOF Collaboration

Established in the year 2000 (MoU signed in 2008)

- 130 researchers, mostly from Europe (participation from Japan, India and the USA)
- 30+ research institutions involved
- typically, 10 PhD students/year
- management: Collaboration Board, Executive Committee, Editorial Board, various working groups

# Publications & experimental data dissemination

- 29 papers published in 2020
  7 in peer reviewed journals + 22 in conference proceedings
- overall 210 papers published
  121 in peer-reviewed journals, 45 in Phys. Rev. C, 32 in NIMA
- 75/85 in Open Access in the last 5 years

https://twiki.cern.ch/NTOFPublic/ListOfPublications

- 116 data sets included in the Experimental Nuclear Reaction Database (EXFOR @ IAEA), 91% of all measurements performed

CERN

nTOF

O. Aberle[1]
V. Alcayne[2]
S. Amaducci[3,4]
J. Andrzejewski[5]
L. Audouin[6]
V. Babiano-Suarez[7]
M. Bacak[1,8,9]
M. Barbagallo[1,10]
S. Bennett[11]
E. Berthoumieux[9]
J. Billowes[11]
D. Bosnar[12]
A. Brown[13]
M. Busso[10,14,15]
M. Caamaño[16]
L. Caballero-Ontanaya[7]
F. Calviño[17]
M. Calviani[1]
D. Cano-Ott[2]
A. Casanovas[17]
F. Cerutti[1]
E. Chiaveri[1,11]
N. Colonna[10]
G. Cortés[17]
M. A. Cortés-Giraldo[18]
L. Cosentino[3]
S. Cristallo[14,19]
L. A. Damone[10,20]
P. J. Davies[11]
M. Diakaki[21,1]
C. Domingo-Pardo[7]
R. Dressler[23]
Q. Ducasse[24]
E. Dupont[9]
I. Durán[16]
Z. Eleme[25]
B. Fernández-Domínguez[16]
A. Ferrari[1]
P. Finocchiaro[3]
V. Furman[26]
K. Göbel[27]
R. Garg[22]
A. Gawlik[5]
S. Gilardoni[1]
I. F. Gonçalves[28]
E. González-Romero[2]
C. Guerrero[18]
F. Gunsing[9]
H. Harada[29]
S. Heinitz[23]
J. Heyse[30]
D. G. Jenkins[13]
A. Junghans[31]
F. Käppeler[32]
Y. Kadi[1]
A. Kimura[29]
I. Knapová[33]
M. Kokkoris[21]
Y. Kopatch[26]
M. Krtička[33]
D. Kurtulgil[27]
I. Ladarescu[7]
C. Lederer-Woods[22]
H. Leeb[8]
J. Lerendegui-Marco[18]
S. J. Lonsdale[22]
D. Macina[1]
A. Manna[34,35]
T. Martínez[2]
A. Masi[1]
C. Massimi[34,35]
P. Mastinu[36]
M. Mastromarco[1]
E. A. Maugeri[23]
A. Mazzone[10,37]
E. Mendoza[2]
A. Mengoni[38]
V. Michalopoulou[21,1]
P. M. Milazzo[39]
F. Mingrone[1]
J. Moreno-Soto[9]
A. Musumarra[3,40]
A. Negret[41]
R. Nolte[24]
F. Ogállar[42]
A. Oprea[41]
N. Patronis[25]
A. Pavlik[43]
J. Perkowski[5]
L. Persanti[10,14,19]
C. Petrone[41]
E. Pirovano[24]
I. Porras[42]
J. Praena[42]
J. M. Quesada[18]
D. Ramos-Doval[6]
T. Rauscher[44,45]
R. Reifarth[27]
D. Rochman[23]
Y. Romanets[28]
C. Rubbia[1]
M. Sabaté-Gilarte[18,1]
A. Saxena[46]
P. Schillebeeckx[30]
D. Schumann[23]
A. Sekhar[11]
A. G. Smith[11]
N. V. Sosnin[11]
P. Sprung[23]
A. Stamatopoulos[21]
G. Tagliente[10]
J. L. Tain[7]
A. Tarifeño-Saldivia[17]
L. Tassan-Got[1,21,6]
Th. Thomas[27]
P. Torres-Sánchez[42]
A. Tsinganis[1]
J. Ulrich[23]
S. Urlass[31,1]
S. Valenta[33]
G. Vannini[34,35]
V. Variale[10]
P. Vaz[28]
A. Ventura[34]
D. Vescovi[10,14]
V. Vlachoudis[1]
R. Vlastou[21]
A. Wallner[47]
P. J. Woods[22]
T. Wright[11]
P. Žugec[12]

# The n_TOF Collaboration

# The n_TOF Collaboration

[1]European Organization for Nuclear Research (CERN), Switzerland
[2]Centro de Investigaciones Energéticas Medioambientales y Tecnológicas (CIEMAT), Spain
[3]INFN Laboratori Nazionali del Sud, Catania, Italy
[4]Dipartimento di Fisica e Astronomia, Università di Catania, Italy
[5]University of Lodz, Poland
[6]Institut de Physique Nucléaire, CNRS-IN2P3, Univ. Paris-Sud, Université Paris-Saclay, F-91406 Orsay Cedex, France
[7]Instituto de Física Corpuscular, CSIC - Universidad de Valencia, Spain
[8]TU Wien, Atominstitut, Stadionallee 2, 1020 Wien, Austria
[9]CEA Irfu, Université Paris-Saclay, F-91191 Gif-sur-Yvette, France
[10]Istituto Nazionale di Fisica Nucleare, Sezione di Bari, Italy
[11]University of Manchester, United Kingdom
[12]Department of Physics, Faculty of Science, University of Zagreb, Zagreb, Croatia
[13]University of York, United Kingdom
[14]Istituto Nazionale di Fisica Nucleare, Sezione di Perugia, Italy
[15]Dipartimento di Fisica e Geologia, Universita' di Perugia, Italy
[16]University of Santiago de Compostela, Spain
[17]Universitat Politècnica de Catalunya, Spain
[18]Universidad de Sevilla, Spain
[19]Istituto Nazionale di Astrofisica - Osservatorio Astronomico di Teramo, Italy
[20]Dipartimento di Fisica, Università degli Studi di Bari, Italy
[21]National Technical University of Athens, Greece
[22]School of Physics and Astronomy, University of Edinburgh, United Kingdom
[23]Paul Scherrer Institut (PSI), Villigen, Switzerland
[24]Physikalisch-Technische Bundesanstalt (PTB), Bundesallee 100, 38116 Braunschweig, Germany
[25]University of Ioannina, Greece
[26]Joint Institute for Nuclear Research (JINR), Dubna, Russia
[27]Goethe University Frankfurt, Germany
[28]Instituto Superior Técnico, Lisbon, Portugal
[29]Japan Atomic Energy Agency (JAEA), Tokai-mura, Japan
[30]European Commission, Joint Research Centre, Geel, Retieseweg 111, B-2440 Geel, Belgium
[31]Helmholtz-Zentrum Dresden-Rossendorf, Germany
[32]Karlsruhe Institute of Technology, Campus North, IKP, 76021 Karlsruhe, Germany
[33]Charles University, Prague, Czech Republic
[34]Istituto Nazionale di Fisica Nucleare, Sezione di Bologna, Italy
[35]Dipartimento di Fisica e Astronomia, Università di Bologna, Italy
[36]Istituto Nazionale di Fisica Nucleare, Sezione di Legnaro, Italy
[37]Consiglio Nazionale delle Ricerche, Bari, Italy
[38]Agenzia nazionale per le nuove tecnologie (ENEA), Bologna, Italy
[39]Istituto Nazionale di Fisica Nucleare, Sezione di Trieste, Italy
[40]Dipartimento di Fisica e Astronomia, Università di Catania, Italy
[41]Horia Hulubei National Institute of Physics and Nuclear Engineering, Romania
[42]University of Granada, Spain
[43]University of Vienna, Faculty of Physics, Vienna, Austria
[44]Department of Physics, University of Basel, Switzerland
[45]Centre for Astrophysics Research, University of Hertfordshire, United Kingdom
[46]Bhabha Atomic Research Centre (BARC), India
[47]Australian National University, Canberra, Australia

# The End

# Additional material

# $^{243}$Am(n,f) cross section measurement with XY Micromegas detectors

N Patronis, M Diakaki et al. (The n_TOF Collaboration)
CERN-INTC-2020-048 ; INTC-P-566

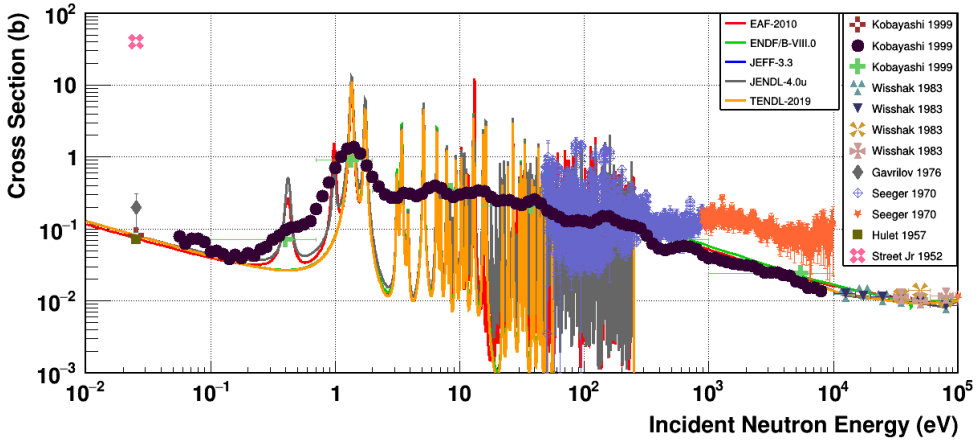


**Figure 1:** Previous measurements of $^{243}$Am(n,f) cross-section up to 100 keV along with the available evaluated libraries (retrieved from the EXFOR database).

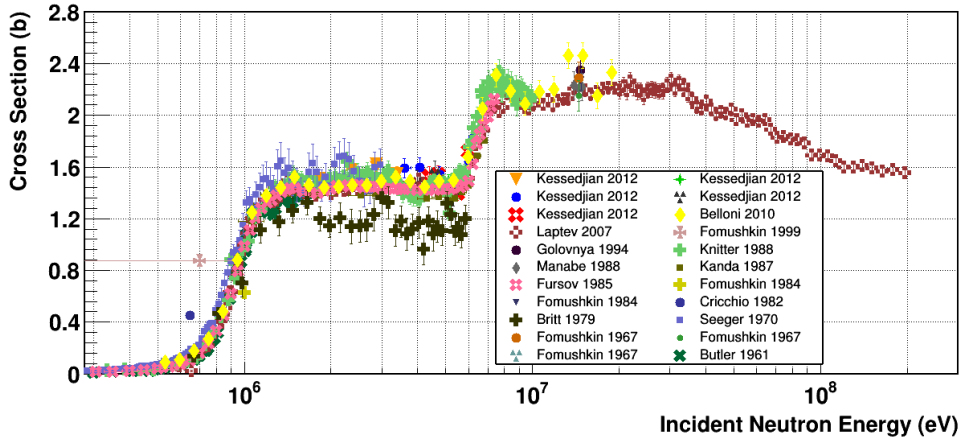


**Figure 2:** Previous measurements of $^{243}$Am(n,f) cross-section above 300 keV (retrieved from the EXFOR database).

# The n_TOF DAQ

A specific pulse shape analysis routine exists for every detector: Silicon Flux Monitor, $C_6D_6$ detectors, PPACs, etc.

**For the $BaF_2$ signals:**

- The TOF is determined by means of a simulated Constant Fraction Discrimination
- Both the fast ($\tau$=0.7ns) and slow ($\tau$=620ns) scintillation components are fitted to a Maxwellian and an exponential (with a fixed $\tau$=620ns) shape, respectively
- Excellent $\alpha/\gamma$ discrimination
- Pileups occurring 300 ns after the first signal are recognised and analysed after performing the necessary baseline correction

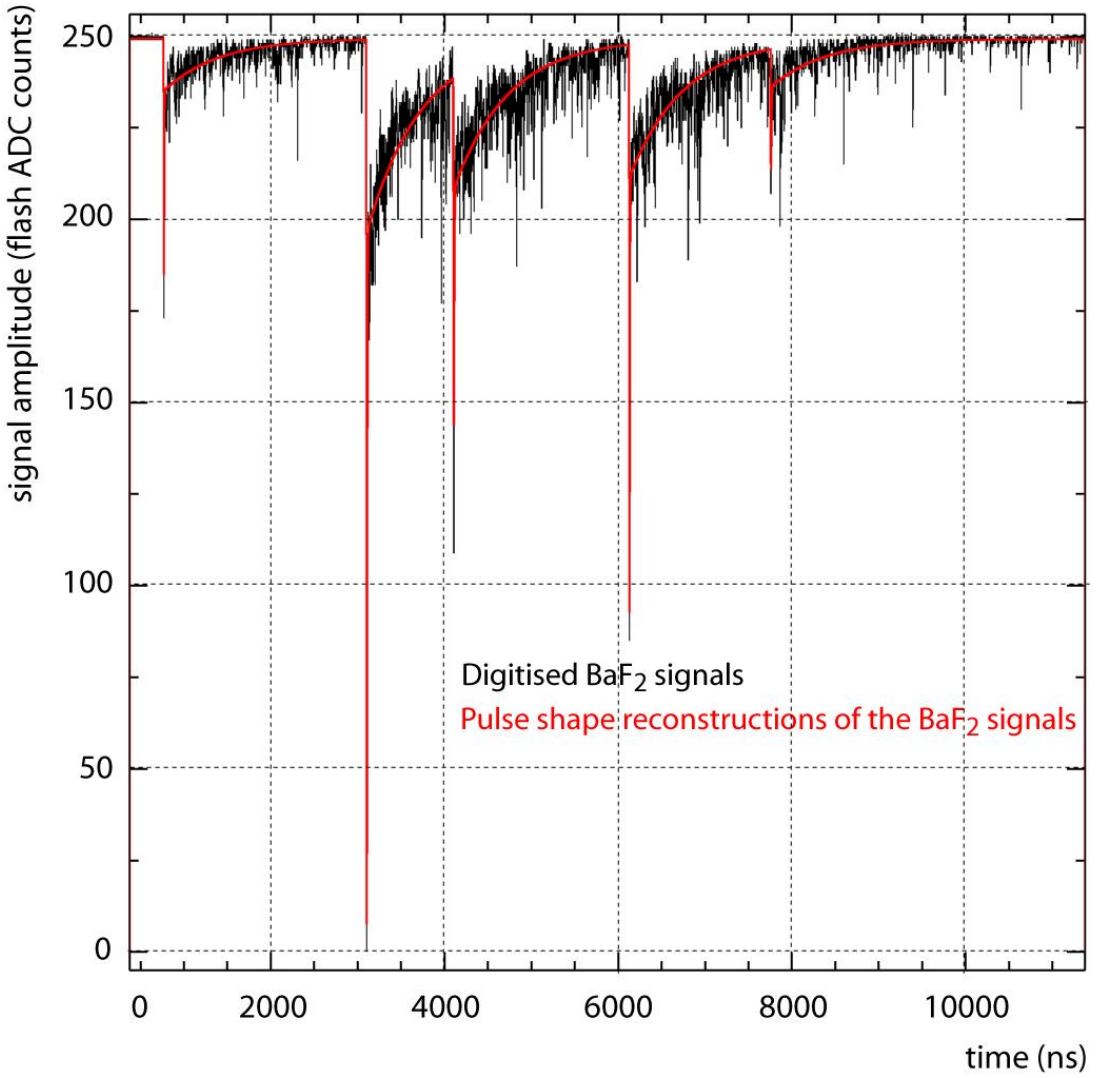


High data transfer rate: ~ 2 TB/day

# Radioisotopes measured at n_TOF

| Isotope | half-life [yr] | mass [g] | N | Activity [Bq] | reaction | note |
|---|---|---|---|---|---|---|
| Be-7 | 0.15 | 7.94E-08 | 6.83E+15 | 1.03E+09 | (n,p) | |
| Be-7 | 0.15 | 2.78E-06 | 2.39E+17 | 3.60E+10 | (n,a) | |
| Al-26 | 7.17E+05 | 1.11E-05 | 2.58E+17 | 7.91E+03 | (n,p); (n,a) | |
| Mn-53 | 3.74E+06 | 8.80E-07 | 1.00E+16 | 5.88E+01 | (n,g) | failed |
| Ni-59 | 7.60E+04 | 1.75E-04 | 1.78E+18 | 5.16E+05 | (n,a) | |
| Ni-63 | 101.2 | 7.72E-02 | 7.38E+20 | 1.60E+11 | (n,g) | |
| Zr-93 | 1.61E+06 | 1.04E+00 | 6.76E+21 | 9.23E+07 | (n,g) | partial results obtained |
| Pm-147 | 2.62 | 8.50E-05 | 3.48E+17 | 2.92E+09 | (n,g) | |
| Sm-151 | 90 | 8.90E-02 | 3.55E+20 | 8.67E+10 | (n,g) | |
| Tm-171 | 1.92 | 3.13E-03 | 1.10E+19 | 1.26E+11 | (n,g) | |
| Tl-204 | 3.78 | 9.00E-03 | 2.66E+19 | 1.54E+11 | (n,g) | |

https://twiki.cern.ch/NTOFPublic/ListOfPublications